Institute of Geophysics
Polish Academy of Sciences

PUBLICATIONS
OF THE INSTITUTE OF GEOPHYSICS
POLISH ACADEMY OF SCIENCES

Geophysical Data Bases, Processing and Instrumentation

429 (D-76)

MONOGRAPHIC VOLUME

Ozone Content Variability in the Ground-level Atmosphere Layer in the Mazowieckie Voivodeship, Central Poland

Izabela Pawlak and Janusz Jarosławski

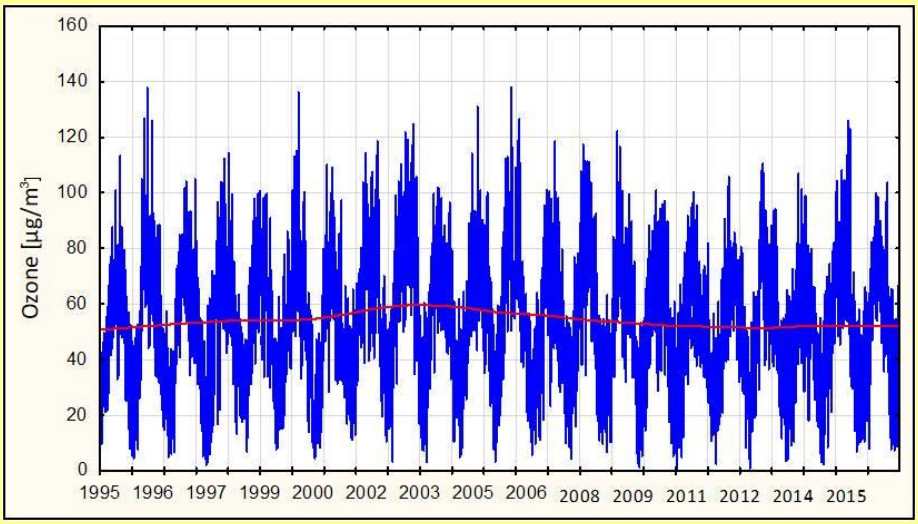

Warsaw 2020 (Issue 3)

INSTITUTE OF GEOPHYSICS
POLISH ACADEMY OF SCIENCES

PUBLICATIONS
OF THE INSTITUTE OF GEOPHYSICS
POLISH ACADEMY OF SCIENCES

Geophysical Data Bases, Processing and Instrumentation

429 (D-76)

MONOGRAPHIC VOLUME

Ozone Content Variability in the Ground-level Atmosphere Layer in the Mazowieckie Voivodeship, Central Poland

Izabela Pawlak and Janusz Jarosławski

Warsaw 2020

ISBN 978-83-66254-01-5 eISSN-2299-8020
DOI: 10.25171/InstGeoph_PAS_Publs-2020-004

Figure “Series of ground-level ozone concentration in Belsk” on the front cover by Izabela Pawlak

Editorial Office
Instytut Geofizyki Polskiej Akademii Nauk
ul. Księcia Janusza 64, 01-452 Warszawa

C O N T E N T S

Editorial note

The present publication is a revised and amended version of I. Pawlak's doctoral thesis defended at the Institute of Geophysics, Polish Academy of Sciences, under the supervision of Professor Janusz Jarosławski.

Abstract

This publication presents an analysis of the variability of ground-level ozone in the Mazowieckie Voivodeship, Central Poland, in 2005−2012 and the forecast of ground-level ozone for the next day using artificial neural network models. The content of ground-level ozone in a given area is mainly determined by meteorological conditions and the presence of appropriate chemical compounds, i.e. ozone precursors. The average ozone mixing ratio is from 20 to 100 ppb, depending on the location of the measurement site.

Despite its low concentration, ozone in the ground layer has a significant impact on natural environment, through the production of free radicals, shaping the greenhouse effect on the Earth and the formation of photochemical smog, to mention just a few effects. High contents of ground-level ozone may result in the occurrence of episodes that are harmful to human health.

The analysis of ground-level ozone measurements in various time scales resulted in the following findings: (1) on an annual scale − the occurrence of a characteristic maximum in the spring-summer period and the minimum in the autumn-winter period, (2) on a daily scale − the occurrence of the highest ground-level ozone content in the afternoon and the lowest just before the sunrise, and (3) on a weekly scale − the existence of a weekend ozone phenomenon.

The analysis of the long-term (1995-2016) ozone measurement series at Belsk gave grounds for distinguishing the three periods, representing an increase, decrease and re-increase of ozone content in the ground-level atmosphere in this locality.

Models for forecasting the maximum 1-hour daily ozone concentration for the next day over the period of April–September 2015 were constructed using the Statistica 10 "Automatic Neural Networks" program package. The quality of the forecast based on neural models was verified for data from the same months of 2014. The results testify to the ability of the network to generalize the training-acquired knowledge for new, previously unexamined cases. A comparison of neural network modeling results with those of the Global Environmental Multiscale-Air Quality (GEM-AQ) troposphere chemistry model shows that the Unidirectional Multi-Layer Perceptron (MLP) type models applied in this study are an effective tool for the next-day ground-level ozone forecasting.

ANALIZA ZMIENNOŚCI ZAWARTOŚCI OZONU W PRZYZIEMNEJ WARSTWIE ATMOSFERY W WOJEWÓDZTWIE MAZOWIECKIM

Streszczenie

Głównym celem badawczym była ocena zmienności zawartości ozonu przyziemnego w województwie mazowieckim w latach 2005–2012 oraz skonstruowanie modeli realizujących prognozę stężenia ozonu przyziemnego na kolejny dzień z wykorzystaniem sztu-cznych sieci neuronowych. Dane pomiarowe użyte w pracy pochodzą z sześciu stacji zlokalizowanych na terenie województwa mazowieckiego, reprezentujących warunki zarówno tła regionalnego jak i miejskiego.

W pierwszej części pracy wykonano analizę statystyczną zmienności czasowej i przestrzennej stężenia ozonu w przyziemnej warstwie atmosfery, która determinowana jest głównie przez panujące warunki meteorologiczne i obecność odpowiednich związków chemicznych – prekursorów ozonu. Wyniki obliczeń wskazują, że najwyższe wartości stężeń ozonu przyziemnego zanotowano na stacjach tła regionalnego zaś najniższe na stacjach tła miejskiego. Na wszystkich analizowanych stacjach zaobserwowano charakte-rystyczny cykl zmian stężeń ozonu, z maksimum w okresie wiosenno-letnim oraz minimum w okresie jesienno-zimowym. Stwierdzono, że uniwersalny schemat zmienności koncentracji ozonu w ciągu doby (z wyraźnym maksimum w godzinach popołudniowych oraz minimum przed wschodem słońca) w skali roku ulega znacznym modyfikacjom. W wyniku analizy zmienności stężeń ozonu w ujęciu tygodniowym wykazano istnienie weekendowego zjawiska ozonowego na niektórych stacjach. Analiza długookresowej zmienności wartości stężenia ozonu przyziemnego na stacji Belsk (1995–2016) uwidoczniła istnienie 3 okresów, w czasie których zaobserwowano wzrost, spadek oraz ponowny powolny wzrost zawartości ozonu przyziemnego. Analiza współczynników korelacji pomiędzy stężeniem ozonu przy-ziemnego a wybranymi parametrami meteorologicznymi pozwoliła określić charakter zależności pomiędzy badanymi zmiennymi. Wyniki te zostały następnie wykorzystane przy konstrukcji modeli prognostycznych stężenia ozonu w przyziemnej warstwie atmosfery.

W drugiej części pracy przedstawiono prognozę wartości maksymalnego 1-godzinnego stężenia ozonu w ciągu doby na kolejny dzień dla okresu od kwietnia do września 2015 roku (osobno dla każdej analizowanej stacji). Prognoza wykorzystywała sztuczne sieci neuronowe o strukturze MLP (Multi-Layer Perceptron). Sprawdzenie jakości prognozy z użyciem analogicznego jak w 2015 roku zestawu danych wejściowych obejmujących okres od kwietnia do września 2014 roku w większości przypadków wykazało istnienie wysokiej korelacji pomiędzy wartościami prognozowanymi a rzeczywistymi. Jednocześnie stwierdzono, że prognozy charakteryzujące się najwyższą wartością błędów względnych zazwyczaj były efektem przeszacowania przez sieci neuronowe relatywnie niskich rzeczywistych wartości stężeń ozonu. Wykonano porównanie wyników uzyskanych z modeli opracowanych w niniejszej pracy, obejmujących okres od kwietnia do września 2014 z wynikami globalnego modelu chemii troposfery GEM-AQ (Global Environmental Multiscale – Air Quality). Wyniki analizy porównawczej wskazują, że jakość prognoz otrzymanych z modeli wykorzystujących sztuczne sieci neuronowe jest porównywalna a nawet w wielu przypadkach przewyższa jakość prognoz uzyskanych przy wykorzystaniu modeli chemii troposfery.

1. INTRODUCTION

1.1 How the ozone was discovered

Ozone was discovered in 1839 by a German scientist − chemist Christian Friedrich Schönbein − during research on water electrolysis (Wierzbicki 1882). Schönbein's hypothesis that ozone is an allotropic form of oxygen naturally occurring in the atmosphere was soon confirmed by Andrews (1874), and a molecular formula was presented by Soret in 1865 (Rubin 2001).

First measurements of the ozone content in the ground layer of the atmosphere, with the use of Schönbein test papers, were already carried out in the first half of the 19th century by the ozone explorer himself. He made use of the decomposition of potassium iodide under the influence of ozone. Test papers soaked in starch glue containing potassium iodide and then exposed outside were changing their color to blue, depending on the current ozone concentration. The basis for determining the ozone concentration was to compare the color of the Schönbein test paper with a 10-point standard scale according to the principle: the higher the read-out value (the maximum is 10), the greater the amount of ozone in the ambient air (Wierzbicki 1882).

In the mid-nineteenth century there was a network of over 300 ozone-measuring stations, covering the area of North America, Australia and Europe. Despite the fact that in most cases those observations provided rather short, unsystematic measurement series (Bojkov 1986), it is as early as in the mid-nineteenth century that the scientists had knowledge about the spatial variability of ozone. According to Andrews (1874), ozone concentration in large cities was lower than in suburban and rural areas. He claimed that ozone is destroyed by contact with smoke and pollutants that are emitted and accumulated in excess in places with high population density. Moreover, he believed that ozone concentration in mountainous areas is lower than in lowland areas.

Along with the qualitative ozone measurement method proposed by Schönbein, there was also a quantitative method based on the arsenite oxidation process. The measuring technique used a cylinder filled with a mixture of potassium arsenite solution and potassium iodide through which atmospheric air was pumped. Under the influence of ozone, arsenite was transformed into arsenate. The amount of arsenate obtained in this manner was the basis for determining ozone in the air (Bojkov 1986).

1.2 Occurrence and role of ozone in the atmosphere

Problems concerning ozone in the ground layer of the atmosphere are considered very important due to the impact of ozone on the natural environment as well as the human health.

Ozone is a gas that occurs naturally in the atmosphere. About 90% of the total ozone content occurs in the stratosphere, the maximum being usually located at altitudes of 20−25 km ("proper" ozone layer) (Fig. 1). At these altitudes, the average ozone mixing ratio is approximately 10 ppm (10 ozone molecules per 10^6 air molecules). The remaining 10% of the total ozone content is within the troposphere, the average mixing ratio close to the earth's surface being between 20 and 100 ppb (20−100 molecules for every 10^9 air molecules).

Ozone present in the atmosphere has an ability to absorb harmful solar radiation in the UV-C range (100−280 nm − thanks to ozone, the radiation at these wavelengths does not reach the earth's surface) and UV-B (280−315 nm), thus providing protection and enabling the life on Earth. In the early 1980s, the process of ozone layer depletion was observed, especially in the South Pole region, causing an increase in the intensity of ultraviolet radiation, the excess of which is dangerous for natural (aquatic and terrestrial) ecosystems and may have a negative impact on human health (increased number of skin cancer events, eye diseases, weakening of the immune system).

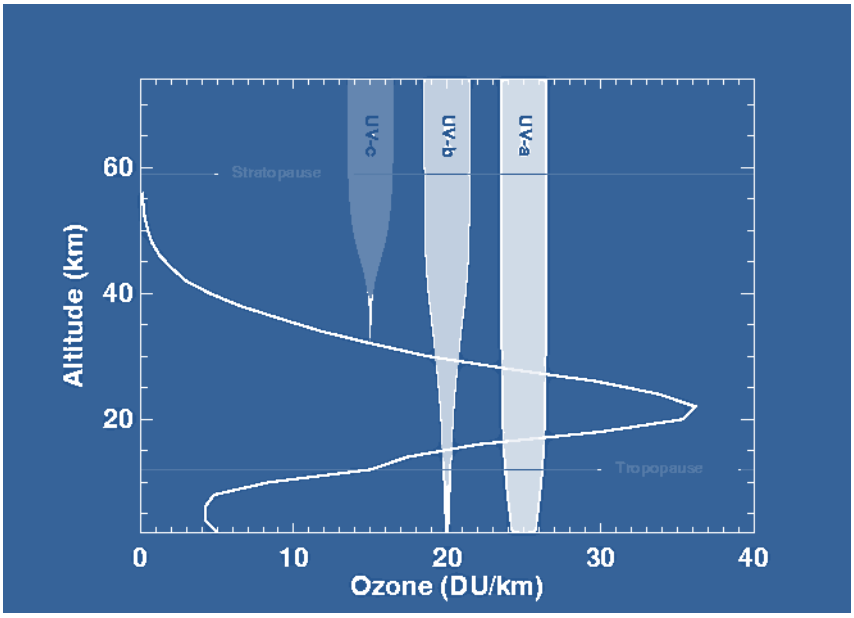

Fig. 1. Vertical profile of ozone content in the atmosphere typical of moderate latitudes (source: https://espo.nasa.gov/solve/content/SOLVE_Science_Overview).

The part of the ozone layer that is present in the troposphere and at the earth's surface, provided that the ozone concentration is high, becomes a toxic air pollution. Especially in the case of ground-level ozone, the main problem is the increase in its concentration observed throughout the 20th century and the occurrence of episodes of high ozone levels dangerous for human health (e.g. eye irritation, coughing, worsening of asthma symptoms), plant condition (e.g. destructive changes in photosynthesis, transpiration) and strength of some materials (e.g. textile; artificial, e.g., rubber or plastic; and organic, e.g., limestone).

The lifetime of an ozone molecule depends on the effectiveness of ozone destruction processes by chemical means or as a result of dry deposition. According to Stevenson et al. (2006), the average lifetime of an ozone molecule in the troposphere is about 22 (± 2) days. This value is not constant and changes depending on the height above sea level: from about 1−2 days in the boundary layer of the atmosphere to several weeks in the upper troposphere. Due to its relatively long lifetime, the ozone molecule can be transported over considerable distances, affecting the ozone budget in places far away from the source area.

Despite its low concentration, ozone found in the ground layer of the atmosphere plays a number of important roles therein:

- ozone is an important greenhouse gas with radiative forcing of 0.40 ± 0.20 W/m^2 (IPCC 2013);
- ozone is the main (next to PAN, NO_x, VOC) component of photochemical smog (The Royal Society 2008);
- the ozone photolysis process is the main source of hydroxyl (OH) radicals in the atmosphere (Guicherit and Roemer 2000).

The ozone occurring in the ground layer of the atmosphere is formed as a result of a series of chemical reactions, including, in particular, volatile organic compounds (VOCs) and nitrogen oxides (NO_x) under the influence of UV radiation (Logan 1985; Aneja et al. 1994; Ordóñez et al. 2005). Due to the non-linear nature of the processes leading to the formation of ozone, the reduction of precursor emissions need not be proportional to the decrease in ground-level ozone. In addition, meteorological conditions in a given area have a very significant impact on the ozone concentration. Another natural source of ozone in the troposphere is the transport of

ozone-rich air from the stratosphere (Stohl et al. 2003). Initially, it was believed that this transport, i.e., the intrusion of stratospheric air into the troposphere, was the dominant source of ozone in the troposphere (Fabian and Pruchniewicz 1977; Viezee et al. 1982). It was not until the early 1970s that the evidence was found ascertaining that the ozone concentration in the troposphere is mainly due to photochemical processes leading to the formation of ozone in situ in the troposphere itself (Fishman and Crutzen 1977, 1978).

The share of the above-mentioned sources in shaping the ozone concentration level varies spatially and temporally throughout the year (Moore et al. 2009). Ozone production as a result of chemical reactions is of great importance in urbanized and industrialized areas where the emission of primary air pollutants is relatively high. Ozone levels in such areas are characterized by the presence of an extensive summer ozone maximum resulting from the significant share of photochemical production during the period of optimum meteorological conditions (high air temperature, intense sunlight). In turn, the transport of ozone-rich stratospheric air masses to the lower troposphere is sometimes so intense and reaches so deep that it is reflected in the high concentrations of ozone recorded at ground stations (Davies and Schuepbach 1994). Therefore, in high mountain regions, areas are found where the direct impact of stratospheric intrusions is undoubtful (Stohl et al. 2003). The seasonal distribution of ozone content characteristic of areas under the dominant influence of stratospheric intrusion usually shows a maximum in the spring (Logan 1985).

1.3 Time-space variability of ground-level ozone on a global scale

In the period covering the second half of the 19th century and the beginning of the 20th century, ground-level ozone was of great interest to scientists. In the second half of the nineteenth century, there were already about 300 observation points, where measurements of ozone concentration in the air were carried out by the commonly used method. the Schönbein test-papers (detailed description of the method: Bojkov 1986); unfortunately, it was only in a few places that the measurements were carried out systematically over at least several years (Bojkov 1986).

One of the longest quantitative series of ground-level ozone measurements at the above-mentioned period was made in the years 1871−1910 at the Montsouris Meteorological Observatory near Paris by Albert Levy. The average annual ozone content measured was about 10 ppb and ranged from 5 to 15 ppb (Volz and Kley 1988). This is the only known ozone measurement series prior to the industrial age made simultaneously using the qualitative Schönbein method and the quantitative chemical method using the oxidation process of the arsenite compound to arsenate.

Another long-term measurement series using the Schönbein method was also made in France (Pic du Midi peak, Pyrenees, 3000 m) (Marenco et al. 1994) in the years 1874−1909. The results indicate that in the period 1874−1895 the average ozone content was around 10 ppb. The seasonal distribution was characterized by a clear spring maximum and winter minimum. From 1895 to the end of the measurement period, an increase in concentration to about 14 ppb was observed, in contrast to the measurement series from Montsouris, in which a decrease in ozone content was noted at that time. The long-term increase in ozone concentrations in the Pic du Midi series can be explained by the simultaneous global increase in methane concentration in the atmosphere, while the corresponding decrease in the ozone concentrations in the Montsouris series by the simultaneous increase in nitric oxide emissions in Paris and, as a result, the intensification of the ozone destruction process according to the reaction: $NO + O_3 \rightarrow NO_2 + O_2$.

In Poland, the first systematic measurements of ground-level ozone were made by Daniel Wierzbicki at the Meteorological Observatory in Kraków. Observations using Schönbein test-papers were carried out in 1854−1878. The average value of ozone concentration over the years

1869−1878 was about 17 ppb, changing within 11−24 ppb. Seasonal variability was characterized by a clear spring maximum and minimum in the autumn-winter period (Pawlak and Jarosławski 2014).

In the 1930s, a ground-level ozone measurement series was made in Arosa (Switzerland), according to which it can be stated that the average annual ozone concentration at that time was about 20 ppb and was close to the ozone concentration measured in Arosa in the 1950s (Staehelin et al. 1994).

As a result of industrial development, atmospheric air quality has started to deteriorate significantly since the early 1950s. Over the years 1950−1990, there was a considerable increase in ozone precursor emissions (NO_x, NMVOC, CH_4, CO) on a global scale, mainly as a result of the development of the fuel and energy industry, agriculture and the intensification of biomass burning. In the case of CO and CH_4 (calculated per carbon), a 1.8-fold increase in concentration was noted; in the case of NMVOC (non-methane volatile organic compounds), there was a 3-fold increase; and in the case of NO_x (calculated per nitrogen), the concentration increased 2.5-fold, the responsible factor being, in particular, the energy sector, mainly the burning of fossil fuels and the development of road transport (van Aardenne et al. 2001).

The longest continuous ground-level ozone measurement series in Central Europe, representative of non-urban conditions, has been performed in Hohenpeisenberg (Germany) since 1971. An analysis of the over 35-year measurement series showed an upward trend in ozone content of 0.31 ± 0.09 ppb/year (Gilge et al. 2010).

Many other stations conducting systematic ozone measurements around the world recorded an upward trend in ground-level ozone concentration in the years 1956−2002, ranging from 0.06 to 2.6% per year, with the highest values in Japan and Europe. It should be added that at most stations the trend varied over time. From the beginning of the measurements until the mid-eighties, a continuous, intensive increase in ozone concentrations was observed, followed by stabilization or continuation of growth, but at a much lower speed (Vingarzan 2004, and the literature therein). This was probably caused by a decrease in NO_x emissions in Europe and North America and a decrease in CO concentration on a global scale (Novelli et al. 2003).

The increase in ozone concentration at the earth's surface over the 100-year period since the beginning of measurements is quite certain, but there is some uncertainty as to the trend of ozone content in the last few decades. This is partly due to the limited number of stations representing real background conditions and partly due to difficulties in comparing data from different measuring periods (Vingarzan 2004). In the work of Logan et al. (2012), stations located at an altitude above 2 km were selected to analyze changes in ozone content over the years 1978−2009 in order to exclude places dominated by the influence of local pollutants and places under the influence of a strong vertical gradient of ozone concentrations, which usually occurs in the layer from the earth's surface to approximately 1 km in height. Based on data from three high mountain stations (Zugspitze 2962 m, Jungfraujoch 3580 m, Sonnblick 3106 m), in the years 1978−2000, an average increase in ozone concentration was noted, amounting to about 15 ppb in winter, spring and summer and to about 11 ppb in autumn, with over 70% increase before 1990. The reasons for the above ozone content distribution can be sought in a change of emission of basic ozone precursors, i.e., NO_x. A slower increase in ozone content occurred simultaneously with a decrease in NO_x content, i.e., since the 1990s (Vestreng et al. 2009; Logan et al. 2012). Also, a rapid increase in the concentration of CH_4 on a global scale, especially since the mid-twentieth century, has significantly slowed down in the late 1990s (Dlugokencky et al. 2011). The CO content has also been on a downward trend since the beginning of the 1990s. In the period 1991–2001, the global average CO content decreased by 0.52 ± 0.10 ppb/year, while in the Northern Hemisphere the decrease was 0.92 ± 0.15 ppb/year (Novelli et al. 2003).

In the paper by Cooper et al. (2014), a review was made of the variability of ground-level ozone content in 2005−2010 depending on the geographical location (latitude and longitude) and altitude. The analysis was based on 20 regional background stations. The results indicate that the lowest ozone concentration values occur within the marine boundary layer in the tropical southern hemisphere (13−14 ppb), and then also within the marine boundary layer in the mid-latitudes of the southern hemisphere (24−26 ppb), as well as in high latitudes of the southern hemisphere (26−27 ppb). Areas within the maritime border zone located at the mid-latitudes of the northern hemisphere are characterized by higher ozone content and values ranging from 28 ppb (Germany) to 49 ppb (Japan). Similarly, high-mountain stations in the northern hemisphere have a higher ozone concentration than those in the southern hemisphere (40−60 ppb). The lowest ozone concentrations at such stations are recorded in the tropical zone and amount to 38−46 ppb, while the highest are on the west coast of Japan (50−59 ppb). It can be noticed that for the stations located in the maritime boundary layer as well as for the high-mountain ones, the highest ozone concentration values occur in the western part of Japan, lying on the windward side on the east of the Asian continent, i.e., the area where the emission of ozone precursor pollutants has been increasing systematically since 1980 (Lee et al. 2014).

As mentioned earlier, spatial variability is reflected in changes in ozone concentration depending on the location of the measurement site defined by its latitude and longitude and also by its height above sea level. Numerous research experiments confirm the thesis about the increase of ozone content with increasing altitude (Moore and Semple 2005, 2009). Usually, the origin of high ozone concentrations lies in the flow of air masses from the stratosphere, although the share of pollutants supplied at high altitude through long-distance transport from areas below is also important (Semple and Moore 2008; Bonasoni et al. 2008). In addition, ozone destruction processes at large altitudes, both those associated with dry deposition and those associated with chemical destruction are significantly reduced. The assessment of the impact of altitude on ozone concentration conducted for 27 European stations located at different altitudes (115−3500 m a.s.l) has shown that the mean ozone concentrations range from 25 to 53 ppb for the stations located at highest and lowest altitudes, respectively. The annual variation of ozone content at high mountain stations shows a clear minimum in the autumn and winter (November−January), reaching about 40−45 ppb and a spring maximum (April) with values of about 60−70 ppb. Sometimes there is a certain deviation from the pattern presented above, observed especially during episodes of high ozone concentrations at low altitudes, e.g., during intense hot-weather waves. Then, the transport of polluted air upwards causes an increase of the monthly average ozone concentrations even in the June−September period, which in combination with high concentrations during spring results in the occurrence of a wide spring-summer ozone maximum (Chevalier et al. 2007). The daily variation of ozone content at high-mountain stations is usually characterized by the lack of variability of ozone concentrations during the day, in contrast to stations located at lower altitudes where a clear maximum is usually recorded in the afternoon and the minimum occurs just before sunrise. However, if slight changes in the distribution of ozone concentrations during the day happen to occur, the opposite situation can often be observed, characterized by higher ozone content during the night than that during the day (Zaveri et al. 1995; Aneja et al. 1994; Naja et al. 2003). According to Aneja et al. (1994), the occurrence of this type of anomaly can be explained by the vertical transport mechanism associated with daily variation in the mixing layer height.

1.4 Aim and scope of the work

This work presents a detailed analysis of the variability of ozone content in the ground layer of the atmosphere in the Mazowieckie Voivodeship over the years 2005−2012. The analysis was

made on the basis of measurements at six monitoring stations (Fig. 2), representing various kinds of the environment:

- Belsk-IG PAN (Belsk): regional background station, located in a rural area, in the Modrzewina Nature Reserve, approx. 60 km south of Warsaw;
- Granica: regional background station, located in a rural area, in the Kampinos National Park, approx. 50 km west of Warsaw;
- Legionowo (Legionowo-Zegrzyńska): urban background station, located in the natural zone, in the eastern part of the town;
- Radom (Radom-Tochtermana): urban background station, located in the shopping and residential zone, in the central part of the city;
- Warszawa-Ursynów (Warsaw Ursynów): urban background station located in the shopping and housing zone in the south part of the city;
- Warszawa-Krucza (Warsaw Krucza): urban background station (heavy traffic) located in the central part of the city.

Recording of air gaseous pollutants as well as meteorological parameters at these stations takes place within the framework of the voivodeship air quality monitoring system. Five of the six stations included in the analysis (Warszawa-Krucza, Warszawa-Ursynów, Radom-Tochterman, Legionowo-Zegrzyńska, Granica) belong to the Regional Inspectorate of Environmental Protection in Warsaw, while the station Belsk-IG PAN belongs to the Institute of Geophysics, Polish Academy of Sciences.

The aim of the study was to answer the following questions:

- What are the physico-chemical processes that decisively determine the ozone content in the ground layer of the atmosphere?
- How do meteorological parameters affect the ozone content in the ground layer of the atmosphere and how does this relation change over the years?
- What was the variability pattern of ground-level ozone in the Mazowieckie Voivodeship in 2005−2012 in various time scales (annual, seasonal, weekly and daily) depending on the type of measuring station?
- What was the variability of ground-level ozone content at the Belsk regional background station in the period 1995−2016?
- Is it possible to construct an effective predictive model of ground-level ozone for the next day using artificial neural networks, based on several basic predictors, that would be able to generate the forecast with an accuracy equivalent to the accuracy attainable by the latest-generation global troposphere chemistry model?

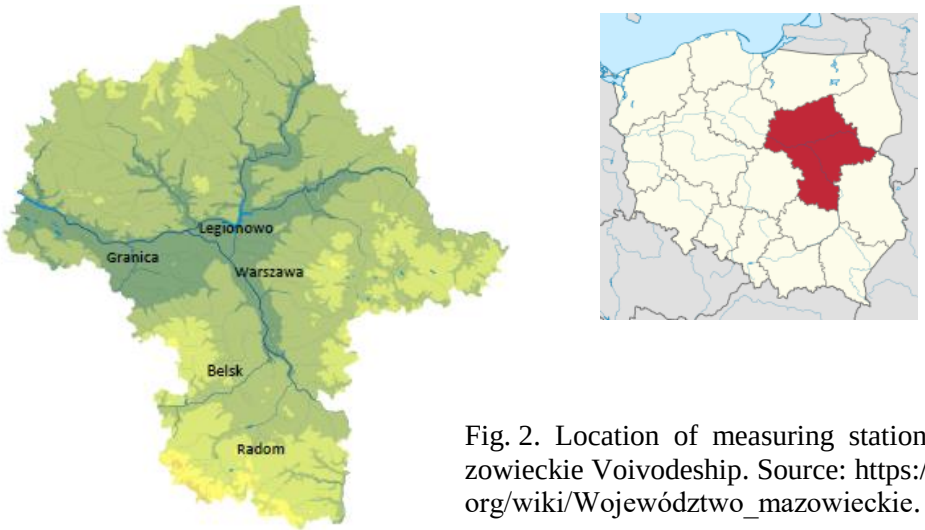

Fig. 2. Location of measuring stations in the Mazowieckie Voivodeship. Source: https://pl.wikipedia.org/wiki/Województwo_mazowieckie.

This book consists of two parts: The first part, covering Chapters 1 to 4, contains a description of the processes determining the ozone content in the ground layer of the atmosphere, as well as the results of statistical analysis regarding the variability of ozone concentration in the Mazowieckie Voivodeship in 2005−2012 at various time scales. In addition, this part gives the results of statistical analysis of the impact of selected meteorological parameters on the ground-level ozone content. These results were then applied for developing the ozone concentration prognostic models based on artificial neural networks.

The second part, covering Chapters 5 to 7, is a presentation of the results obtained using neural network models and their interpretation for selected measurement sites, as well as a comparative analysis of the obtained modeling with the forecasts produced by the global troposphere chemistry model for the same sites.

Chapter 1 presents basic information about ground-level ozone, the history of ozone discovery, and discusses the time-space variability of ground-level ozone on a global scale.

Chapter 2 presents the basic physical-chemical processes affecting the ground-level ozone content.

Chapter 3 presents the analysis of the variability of ground-level ozone at selected stations of the Mazowieckie Voivodeship in the years 2005−2012 in various time scales. It also describes the long-term pattern of ground-level ozone content variability at the Belsk station in the period 1995−2016.

Chapter 4 shows an analysis of the impact of selected meteorological parameters (air temperature, solar radiation, relative humidity and wind speed) on the ozone content in the ground layer of the atmosphere.

Chapters 5 and 6 present the features of artificial neural networks as a tool for developing the ground-level ozone forecasts, and the ground-level ozone forecasting models based on neural networks.

In Chapter 7, the ground-level ozone forecasts for the next day over the period from April to September 2014 were made, using neural networks based on the 2015 data. Having at our disposal the ground-level ozone forecasts for 2014, the accuracy of results obtained by neural models was compared to those obtained from the global tropospheric chemistry model. Based on the comparative analysis, the accuracy was evaluated of the neural model forecasts *versus* that of the latest-generation global pollution forecast model.

2. PROCESSES ESTABLISHING THE OZONE CONTENT IN THE GROUND LAYER OF THE ATMOSPHERE

The ozone content in the ground layer of the atmosphere depends on a number of physico-chemical processes responsible for its formation, transport and destruction (Cape 2008).

Chemical processes determining the ozone content of the ground layer of the atmosphere include a series of cycles of chemical reactions leading to the production or destruction of ozone. Physical processes affecting the value of ground-level ozone are primarily the processes of dry deposition of ozone on the ground and air mass transport processes.

2.1 Chemical processes

2.1.1 Chemical reaction cycles producing the ground-level ozone

In the troposphere and at the surface of the earth, the production of ozone requires the presence of oxygen atoms, whose source is the photodissociation reaction of nitrogen dioxide:

$$\mathrm{NO_2} + h\nu\ (\lambda < 424\ \mathrm{nm}) \rightarrow \mathrm{NO} + \mathrm{O}\,. \tag{1}$$

The newly formed oxygen atom, joining an oxygen molecule in the presence of an additional molecule (M, which is usually an oxygen or nitrogen molecule), leads to the formation of an ozone molecule (Eq. 2). Thus far, this is the only known method of ozone production in the surface layer of the atmosphere:

$$O + O_2 + M \rightarrow O_3 + M\,. \tag{2}$$

In turn, nitric oxide reacts quickly with ozone to reproduce nitrogen dioxide and oxygen:

$$NO + O_3 \rightarrow NO_2 + O_2\,. \tag{3}$$

The reaction cycle (1−3) discussed above is relatively fast and leads to a certain constant level of overground ozone, depending on the initial concentration of NO, NO_2, O_3 and the intensity of UV radiation. The process represented by reaction (3) is called the titration reaction between NO and O_3. Each NO molecule is responsible for removing one O_3 molecule, thus preventing the accumulation of ozone (Chou et al. 2006).

As can be seen from the above, the net ozone production can only occur when the nitric oxide molecule is converted to the nitrogen dioxide molecule without a loss of the ozone molecule. When free radicals are present in the troposphere, nitric oxide also reacts with them, contributing to an increase in nitrogen dioxide content without removing ozone, and as a result leading to an increase in ozone concentration:

$$RO_2 + NO \rightarrow RO + NO_2\,. \tag{4}$$

The production of free radicals is a result of oxidation of, e.g., volatile organic compounds (VOC) and carbon monoxide. The simplest reaction cycle leading to the formation of free radicals and, consequently, ozone is the carbon monoxide (CO) cycle, which reacts with a hydroxyl radical (OH) to form a carbon dioxide molecule and a hydrogen atom

$$CO + OH \rightarrow CO_2 + H\,. \tag{5}$$

The hydrogen atom reacts immediately with the oxygen molecule in the presence of a third molecule (M) which absorbs the excess energy:

$$H + O_2 + M \rightarrow HO_2 + M\,. \tag{6}$$

If the troposphere contains a sufficiently large amount of nitrogen oxides (NO > 10 ppt), the newly formed hydroperoxide (HO_2) quickly reacts with them, resulting in the formation of nitrogen dioxide:

$$HO_2 + NO \rightarrow OH + NO_2 \tag{7}$$

At this moment there occurs the process that plays the key role in the whole cycle, i.e., the photodissociation of nitrogen dioxide, giving rise to the formation of atomic oxygen and the reconstitution of nitric oxide:

$$NO_2 + h\nu\ (\lambda < 424\ \text{nm}) \rightarrow NO + O\,. \tag{1, repeated}$$

The final stage of the cycle is the production of an ozone molecule:

$$O + O_2 + M \rightarrow O_3 + M\,. \qquad \text{(2), repeated}$$

The net effect of the above series of reactions is as follows:

$$CO + 2O_2 + h\nu \rightarrow CO_2 + O_3\,. \qquad (8)$$

As mentioned above, reaction (7) only occurs when the nitrogen oxides (NO) are sufficiently numerous. When their concentration is low, reaction (7) competes with the following reaction (9):

$$HO_2 + O_3 \rightarrow OH + 2O_2\,. \qquad (9)$$

Of great importance is the speed of individual reactions. Reaction (7) is much faster than reaction (9), which, provided that the number of nitrogen oxides is sufficient, guarantees chemical processes leading to ozone production.

Similar to reactions for carbon monoxide (CO) molecule, analogous cycles take place with the participation of volatile organic compounds (VOCs), including, e.g., methane (CH_4), present in the atmosphere in the highest concentration among all hydrocarbons (vanLoon and Duffy 2008).

The methane oxidation process is important in shaping ozone concentrations in the lower troposphere because almost 1/4 of the hydroxyl radicals react with methane, thus evoking several reaction chains resulting in either the production or destruction of ozone. Likewise in the case of carbon monoxide, the number of available nitrogen oxides plays a key role (Crutzen and Zimmermann 1991). Provided that the NO_x content is sufficiently high, the following reaction cycle occurs, initiated by a hydroxyl radical and a methane molecule:

$$CH_4 + OH \rightarrow CH_3 + H_2O\,. \qquad (10)$$

As a result, a methyl radical (CH_3) is formed, which reacts very quickly with oxygen to form a methyl peroxy radical according to the following formula:

$$CH_3 + O_2 + M \rightarrow CH_3O_2 + M\,. \qquad (11)$$

If the concentration of nitrogen oxides is sufficiently high, the newly formed CH_3O_2 radical reacts with nitric oxide to form nitrogen dioxide, which is key to the ozone formation:

$$CH_3O_2 + NO \rightarrow CH_3O + NO_2\,. \qquad (12)$$

The methoxy radical thus formed, in reaction with oxygen, creates a hydroperoxide radical (the following Eq. (13)), which in a subsequent reaction with nitric oxide contributes to the formation of nitrogen dioxide (rewritten Eq. (7)):

$$CH_3O + O_2 \rightarrow CH_2O + HO_2\,. \qquad (13)$$

During the cycle, two nitrogen dioxide molecules are formed, which subsequently, as a result of the photodissociation process, form oxygen atoms (Eq. (1)) necessary for ozone formation (Eq. (2)):

$$NO_2 + h\nu\ (\lambda < 424\ \text{nm}) \rightarrow NO + O\,, \qquad \text{(1), repeated}$$

$$O + O_2 + M \rightarrow O_3 + M\,. \qquad \text{(2), repeated}$$

Net equation:

$$CH_4 + 4O_2 \rightarrow CH_2O + H_2O + 2O_3\,. \qquad (14)$$

As a result of the above cycle, two ozone molecules are formed from one molecule of methane. In an environment where the amount of NO_x is small, the following methane reaction cycle with the participation of methane takes place:

$$CH_4 + OH \rightarrow CH_3 + H_2O\,, \qquad \text{(10), repeated}$$

$$CH_3 + O_2 + M \rightarrow CH_3O_2 + M\,, \qquad \text{(11), repeated}$$

$$CH_3O_2 + HO_2 \rightarrow CH_3O_2H + O_2\,, \qquad (15)$$

$$CH_3O_2H + h\nu\ (\lambda < 330\ \text{nm}) \rightarrow CH_3O + OH\,, \qquad (16)$$

$$CH_3O + O_2 \rightarrow CH_2O + HO_2\,. \qquad \text{(13), repeated}$$

Net equation:

$$CH_4 + O_2 \rightarrow CH_2O + H_2O\,. \qquad (17)$$

In the above chain, reaction (16) may sometimes be substituted by a reaction of the form (18):

$$CH_3O_2H + OH \rightarrow CH_2O + H_2O + OH\,. \qquad (18)$$

Then the net effect of the above cycle is as follows:

$$CH_4 + OH + HO_2 \rightarrow CH_2O + 2H_2O\,. \qquad (19)$$

As follows from this reasoning, the lack of nitrogen oxides in the above reactions results in the absence of nitrogen dioxide and thus of ozone. In both cases, the final effect is the creation of formaldehyde (CH_2O), the first main product for the oxidation of methane, which can stay in the atmosphere even for 1.5 days. Formaldehyde undergoes further reactions: with hydroxyl radicals (OH) or photolysis ($\lambda < 350$ nm), which produce hydroperoxide radicals and carbon monoxide.

In the oxidation cycles of carbon monoxide as well as methane, the ozone production process critically depends on the concentration of nitrogen oxides in the atmosphere. It is only with a sufficient amount of NOx that the oxidation cycles discussed above ultimately give raise to an ozone molecule. In the opposite situation, hydroxyl and hydroperoxide radicals are removed from the atmosphere, delaying ozone formation.

2.1.2 Chemical reactions leading to ozone destruction at the earth's surface

The mechanism of photochemical destruction of an ozone molecule depends on the wavelength of solar radiation causing its decay. At a wavelength greater than 310 nm, there occurs the ozone photolysis, resulting in the formation of an oxygen atom in the ground state:

$$O_3 + h\nu\ (\lambda > 310\ \text{nm}) \rightarrow O(^3P) + O_2\,, \qquad (20)$$

which subsequently, by joining the molecular oxygen, reproduces the ozone molecule:

$$O(^3P) + O_2 + M \rightarrow O_3 + M\,. \tag{21}$$

If the wavelength is shorter than 310 nm, the photodissociation of ozone leads to the formation of oxygen atoms in the excited state:

$$O_3 + h\nu\ (\lambda < 310\ \text{nm}) \rightarrow O(^1D) + O_2\,. \tag{22}$$

Part of these atoms, due to reaction with an oxygen or nitrogen particle, quickly transform to the ground state, while part of it react with a water vapor molecule to become a source of hydroxyl (OH) radicals:

$$O(^1D) + H_2O \rightarrow 2OH\,. \tag{23}$$

The reactions presented in the previous section:

$$NO + O_3 \rightarrow NO_2 + O_2\,, \tag{3}, \text{repeated}$$

$$CO + OH \rightarrow CO_2 + H\,, \tag{5}, \text{repeated}$$

$$H + O_2 + M \rightarrow HO_2 + M\,, \tag{6}, \text{repeated}$$

$$HO_2 + O_3 \rightarrow OH + 2O_2\,, \tag{9}, \text{repeated}$$

together with the ozone photolysis process, form a cycle of chemical reactions leading to the destruction of ozone in the ground layer of the atmosphere.

2.1.3 The role of NOx and VOC in the formation of ground-level ozone

Ozone formed in the ground layer of the atmosphere as a result of photochemical processes shows a non-linear dependence on the concentration of its precursors (Atkinson 2000). Sometimes, the ozone process depends on NO_x only, being almost independent of VOC, while in other cases its effectiveness increases with increasing VOC and does not depend on the concentration of NO_x. Of equal importance as the very presence of VOC and NO_x is their quantitative ratio (Finlayson-Pitts and Pitts 1993).

When the production of radicals in the troposphere keeps to be at a high level, the course of chemical reactions depends on the concentration of nitrogen oxides therein. At a high concentration of nitrogen oxides, there occurs a reaction that enhances the concentration of nitrogen dioxide and, consequently, also ozone:

$$HO_2 + NO \rightarrow OH + NO_2 \tag{7}, \text{repeated}$$

$$NO_2 + h\nu\ (\lambda < 424\ \text{nm}) \rightarrow NO + O\,. \tag{1}, \text{repeated}$$

$$O + O_2 + M \rightarrow O_3 + M\,. \tag{2}, \text{repeated}$$

When the concentration of nitrogen oxides is low, it is the reaction leading to ozone destruction that turns out to be dominant:

$$HO_2 + O_3 \rightarrow OH + 2O_2\,, \tag{9}, \text{repeated}$$

When we are dealing with a state of a very high NO_x emission in the troposphere, the amount of radicals is not sufficient to react with all nitric oxide molecules. Then along with the reaction:

$$OH + NO_2 + M \rightarrow HNO_3 + M, \tag{24}$$

there appears the reaction of ozone removal from the atmosphere:

$$O_3 + NO \rightarrow NO_2 + O_2. \tag{3}, \text{repeated}$$

The process of ozone removal by nitric oxide is particularly effective at night, when the ozone production process vanishes and, due to the continuous NO_x emission, the ozone destruction reaction becomes the dominant one. Similarly, in winter, when ozone production is much slowed down, low ozone concentrations occur in many contaminated areas (Parrish et al. 1991). Moreover, when NO_x emissions prevail over the production of radicals, atmospheric purification processes that occur through the oxidation of compounds such as CO or HCHO are significantly reduced.

As can be seen from the above, an increase in VOC content usually means an increase in ozone concentration, whereas an increase in NO_x can lead to either an increase or a decrease in ozone, depending on the VOC/NO_x ratio. With a certain amount of VOC in the air, the optimal NO_x content ensures maximum ozone concentration in the ground layer of the atmosphere. The dependence of ozone production on the value of VOC and NO_x concentrations is illustrated in Fig. 3, showing ozone isoplets as a function of VOC and NO_x concentration. The graph shows the non-linearity of ozone formation in relation to the content of VOC and NO_x in the air. When the NO_x content is low (VOC saturated regime), the likelihood of ozone formation increases with increasing NO_x and almost does not depend on the VOC content. When the NO_x content is high (NO_x saturated regime), the likelihood of ozone production increases with decreasing NO_x and increasing VOC (Sillman 1999).

To illustrate the relationships discussed above, Fig. 3 presents 3 points representing different concentrations of the studied components. Point 1 can be treated as the initial situation characterizing the area with high VOC concentration and low NO_x concentration. A significant

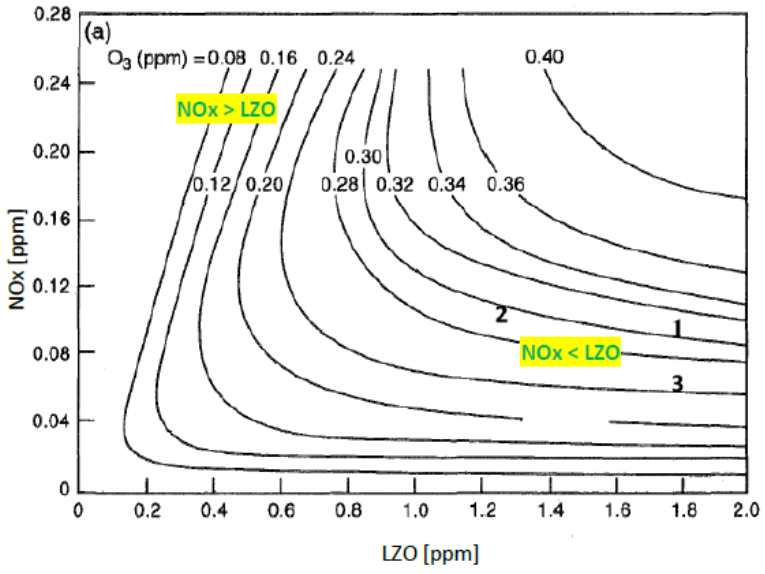

Fig. 3. Maximum ozone isoplet values for given NOx and VOC concentrations obtained on the basis of the EKMA (Empirical Kinetic Modeling Approach) (source: Finlayson-Pitts and Pitts 1993, revised version).

reduction in VOC concentration causes a shift to Point 2. Despite the reduction of VOC emissions by almost 50%, we do not observe any significant changes in ozone concentration. On the other hand, a slight reduction in NO_x concentration causes a shift to Point 3, characterized by a significantly lower ozone content. Thus, in order to reduce the ozone concentrations it is necessary to make a skilful reduction of emission of basic ozone precursors, such as nitrogen oxides and volatile organic compounds, keeping in mind that the reduction of NO_x will be effective in places where VOC concentration dominates, while the reduction of VOC concentration will be effective in areas of NO_x dominance.

2.1.4 Ozone as a component of photochemical smog

Smog is defined as an episode of sudden and severe air pollution (Juda-Rezler 2006). The very term "smog", meaning a combination of smoke and fog, was first used at the beginning of the 20th century to describe the phenomenon of intense air pollution over London. Soot particles floating above the city and numerous impurities (sulfur dioxide, carbon monoxide, organic compounds, nitrogen dioxide), which are a result of burning coal, are called classic smog (as well as smog of London, black or winter-type).

Photochemical smog appeared in the 1940s in Los Angeles (Haagen-Smit 1952). It is characterized by the presence of high concentration of ozone and other oxidants (e.g., peroxide acetyl nitrate, PAN, hydrogen peroxid, H_2O_2). These substances, defined as secondary pollution, arise as a result of photochemical processes involving NMVOC (non-methane volatile organic compounds) and nitrogen oxides resulting from the combustion of liquid fuels, mainly in the transport sector.

In addition to the presence of an appropriate amount of nitrogen oxides and hydrocarbons, the following meteorological conditions are necessary for the creation of photochemical smog:

- high temperature to enhance the speed of some chemical reactions,
- intense solar radiation to initiate the photochemical processes,
- no wind (stationary atmosphere allows reagents to remain in place).

Intense photochemical smog episodes are often reported under conditions of temperature inversion in the boundary layer. The lack of convective movement limits the mixing of air components and is suitable for their retention over contaminated area (Rani et al. 2011). The longer the duration of thermal inversion, the higher the concentration of combustion products. According to Falkowska and Korzeniewski (1998), appropriate orographic conditions may extend the duration of photochemical smog up to several days.

The intensity of the photochemical smog also depends on the time of day. During the formation of Los Angeles-type smog, the concentrations of nitrogen oxides, hydrocarbons and oxidants formed during the day change significantly. A typical diurnal pattern of a photochemical smog production is shown in Fig. 4.

On the basis of this figure it is possible to trace the stages leading to the formation of photochemical smog:

- from the very early morning hours, the increase in traffic is associated with increasing concentration of hydrocarbons and nitric oxide,
- in the late morning there is an intense increase in the concentration of nitrogen dioxide caused by the conversion of primary NO to secondary NO_2,
- during the day, as solar radiation intensifies, the photochemical processes start to produce a decrease in concentrations of hydrocarbons and nitrogen dioxide. At the same time, there appears an increase in the concentration of oxidants (including ozone and PAN) and aldehydes, which reach their maximum values in the afternoon,
- after the sunset, when photochemical processes vanish, a decrease in the concentration of oxidants and aldehydes is observed, lasting over the night.

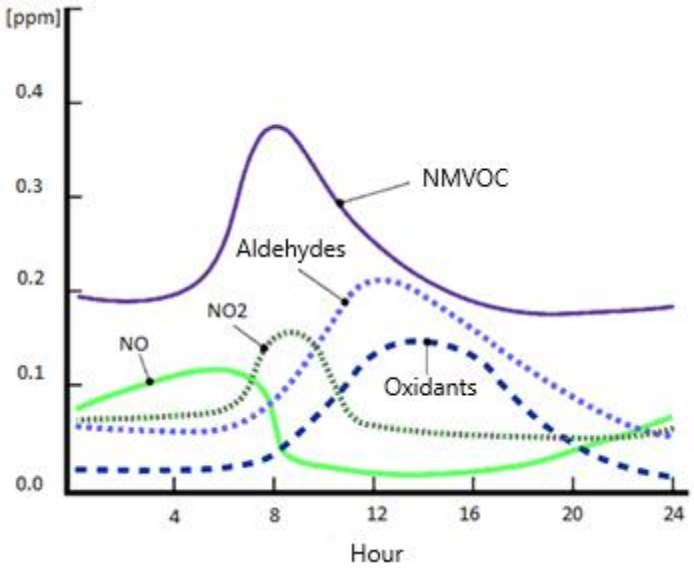

Fig. 4. The content of the main components of photochemical smog (source: http://mtweb.mtsu.edu/nchong/Smog-Atm1.htm; revised version).

As results from the above, during the photochemical smog the concentration of such chemicals as nitrogen oxides, hydrocarbons, ozone, PAN, other oxidants or aldehydes reach above their average values. This situation, depending on the prevailing meteorological and orographic conditions, may persist for more than ten days.

2.2 Physical processes

2.2.1 Dry deposition on the earth's surface

The mechanism of dry ozone deposition on the earth's surface is an important source of ozone removal from the ground layer of the atmosphere (Güsten et al. 1996). The effectiveness of this process depends on the concentration of ozone, the intensity of air turbulence, and the adsorption capacity of the surface (Seinfeld and Pandis 2006).

The process of dry deposition of gaseous pollutants consists of the three stages:

- transport of gas in the overground, turbulence layer (the greater the degree of atmospheric turbulence, the faster the transport of gas pollution to the earth's surface,
- gas transport in the sub-laminar layer very close to the earth's surface (determined by the molecular diffusion of gas),
- gas absorption by the receptor (determined by the ability of the surface substrate to absorb a given pollutant).

As stated by Juda-Rezler (2006), the speed of dry settlement depends on a number of factors, namely:

- physical and chemical characteristics of pollution,
- ground properties (e.g., soil moisture, type of ground cover, aerodynamic roughness of the substrate),
- parameters of vegetation covering the area (e.g., type of vegetation, ratio of the area covered by pollution-absorbing plants to the whole area, the degree of opening of stomata),
- meteorological conditions (e.g., humidity, wind speed, temperature).

From the study of Pio and Feliciano (1996) it follows that the key factor affecting the rate of dry ozone deposition is the degree of stomata opening. The analysis of continuous measurements made over a period of one year in the grassy area on the west coast of Portugal has shown

a clear variation in the rate of dry deposition during the day. Much higher values were recorded during the daytime (when as a result of absorption of solar radiation stomata are open) than at night. The authors also observed a clear seasonality in the dry deposition rate, consistent with the vegetative cycle. During the full vegetation period, the V_d[4] (dry deposition velocity [m/s]) values fluctuated within the range of 0.2−0.5 cm/s, while outside the vegetation period, when the stomatal activity is weaker, the values fell to 0.1 cm/s. Research carried out by Güsten et al. (1996) from March to April 1993 in the Libyan desert showed relatively low values of the dry deposition speed on a sand substrate in comparison to the deposition on an area covered with vegetation. The maximum V_d values recorded during the day were of about 0.20 cm/s, while the average V_d for the entire measuring period was 0.065 cm/s only. It can be concluded that the highest values of the speed of dry ozone deposition are in the forest, then go the grassy areas, the lowest values being in desert areas. It can be stated that higher V_d values occur in areas with adequate soil moisture, covered with vegetation characterized by high photosynthetic activity during the growing season, and lower V_d values are in areas devoid of vegetation and also in months that do not belong to the growing season in a given area.

2.2.2 Air transport from the stratosphere

Downward-moving stratospheric air masses can significantly affect ozone concentrations in the troposphere (Fabian and Pruchniewicz 1977) due to the relatively long lifetime of ozone molecules, which in the free troposphere may last as long as two months (Fishman et al. 1979).

The exchange of air masses between the stratosphere and the troposphere is part of global atmospheric circulation, including the air transport through the tropopause (Mohanakumar 2008). Global processes shaping the exchange between the lower stratosphere and the troposphere are controlled by the large-scale Brewer-Dobson circulation (Holton et al. 1995), which is responsible for transporting ozone and other air components from the equatorial areas towards the poles. This circulation is generated by waves formed in the troposphere, which then break (lose stability) in the stratosphere and induce the movement of air masses towards high latitudes as well as their flow towards the earth's surface (Tarasick and Slater 2008).

In medium latitudes, the ozone transport from the stratosphere is mainly governed by processes accompanying the phenomena of tropopause folding and cut-off lows (Mohanakumar 2008; Bonasoni et al. 2000).

The transport of stratospheric air occurs when the boundary area between the stratosphere and the troposphere is distorted and deviates from the natural horizontal position in the center of a jet stream. Intrusions of dry, ozone-rich air, characterized by high potential vorticity, move from the stratosphere to the troposphere. By using profiles of ozone concentration, potential vorticity as well as temperature, pressure and humidity, it is possible to identify the phenomenon of tropopause folding and the transfer of ozone formed in the stratosphere to the troposphere layer (Beekmann et al. 1997).

Stratospheric intrusions at an altitude of about 6−8 km a.s.l. are characterized by very high ozone concentrations, in the range of 240−400 ppb. At lower altitudes, the ozone concentration, as a result of mixing with ambient air, is in the range of 100−200 ppb (Johnson and Viezee 1981).

In the course of transport into the troposphere, the majority of stratospheric intrusions, which carry ozone-rich air masses, undergo intense mixing processes in the free troposphere, above 700 hPa (Viezze et al. 1983). Sometimes, when the intrusion moves down, it breaks into smaller and smaller fragments and, as a result, mixes with the surrounding air (Bithell et al. 1999). Phenomena of direct stratospheric air reaching the earth's surface are rarely recorded and may last up to several days (Hocking et al. 2007; Viezze et al. 1983).

The participation of stratospheric ozone in the formation of ozone content in the troposphere exhibits clear seasonality. Deep stratospheric intrusions most often occur in late winter (Stohl et al. 2003).

3. ANALYSIS OF TIME-SPACE VARIABILITY OF OZONE IN THE GROUND LAYER OF THE ATMOSPHERE IN THE MAZOWIECKIE VOIVODESHIP OVER THE YEARS 2005−2012

Ozone in the ground layer of the atmosphere is classified as a secondary air pollution due to the fact that it is not directly emitted into the atmosphere. Its concentration is a function of many factors, such as meteorological conditions, season of the year, atmospheric pollution of ozone precursors and the rate of photochemical reactions.

In order to get a full understanding of mechanisms affecting the concentration of ozone in the ground layer of the atmosphere in a given place and be able to make a prediction of concentration changes, one needs to have the results of systematic measurements on local and regional scales. It is necessary to register not only the concentrations of ozone, but also of the chemical compounds that are its precursors (VOC, NO_x, CO). Constant monitoring of meteorological parameters is equally important.

In this study, a thorough analysis of space-time variability of ground-level ozone content was based on data from six measuring stations (Warszawa-Krucza, Warszawa-Ursynów, Radom-Tochterman, Legionowo-Zegrzyńska, Belsk-IG PAN, Granica) over the period from January 2005 through December 2012.

The ground-layer ozone variability presented in this chapter is divided into 5 parts:

- changes in the years 2005−2012,
- annual changes,
- changes on a weekly scale,
- changes in the 24-hour scale.

This division was applied due to various mechanisms determining changes in ozone concentrations in different time scales.

In addition, long-term changes in ground-level ozone were presented based on a measurement series in Belsk in 1995−2016.

3.1 Variability of ozone concentration in the ground layer of the atmosphere over the years 2005−2012

Table 1 presents average annual ozone concentrations in the ground atmosphere layer in the period 2005−2012 at the six stations used for the analysis.

Table 1

Mean annual values of ozone concentration in the ground layer of the atmosphere

Year / Station	2005	2006	2007	2008	2009	2010	2011	2012	Mean
	[μg/m^3]								
Granica	51.3	52.9	50.6	49.5	46.1	49.9	50.0	48.7	49.9
Belsk	57.4	60.8	52.7	55.6	52.2	51.8	52.2	50.2	54.1
Legionowo	53.6	49.8	46.2	45.1	44.1	47.2	45.3	45.4	47.1
Warszawa-Ursynów	50.4	50.0	38.2	46.5	43.7	46.4	45.2	44.7	45.6
Warszawa-Krucza	42.4	41.9	38.5	41.6	41.1	42.6	41.0	40.6	41.2
Radom	43.1	44.9	46.0	43.9	42.6	38.7	48.8	43.5	43.9

Analyzing the above data, it can be concluded that the highest ozone content was recorded at regional background stations where the average annual ozone concentration values ranged from 50.2 to 60.8 μg/m^3 (Belsk) and from 46.1 to 52.9 μg/m^3 (Granica). Much lower concentrations were recorded at urban background stations, in particular at the Warszawa-Krucza station (values in the range from 38.5 to 42.6 μg/m^3).

At four out of six stations analyzed (Granica, Belsk, Legionowo, Warszawa-Ursynów) there is a noticeable downward trend in ground-level ozone concentration. The exceptions are the stations: Warszawa-Krucza and Radom, where the average annual values remain constant throughout the entire period under analysis.

3.2 Annual variability of ozone concentration in the ground layer of the atmosphere

The concentration of ozone in the ground layer of the atmosphere shows a clear variability throughout the year. Plots of average monthly values of ozone concentration in the ground layer of the atmosphere in 2005−2012 are presented in Fig. 5.

The annual variability of ozone content depends on many factors, to mention, in particular: (1) geographical location, (2) meteorological conditions, (3) proximity of potential sources of ozone precursors (Logan 1985), as well as the intensity of chemical processes, deposition processes and transport (both in horizontal and vertical directions) (Monks 2000).

A characteristic annual cycle of ozone concentrations was recorded at all stations analyzed, with the maximum in the spring and summer season and the minimum in the autumn and winter season. At the cites of the regional background (Granica, Belsk) the maximum ozone concentration was recorded in April, while in the cites of the urban background (especially Warszawa-Krucza and Radom) the maximum occurred in the period from April to July. Ozone maxima recorded in the spring and summer are primarily associated with increased photochemical production of ozone (Wang et al. 1998). In the autumn and winter months, when the efficiency of photochemical processes decreases, the concentration of ground-level ozone reaches minimum values in the yearly scale.

Analyzing the distribution of ozone concentrations in terms of the type of measuring station, the highest ozone values were recorded at regional background stations, Belsk and Granica, located in rural areas, at a significant distance from potential sources of pollution (Fig. 5). Maximum average values (2005−2012) for the above stations were recorded in April and amounted to 76.8 and 73.3 μg/m^3, respectively. The minimum values, of 27.1 and 24.4 μg/m^3, respec-

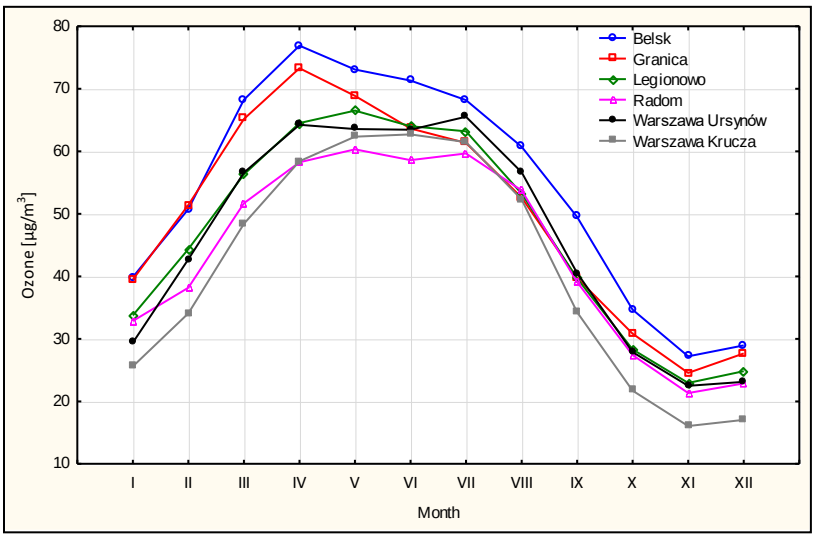

Fig. 5. The average annual variation of ozone concentration in the ground layer of the atmosphere in 2005−2012.

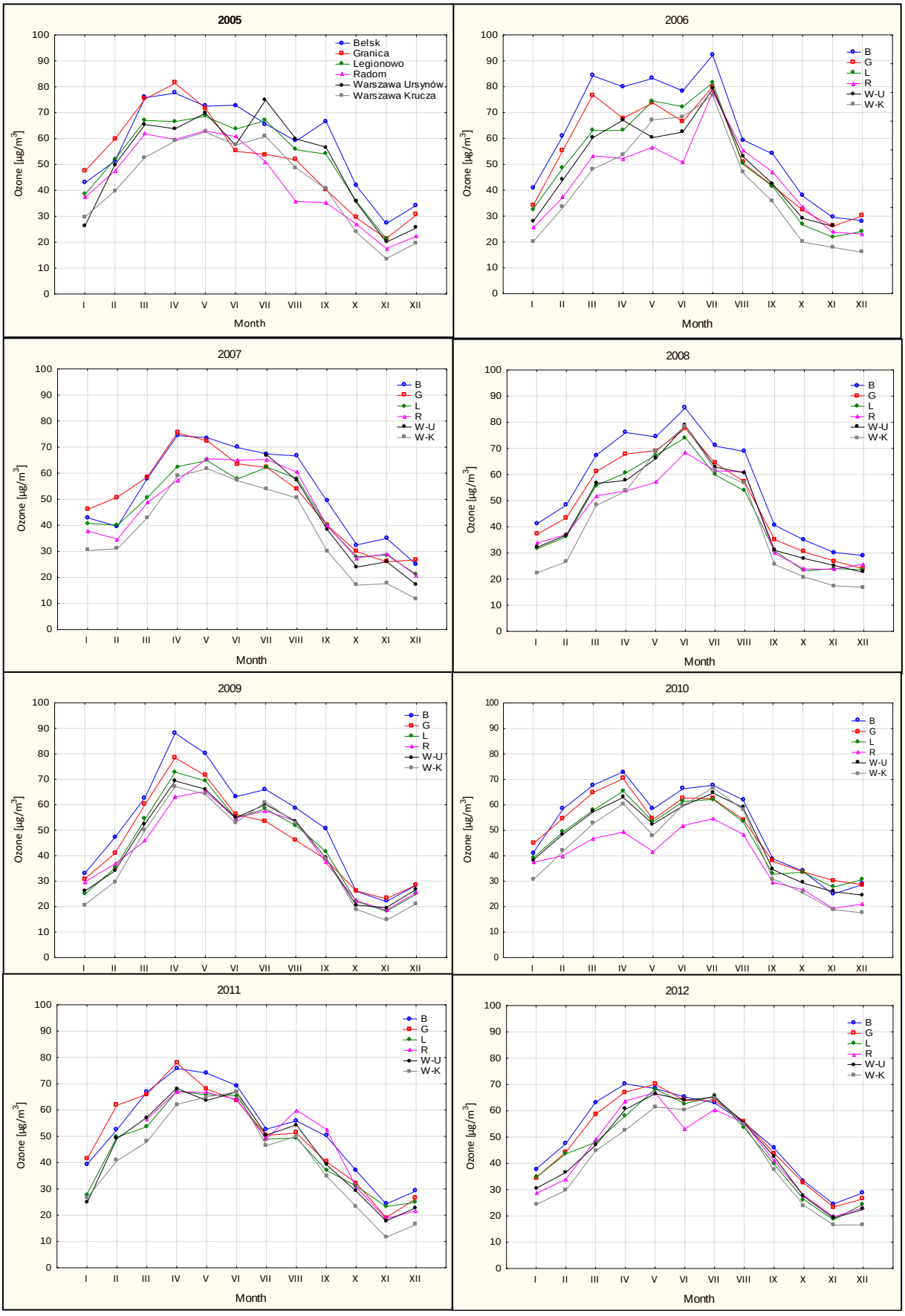

Fig. 6. The annual variations of ground-level ozone in the years 2005−2012.

tively, were observed in November. Much higher ozone concentrations found at regional background stations, as compared to those at other stations, are due to a limited number of mechanisms leading to ozone destruction in areas located away from urban agglomerations (Saitanis 2003). First of all, it is the lack of intensive NO emission that limits the processes of ozone destruction as a result of the reaction $NO + O_3 \rightarrow NO_2 + O_2$. Relatively low ozone concentrations were recorded at urban background stations where the maximum values observed from May through July ranged from 60.3 $\mu g/m^3$ (Radom) to 66.5 $\mu g/m^3$ (Legionowo) (Fig. 5; Table 1). Minimum values at all the stations were recorded in November and ranged from 16.2 $\mu g/m^3$ (Warszawa-Krucza) to 22.8 $\mu g/m^3$ (Legionowo). A significant diversity of ozone content depending on the location of the measuring station points to a strong impact of local conditions in shaping ozone concentrations.

Figure 6 presents average monthly values of ground-level ozone concentrations for all the stations in each year covered by the analysis (2005−2012). In most cases, the high ozone concentrations were recorded in April, constituting the yearly maximum in 2007, 2009, 2011, and 2012. In the years 2006 and 2010 there was a double maximum, occurring in March and July, as well as April and July, respectively. The year 2008 was different from the others included in the analysis, since the maximum ozone concentration was recorded at all the stations in June. This was due to the exceptionally favorable weather conditions in this month (high temperature, intense solar radiation, no wind).

Due to the multiplicity of factors determining the variability of ozone content, significantly different concentrations may be recorded at two stations in the same city, where the meteorological conditions are, of course, very similar. In this work, such examples are the stations Warszawa-Krucza and Warszawa-Ursynów. In this case, the impact of the location (and the resulting different concentration levels of ozone precursors NO_x, VOC, and CO) of the measuring station on the ground-level ozone concentration is significant (Fig. 6). Each month (2005−2012 average), the ozone content at the Warszawa-Ursynów station was higher than at the Warszawa-Krucza station. The differences ranged from 0.8 $\mu g/m^3$ (June) to 8.8 $\mu g/m^3$ (February) with the average difference for 2005−2012 being 5.1 $\mu g/m^3$. The maximum differences were even in excess of 16 $\mu g/m^3$ (September 2006). Only in 12% of cases the average monthly ozone content recorded at Warszawa-Ursynów was lower than at Warszawa-Krucza, and the differences ranged from 0.9 $\mu g/m^3$ (July 2009) to 16 $\mu g/m^3$ (December 2006).

3.3 Weekly variability of ozone concentration in the ground layer of the atmosphere

The occurrence of higher ozone concentrations in the ground layer of the atmosphere on work-free days (Saturday–Sunday) compared to workdays (Monday–Friday) was first observed and described in the 1970s (Cleveland et al. 1974). Along with higher ozone concentrations on work-free days, lower concentrations of primary impurities (e.g., VOC, NO_x), which are precursors of ozone formation, were observed.

The phenomenon of the occurrence of higher ozone concentrations on Saturdays and Sundays is mostly related to large cities (Pont and Fontan 2001; Bronnimann and Neu 1997; Wang et al. 2013; Atkinson-Palombo et al. 2006) where the emission of primary pollutants due to intensive traffic is larger and significantly variable during the week.

3.3.1 Causes of weekend ozone phenomenon

According to the CARB (California Air Resources Board) report (https://www.arb.ca.gov/research/weekendeffect/arb-final/wee_sr_ch3.pdf) the so-called weekend phenomenon is associated with the occurrence of the following circumstances:

- Reduction of NO_x emissions on work-free days. The decrease in traffic intensity is associated with a decrease in NO_x emissions, modifying the chemical processes (described in Chapter 2) leading to the formation of ozone.
- Delay of NO_x emissions on work-free days. The daily distribution of NO_x emissions at the weekend differs from the distribution on workdays; among other things, it is characterized by a shift in the daily maximum of NO_x emissions by several hours. This type of NO_x distribution contributes to more efficient ozone production.
- Increased supply of solar radiation as a result of reduced soot emissions (lower share of elemental carbon in suspended dust) on work-free days.

As a result of reduced road traffic (especially diesel vehicles), the number of soot particles is smaller during the weekend, which results in a smaller amount of the absorbed UV radiation.

Despite numerous studies on the genesis of the weekend ozone phenomenon (Fujita et al. 2002; Yarwood et al. 2002), it is still difficult to unequivocally determine the reason for the occurrence of lower ozone concentrations on weekdays compared to weekends. There is a consistent view, supported by many authors, that the main reason for this phenomenon is the reduction of NO_x emissions in an environment characterized by a NO_x saturated regime (Heuss et al. 2003; Yarwood et al. 2003; Debaje and Kakade 2006; Pawlak and Jarosławski 2015). The reduction of NO_x emissions (especially NO), due to reduced traffic (mainly trucks) on Saturdays and Sundays, results in a decrease in the efficiency of the ozone removal process according to the reaction $NO + O_3 \rightarrow NO_2 + O_2$, followed by the process involving NO_2, which, instead of ozone, produces HNO_3, according to the reaction $NO_2 + OH \rightarrow HNO_3$. In addition, when VOC molecules are available in the air (and hence, free radicals, RO_2 resulting from the oxidation of VOC), a reaction occurs when NO_2 is produced without consumption of ozone: $RO_2 + NO \rightarrow NO_2 + RO$. As described in Chapter 2, the net effect of ozone production depends on the quantitative ratio of VOC to NO_x. According to Atkinson et al. (2006), urban areas have a lower VOC/NO_x ratio compared to rural areas. In these places, at the weekend, when the NO_x content drop is significantly greater than the VOC content drop, the ozone content increases. The reverse situation, when the lower ozone values occur at the weekend than on workdays, is due to a reduction in the NO_x content in an environment with a reduced NO_x content regime.

3.3.2 Analysis of the variability of ground-level ozone and nitrogen oxides on individual days of the week

This section presents an analysis of ground-level ozone variability on a weekly basis. It employs the 1-hour O_3 measurement data, as well as NO, NO_2, and NO_x data from all measuring stations analysed over the years 2005−2012. The occurrence of ozone weekend phenomenon was examined on the basis of average daily concentrations of ozone and other pollutants.

In order to determine whether there are differences between the ozone concentrations at weekends and on workdays at the stations subject to the analysis, the average ground-level ozone concentrations on Monday, Tuesday, Wednesday, Thursday, and Friday were compared with those on Saturday and Sunday.

In Fig. 7, daily diagrams are presented of O_3, NO, NO_2, and NO_x concentration at the stations Granica, Belsk, Legionowo, Warszawa-Krucza, Radom, and Warszawa-Ursynów). The diagrams were made on the basis of 1-hour values of pollution concentrations averaged over the period 2005−2012.

Analyzing the above graphs, it is easy to notice a significant similarity in the distribution of ozone and other pollutants at regional background stations. A characteristic daily course of ozone concentrations was observed, with a maximum in the afternoon, reaching over 70 $\mu g/m^3$, and a minimum in the early morning, just before the sunrise, amounting to about 30 $\mu g/m^3$ at Granica and 40 $\mu g/m^3$ at Belsk. The daily course of nitrogen compounds shows very little var-

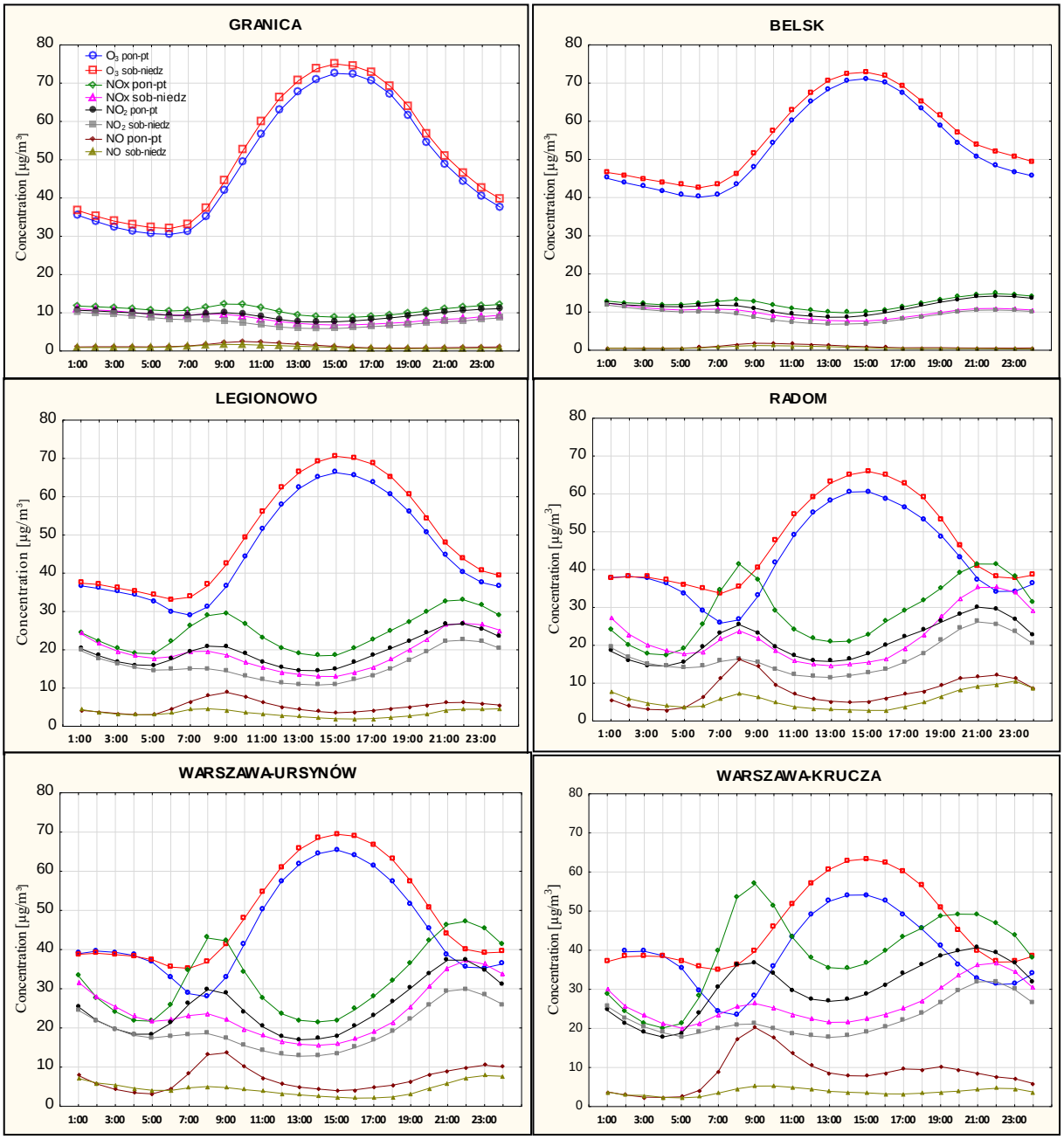

Fig. 7. Average daily variations of O_3, NO_x, NO_2, and NO concentrations in 2005−2012. Explanation of line labels in the Granica station panel.

iation during the day, in particular the NO 2.5 µg/m^3. This is probably due to the lack of local NO_x sources, mainly road traffic in the vicinity of both stations, as opposed to the situation in cities. As follows from further analysis of the above charts, the plots of ozone and nitrogen oxides concentrations at weekends and on workdays at regional background stations differ slightly, both in terms of shape and concentration values. However, a certain relationship was observed at both stations: lower ozone concentrations on workdays compared to weekends and higher NO, NO_2, and NO_x concentrations on workdays than on weekends. Urban background stations, in contrast to regional background stations, are characterized by a significant variation in NO, NO_2, and NO_x concentrations during the day, especially on workdays. The concentration of nitrogen oxides reaches maximum values in the morning, between 06:00 and 10:00, and in

the evening, between 20:00 and 23:00, while the ozone concentration reaches maximum values in the afternoon, between 13:00 and 17:00.

As for urban background stations (Legionowo, Radom, Warszawa-Ursynów, and Warszawa-Krucza), the differences in O_3, NO, NO_2, and NO_x concentrations between the workdays and the weekend are much larger than for Belsk and Granica stations. The exception is the night-time (hours 24:00 through 04:00) when the concentrations on workdays are comparable to those on the weekend. The distribution of NO_2 and NO_x concentrations shows the existence of two maxima, the first in the morning (06:00 through 10:00) and the second in the evening (19:00 through 23:00), visible especially on workdays. At the weekend, the shape of the distribution is similar to that on workdays, although the NO_2 and NO_x concentrations are much lower. Generally, it can be stated that at each city station the ozone concentrations recorded at the weekend are higher than those recorded on workdays. In the case of nitrogen oxides, an opposite pattern is observed at all the stations: their concentration is higher on workdays than on weekends.

The daily behavior of the concentration of the components under study can be described in four phases:

(1) The phase lasting from 4:00 to 8:00 is characterized by a rapid and significant increase in NO_x concentration as a result of increased traffic during the morning rush hours. Freshly emitted NO compounds without solar radiation react with O_3 to form NO_2, thereby increasing the amount of NO_2 and reducing the amount of O_3. In this phase, the difference between NO, NO_2, and NO_x concentrations recorded on weekends and on workdays is particularly large. Analyzing data from the Warszawa-Krucza station, these differences are 13, 15, and 28 $\mu g/m^3$, respectively. So significant differences are probably due to the lack of heavy traffic on work-free days (Saturday and Sunday);

(2) The phase lasting from 08:00 to 15:00, i.e., until the ozone concentration reaches its maximum value. During this time, as a result of increased solar radiation, temperature rise and accumulation of NO_2 compounds, photochemical ozone production processes dominate, especially in the first hours of the phase. Ozone concentration increases, reaching at some point its maximum value during the day. During this time, the ozone concentration grows to reach a value that is over two times greater than its daily minimum, while the concentration of nitrogen oxides successively decreases;

(3) The phase lasting from 15:00 to 21:00 is characterized by a gradual decrease in O_3 concentration, which is probably caused by the weakening of solar radiation and a decrease in temperature, and consequently a significant reduction of photochemical ozone production processes. At the same time, the NO_x accumulation process begins, which becomes possible due to heavy traffic during the evening rush hours. The amount of NO_x accumulated through this time is comparable to the amount of NO_x accumulated in the first phase during the morning rush hours;

(4) The phase lasting from 21:00 to 04:00 has relatively constant values of O_3 and NO concentration. Generally, it can be stated that during this time ozone and nitrogen oxides concentrations on workdays and on weekends are comparable, particularly over the time from the midnight to the end of the phase. The minimum in the variability of concentrations at night is probably caused by the disappearance of photochemical processes and the reduction of pollutant emissions occurring concurrently.

It can be expected that the phenomenon of higher ozone concentrations at the weekend than on workdays at a statistically significant level ($\alpha = 0.05$) will occur at urban background stations, while it will be definitely absent at regional background stations. The above hypothesis will be verified (confirmed or rejected) in the course of further calculations and considerations.

Figure 8 presents weekly ozone concentration variability expressed as a percentage deviation of ozone concentration on individual days of the week from the weekly average (adopted as 0 on the Y axis) in 2005–2012 for all the measuring stations analyzed. The weekly average is the ozone concentration value averaged over all the weeks in 2005−2012; similarly, the average ozone content on each day of the week is the ozone concentration value averaged separately for each day of the week in 2005−2012.

For stations Belsk and Granica, positive deviations were recorded on Saturday, Sunday, and Monday. On Monday, a positive deviation from the weekly average was still present (although on a very small scale), which could have been caused by the lack of heavy traffic in rural areas, unlike in large cities, where on Monday, due to the beginning of the working week, this traffic is definitely higher than the day before (Sunday). Hence, lower NO_x emissions (especially NO) reduce the ozone destruction and at the same time allow to maintain elevated ozone concentrations also on Monday (lower NO_x concentration compared to the weekly average at regional background stations also occurred on Monday). On other days of the week, deviations of ozone concentrations from the weekly average were negative.

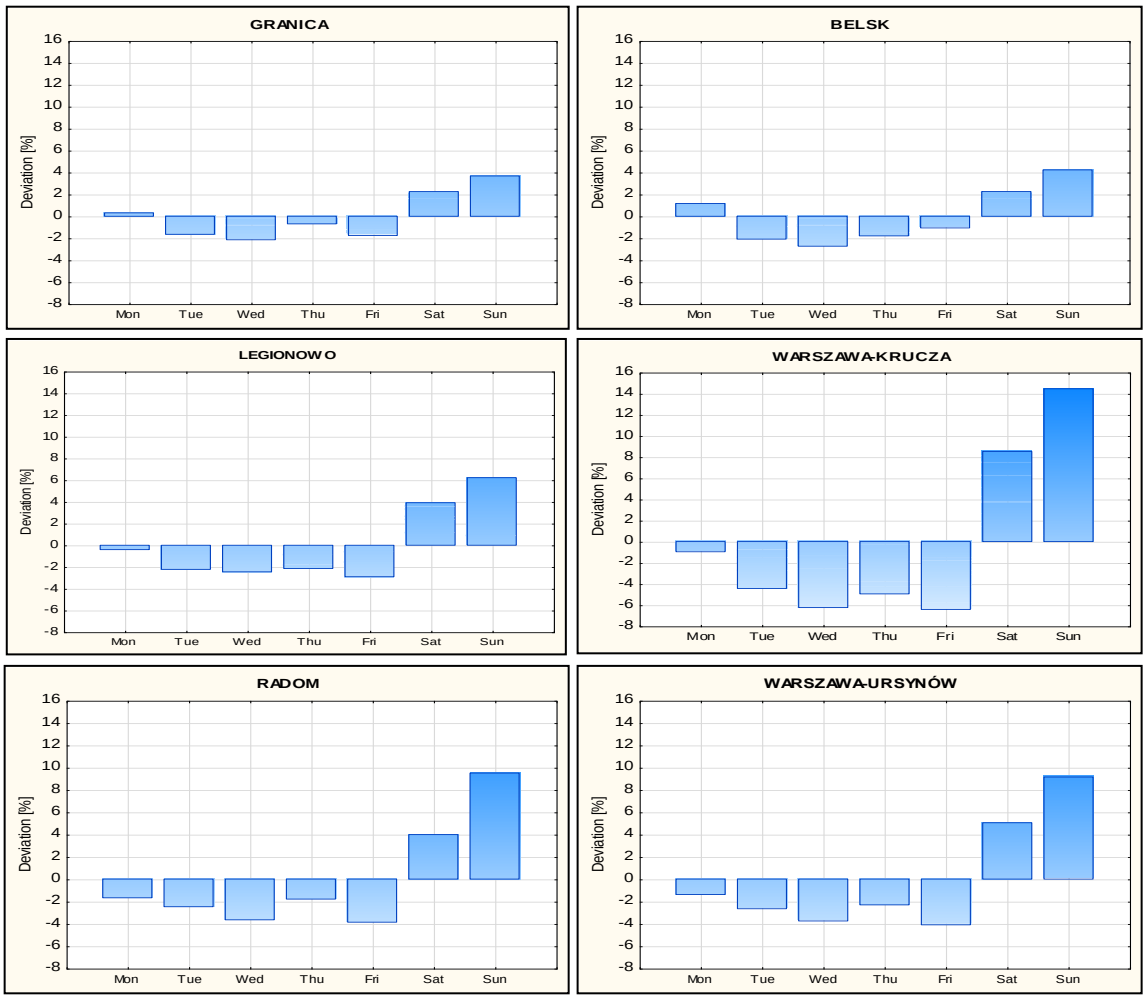

Fig. 8. Percentage deviations of ozone concentrations on individual days of the week in relation to the many-year weekly average.

Fig. 9. Percentage deviations of NO_x concentration on individual days of the week from the many-year weekly average (2005−2012).

Analyzing the urban background stations (Legionowo, Warszawa-Krucza, Radom, Warszawa-Ursynów) it can be seen that positive deviations from the weekly average occur only on Saturday and Sunday, and, as in the case of rural stations, the highest deviations were on Sunday. On the other days of the week, the deviations from the weekly average were negative, the largest deviation at all city stations being recorded on Friday.

Looking at Fig. 9, which shows the percentage deviation of NO_x content from the many-year weekly average (2005−2012), one can notice a characteristic distribution of deviations of the opposite nature than in the case of ozone.

At regional background stations (Granica, Belsk) deviations of NO_x concentration from the weekly average on Saturday, Sunday, and Monday were negative. On the other days of the week, i.e., Tuesday, Wednesday, Thursday, and Friday, the deviations were positive, the largest being on Friday, at both stations amounting to 9.9% (1 and 1.2 μg/m^3).

At all the city stations, except of the Warszawa-Krucza, negative percentage deviations from the weekly average were recorded on Saturdays and Sundays. Negative deviations from the weekly average value at Warszawa-Krucza were also recorded on Monday, although this value is negligible and amounts to –0.4% (–0.1 μg/m^3). Positive deviations at the stations Legionowo, Radom, and Warszawa-Ursynów were recorded from Monday to Friday, while at the Warszawa-Krucza from Tuesday to Friday. For all four stations, the largest positive deviations from the long-term weekly average were recorded on Tuesday.

Average values of concentrations of ozone and nitrogen oxides for particular days of the week are presented in Tables 2 and 3. At regional background stations (Granica, Belsk) the lowest values were recorded on Wednesday and the highest on Sunday. For all city stations (Legionowo, Warszawa-Krucza, Radom, and Warszawa-Ursynów) the lowest values on a weekly basis were recorded on Fridays, while the highest on Sundays, as in the case of regional background stations.

In the case of NO_x, the lowest concentration values per week were recorded on Sunday at all the stations. At regional background stations these values ranged from 7.9 to 8.9 μg/m^3, while at urban background stations in the range from 17.7 μg/m^3 (Legionowo) to 23.9 μg/m^3 (Warszawa-Krucza). The highest concentrations were recorded on different days, depending on the type (location) of measuring station. At Granica and Belsk, the maximum values were recorded on Friday. At all urban stations, the maximum on a weekly basis was recorded on Tuesday and, depending on the station, concentration values ranged from 25.7 μg/m^3 (Legionowo) to 41.9 μg/m^3 (Warszawa-Krucza).

Table 2

Weekly variability of ground-level ozone concentration in 2005−2012

Station	O_3 [μg/m^3]										
	Day of the week							Value		Day	
	Mon	Tue	Wed	Thu	Fri	Sat	Sun	Min	Max	Min	Max
Granica	49.9	48.9	48.7	49.4	48.9	50.9	51.6	48.7	51.6	Wed	Sun
Belsk	54.7	53.0	52.6	53.1	53.5	55.3	56.4	52.6	56.4	Wed	Sun
Legionowo	47.2	46.3	46.2	46.4	46.0	49.2	50.3	46.0	50.3	Fri	Sun
Warszawa-Krucza	41.0	39.5	38.8	39.3	38.7	44.9	47.4	38.7	47.4	Fri	Sun
Radom	43.1	42.7	42.2	43.0	42.1	45.6	48.0	42.1	48.0	Fri	Sun
Warszawa-Ursynów	45.1	44.5	44.0	44.6	43.8	48.0	49.9	43.8	49.9	Fri	Sun

Note: The minimum values are in blue, the maximum values are in red.

Table 3
Weekly variability of ground-level NO_x concentration in 2005−2012

Station	NO_x [µg/m^3]										
	Day of the week							Value		Day	
	Mon	Tue	Wed	Thu	Fri	Sat	Sun	Min	Max	Min	Max
Granica	9.7	11.0	11.0	11.1	11.2	9.6	7.9	7.9	11.2	Sun	Fri
Belsk	11.1	12.7	12.7	12.7	12.8	10.9	8.9	8.9	12.8	Sun	Fri
Legionowo	23.9	25.7	24.3	23.9	25.2	20.7	17.7	17.7	25.7	Sun	Tue
Warszawa-Krucza	35.4	41.9	39.5	39.7	39.3	29.0	23.9	23.9	41.9	Sun	Tue
Radom	29.2	30.7	28.7	27.8	29.8	24.9	20.5	20.5	30.7	Sun	Tue
Warszawa-Ursynów	32.1	33.2	31.7	31.2	32.4	25.6	22.5	22.5	33.2	Sun	Tue

Note: The minimum values are in blue, the maximum values are in red.

In Table 4 there are listed average differences between O_3 and NO_x content at the weekend (Saturday, Sunday) and the content of these compounds on workdays (Monday–Friday) in 2005−2012. In order to determine whether the differences in the concentration of individual substances on workdays and at the weekend are statistically significant ($\alpha = 0.05$), the following statistical tests were performed for the set of average daily ozone and nitrogen oxides concentrations determined for each day of the week:

(1) Test F, allowing to determine whether the analyzed samples have equal/unequal variance,

(2) Two-sample *t* test with equal or unequal variances. In a situation when *t* was greater than t_c or when *t* was less than $-t_c$, the difference was considered statistically significant at the level of $\alpha = 0.05$.

Table 4 presents the average O_3 and NO_x concentrations on workdays and on weekends, averaged over the years 2005−2012 together with the results of Student's *t*-test (t, t_c, p). As can be seen, it is only at the Warszawa-Krucza station that the statistical significant ($\alpha = 0.05$) differences in ozone content on workdays and on weekends were recorded over the analyzed period of time (2005−2012). In this case, the difference of concentrations amounted to 5.1 µg/m^3. At other stations, these values ranged from 1.5 µg/m^3 (Belsk) to 3.2 µg/m^3 (Warszawa-Ursynów). Analyzing the differences in NO_x concentrations, it can be seen that the differences between the workdays and weekends are statistically significant at all the analyzed stations. Negative differences represent higher content of nitrogen compounds on workdays than on weekends. The smallest differences were recorded at regional background stations (from –2.1 to –2.5 µg/m^3), and the largest at the Warszawa-Krucza station (–12.8 µg/m^3).

In order to check a possible seasonality of the weekend phenomenon, an analysis was made of the significance of differences in the concentrations of O_3 and NO_x in the workdays and on the weekend for four seasons. The results are presented in Table 5.

Table 4

Mean concentrations of O_3 and NO_x on workdays and the weekends with the differences between them and the results of Student's *t*-test

2005−2012	Mean O_3 [μg/m^3]		Difference [μg/m^3]/%	*t*	t_c	*p*
	Sat–Sun	Mon–Fri				
Granica	51.2	49.7	1.6/2.9	1.3	2.1	0.208
Belsk	55.8	54.4	1.5/2.5	0.9	2.1	0.385
Legionowo	49.8	47.5	2.3/4.6	1.3	2.1	0.229
Warszawa-Krucza	46.1	41.0	5.1/11.1	**3.9**	**2.1**	**0.002**
Radom	46.8	44.0	2.8/6	1.5	2.1	0.157
Warszawa-Ursynów	48.9	45.8	3.2/6.3	1.3	2.1	0.220
2005−2012	Mean NOx [μg/m^3]		Difference [μg/m^3]/%	*t*	t_c	*p*
	Sat–Sun	Mon–Fri				
Granica	8.7	10.8	–2.1/19.4	**3.14**	**2.14**	**0.007**
Belsk	9.9	12.4	–2.5/20.2	**3.92**	**2.14**	**0.002**
Legionowo	19.2	24.6	–5.4/22	**5.16**	**2.14**	**0.000**
Warszawa-Krucza	26.4	39.2	–12.8/32.7	**3.46**	**2.36**	**0.010**
Radom	22.7	29.2	–6.5/22.3	**3.53**	**2.14**	**0.003**
Warszawa-Ursynów	24.1	32.1	–8.1/24.9	**7.72**	**2.14**	**0.000**

Note: Statistically significant cases ($\alpha = 0.05$) are bolded.

For all seasons, statistically significant differences in average concentrations of the studied pollutants between the weekend and workdays occur only at the Warszawa-Krucza station (likewise in the analysis of the whole year). However, an additional two features can be noticed that were not visible during the entire year, namely:

(1) in winter, differences in ozone content at the weekend are statistically significantly higher than on workdays also at the three remaining stations: Warszawa-Ursynów, Radom and Belsk;

(2) in summer, regional background stations (Granica, Belsk) are exceptional by being characterized by higher ozone concentrations on weekends than on workdays. Although these differences are negligible (approx. –0.2 μg/m^3) and statistically insignificant, still the tendency that is opposite to that in all other localities and seasons may point to a different chemical regime at this time of the year.

In order to clarify the situation described in point 2, an analysis was made to determine what is the interaction between O_3 and NO_x and establish the chemical regime in various seasons of the year. The scatter charts shown in Fig. 10 present the degree of correlation between daily average O_3 and NO_x concentrations in individual seasons throughout the entire period 2005−2012. The analysis was made for stations of the regional background, Granica and Belsk, because it is only at these stations that a specific summer pattern was observed, namely, the occurrence of higher ozone content on workdays than on weekends.

Table 5
Mean concentrations, per seasons, of O_3 i NO_x in workdays and weekends

2005−2012 spring	O_3 [μg/m^3]			NO_x [μg/m^3]		
	Sat–Sun	Mon–Fri	Difference	Sat–Sun	Mon–Fri	Difference
Granica	69.91	68.68	1.22	7.23	8.84	–1.60
Belsk	73.69	72.42	1.28	8.95	10.47	**–1.52**
Legionowo	64.27	61.80	2.47	18.74	23.04	**–4.30**
Warszawa-Krucza	60.73	54.79	**5.94**	28.28	35.63	**–7.35**
Radom	59.15	55.89	3.26	23.02	26.99	–3.97
Warszawa-Ursynów	64.16	60.24	3.93	25.40	31.66	–6.26
2005−2012 summer	O_3 [μg/m^3]			NO_x [μg/m^3]		
	Sat–Sun	Mon–Fri	Difference	Sat–Sun	Mon–Fri	Difference
Granica	59.18	59.39	–0.21	5.71	6.54	–0.83
Belsk	66.54	66.75	–0.22	7.05	8.62	**–1.57**
Legionowo	61.44	59.70	1.74	13.53	17.04	**–3.50**
Warszawa-Krucza	63.10	57.10	**6.00**	20.59	28.90	**–8.30**
Radom	59.85	56.80	3.05	16.54	20.81	**–4.26**
Warszawa-Ursynów	64.11	60.91	3.20	16.84	23.84	**–7.00**
2005−2012 autumn	O_3 [μg/m^3]			NO_x [μg/m^3]		
	Sat–Sun	Mon–Fri	Difference	Sat–Sun	Mon–Fri	Difference
Granica	32.27	31.53	0.74	9.78	11.67	**–1.89**
Belsk	38.34	36.62	1.72	11.26	13.67	**–2.41**
Legionowo	32.71	29.61	3.10	21.14	27.72	**–6.58**
Warszawa-Krucza	27.71	22.67	**5.04**	28.42	40.73	**–12.31**
Radom	31.56	28.51	3.06	24.82	33.76	**–8.95**
Warszawa-Ursynów	33.15	29.22	3.93	29.38	38.10	**–8.72**
2005−2012 winter	O_3 [μg/m^3]			NO_x [μg/m^3]		
	Sat–Sun	Mon–Fri	Difference	Sat–Sun	Mon–Fri	Difference
Granica	42.64	36.76	5.88	12.64	16.47	–3.83
Belsk	43.57	37.20	**6.38**	12.57	17.04	**–4.47**
Legionowo	38.81	32.46	6.36	23.58	30.05	**–6.47**
Warszawa-Krucza	31.10	22.18	**8.92**	26.45	37.13	**–10.68**
Radom	35.12	27.79	**7.33**	25.31	33.97	**–8.65**
Warszawa-Ursynów	36.41	29.19	**7.22**	24.53	34.56	**–10.03**

Note: Statistically significant cases (α = 0.05) are bolded.

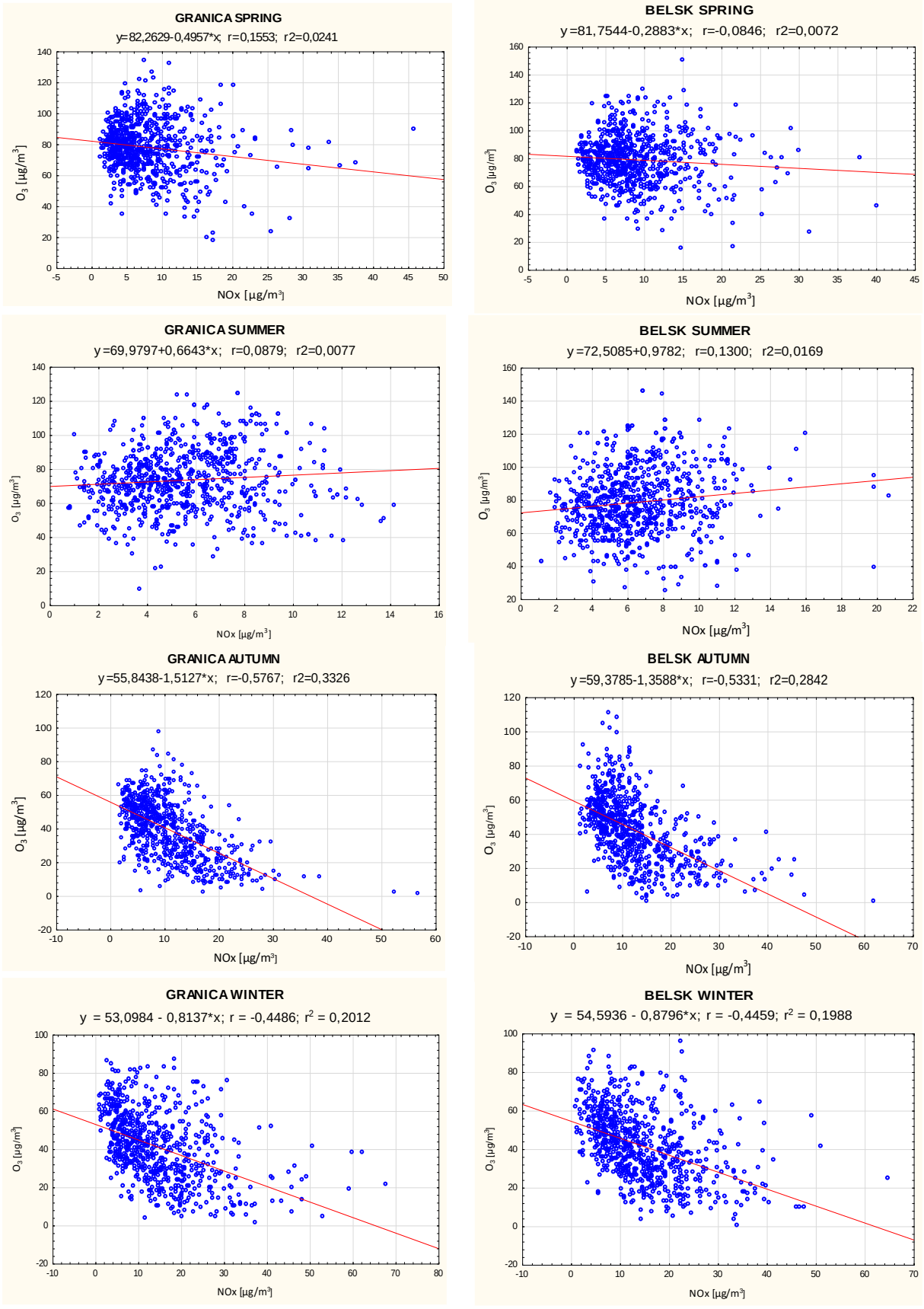

Fig. 10. Relationship between the concentrations of O_3 and NO_x at different seasons over the years 2005−2012.

As follows from Fig. 10, it is only in the autumn and winter that a clear negative correlation is observed. This means that along with the increasing NO_x content, the O_3 content decreases. This gives evidence for the fact that a chemical regime in a given environment is characterized by a high NO_x/VOC content ratio (Seinfeld and Pandis 2006). Hence, as shown in Table 5, the lower NO_x concentrations on weekends (than on workdays) result in higher O_3 concentrations on weekends, and, consequently, the higher NO_x concentrations on workdays result in lower O_3 concentrations on these days. In spring and summer, correlation coefficient values are very low. Hence, it cannot be clearly determined which chemical regime (NO_x/VOC ratio) dominates in this season.

3.3.3 Comparative analysis of O_x content on workdays and on weekends

In the cycle of reactions settling the balance between NO, NO_2, and O_3 (Eqs. (2) to (4), Chapter 2), two groups of cycle's components can be distinguished: the NO_x group ($NO + NO_2$) and the O_x group ($O_3 + NO_2$). The reactions presented below show the possible paths leading to an increase or decrease in the concentration of components in individual groups. The first of these, previously presented reaction (4), indicates the possibility of NO_2 production without automatic consumption of O_3. The reaction of NO with RO_2 means the possibility of production as well as cumulation of O_3. The second, reaction (24), indicates the main pathway of reducing the O_x content through the reaction of NO_2 with OH. At the same time, this reaction weakens the ozone production potential (Sadanaga et al. 2008).

$$RO_2 + NO \rightarrow RO + NO_2 . \qquad \text{(4), repeated}$$

$$OH + NO_2 + M \rightarrow HNO_3 + M \qquad \text{(24), repeated}$$

Reaction (4) contributes to an increase in the O_x content, while reaction (24) causes a decrease in the O_x content. Hence, both the increase and decrease of the O_x concentration is reflected in the enhancement or inhibition of photochemical ozone production. Comparing the O_x content on workdays with that on the weekend, it can be established whether the photochemical ozone production potential is greater on workdays or on the weekend, and also determine the factors shaping the phenomenon of higher O_3 concentrations at the weekend compared to other days of the week. Namely, if the amount of O_x on workdays is comparable with O_x values on the weekend, it means that the occurrence of the phenomenon of higher ozone content at the weekend compared to workdays is due to the reaction of O_3 removal by NO (reaction 3) (Sadanaga et al. 2012)

Table 6 presents O_x content on workdays and on weekends, and the corresponding differences, for all stations analyzed in 2005−2012. In order to determine whether the differences in the amount of O_x on workdays and at the weekend are statistically significant ($\alpha = 0.05$), analogous calculations as those for O_3 and NO_x (see Table 4) were made, namely:

(1) calculations of daily average O_x content for each day of the week, at all measuring stations in 2005−2012,

(2) calculations of average O_x content on workdays and weekend averaged for the years 2005−2012,

(3) F test, allowing to determine whether the analyzed samples have equal/unequal variance,

(4) two-sample *t*-test assuming equal or unequal variances; when *t* was greater than t_c or when *t* was less than $-t_c$, the difference was treated as statistically significant at the level $\alpha = 0.05$.

Table 6

Mean values of O_x content in workdays and on weekends with the differences between them and the results of *t*-Student test in the years 2005−2012

2005−2012	Mean O_x [μg/m^3]		Difference [μg/m^3]/%	*t*	t_c	*p*
	Sat–Sun	Mon–Fri				
Granica	58.5	58.4	0.2/0.2	0.11	2.14	0.913
Belsk	64.8	64.7	0.1/0.2	0.03	2.14	0.980
Legionowo	65.1	65.6	–0.5/0.8	0.26	2.14	0.797
Warszawa-Krucza	65.4	65.9	–0.5/0.8	0.12	2.18	0.908
Radom	63.6	63.6	0.0/0	–0.01	2.14	0.994
Warszawa-Ursynów	68.9	69.7	–0.8	0.30	2.14	0.769

Table 7

Mean values of O_x content in workdays and on weekends at individual seasons and the corresponding differences in the years 2005–2012

2005−2012 spring	O_x [μg/m^3]			2005−2012 autumn	O_x [μg/m^3]		
	Sat–Sun	Mon–Fri	Difference		Sat–Sun	Mon–Fri	Difference
Granica	76.42	76.42	0.00	Granica	41.23	41.17	0.06
Belsk	81.75	81.96	–0.21	Belsk	49.00	49.19	–0.19
Legionowo	79.44	80.52	–1.09	Legionowo	48.69	49.35	–0.66
Warszawa-Krucza	85.79	86.22	–0.43	Warszawa-Krucza	51.57	54.16	–2.59
Radom	76.39	76.93	–0.54	Radom	49.40	49.82	–0.42
Warszawa-Ursynów	85.70	85.85	–0.14	Warszawa-Ursynów	54.74	55.49	–0.76
2005−2012 summer	O_x [μg/m^3]			2005−2012 winter	O_x [μg/m^3]		
	Sat–Sun	Mon–Fri	Difference		Sat–Sun	Mon–Fri	Difference
Granica	64.28	64.95	–0.67	Granica	53.69	51.24	2.45
Belsk	72.74	74.62	–1.88	Belsk	55.36	52.85	2.51
Legionowo	73.26	74.16	–0.90	Legionowo	58.21	56.53	1.68
Warszawa-Krucza	82.26	83.60	–1.34	Warszawa-Krucza	51.55	49.22	2.32
Radom	74.18	74.58	–0.41	Radom	55.16	52.83	2.33
Warszawa-Ursynów	79.14	81.15	–2.01	Warszawa-Ursynów	58.11	56.89	1.22

As can be seen from Table 6, the lowest O_x concentrations were recorded at the station Granica (about 58 μg/m^3), while the highest were at Warszawa-Ursynów (about 69 μg/m^3); O_x concentrations at the remaining stations were similar (within approx. 64−66 μg/m^3). The O_x concentrations on workdays do not differ significantly from those on weekends, regardless of the type of station. In addition, these differences are not statistically significant for every station. The maximum differences between the O_x content on workdays and at the weekend occur at Warszawa-Ursynów and are –0.8 μg/m^3 only. At Radom, on the other hand, the difference is zero. The percentage differences in the O_x content on workdays and on weekends ranged from 0% (Radom) to 1.2% (Warszawa-Ursynów).

Analyzing the distribution of O_x content in individual seasons of the year (Table 7) it can be seen that, similarly to the analysis for the whole year, the differences in O_x content in each case are statistically insignificant and range from –2.59 to 2.51 μg/m^3.

Negative differences were noted in spring, summer and autumn, which means that the O_x content was higher on workdays than on weekends. The differences in each of these seasons were comparable and ranged from 0.0 to –2.59 μg/m^3. In the winter, the pattern was different: the amount of O_x at weekends was higher than on workdays, which resulted in non-negative differences in the O_x content.

The occurrence of non-significant differences in the O_x content on workdays and at the weekend leads to the conclusion that the main reason in shaping the pattern in question is the reaction: $NO + O_3 \rightarrow NO_2 + O_2$, which reduces the concentration of ozone at the earth's surface. An important source of NO emissions is increased traffic, especially in large cities and especially on workdays. The smaller amounts of NO emitted during the weekend result in higher ozone levels on these days, especially at stations of urban background.

3.4 Daily variability of ozone concentration in the ground layer of the atmosphere

Daily cycles of variability of ozone concentrations in the ground layer of the atmosphere in the Mazowieckie Voivodeship are characterized by clear seasonal variability, and changes depending on the location of the station. The pattern depends on the season of the year and, consequently, on the prevailing meteorological conditions as well as the presence of chemical substances affecting the ozone concentration. Analyzing daily changes in ozone concentration, different patterns can be observed for different seasons. In Fig. 11, diagrams of daily changes in the ground-level atmosphere layer at all the stations analyzed in the period 2005−2012 are presented separately for each month.

In the months from April to August, a characteristic cycle of ozone variations was recorded, similar at all the stations. From 08:00, there was a clear increase in ozone content lasting up to afternoon hours as a result of ozone production in photochemical processes involving VOC and NO_x, which, together with a constant increase in air temperature and solar radiation, are more effective. In addition, vertical air mixing processes and, as a result, downward transport of air from higher layers of the ozone-rich atmosphere, additionally affect the high ozone content during the day (Lal et al. 2000). The maximum ozone concentration occurred between 15:00 and 17:00. From 18:00, a gradual decrease in ozone concentration was recorded at all stations, which in Granica, Belsk, Legionowo and Radom continued all the night, reaching the lowest values at 06:00 (Granica, Belsk, Legionowo) and at 07:00 (Radom). The reduction of photochemical processes in the evening as a result of decreasing air temperature and weakening of solar radiation and its dissappearance at night is one of the factors responsible for low ozone concentrations in the evening and at night. An additional contribution comes from the ozone deposition processes on the surfaces (responsible for reducing the ozone concentrations) and chemical processes with the participation of nitric oxide ($NO + O_3 \rightarrow NO_2 + O_2$), responsible for the reduction of ozone in urban areas (Eliasson et al. 2003). Continuous NO emission in

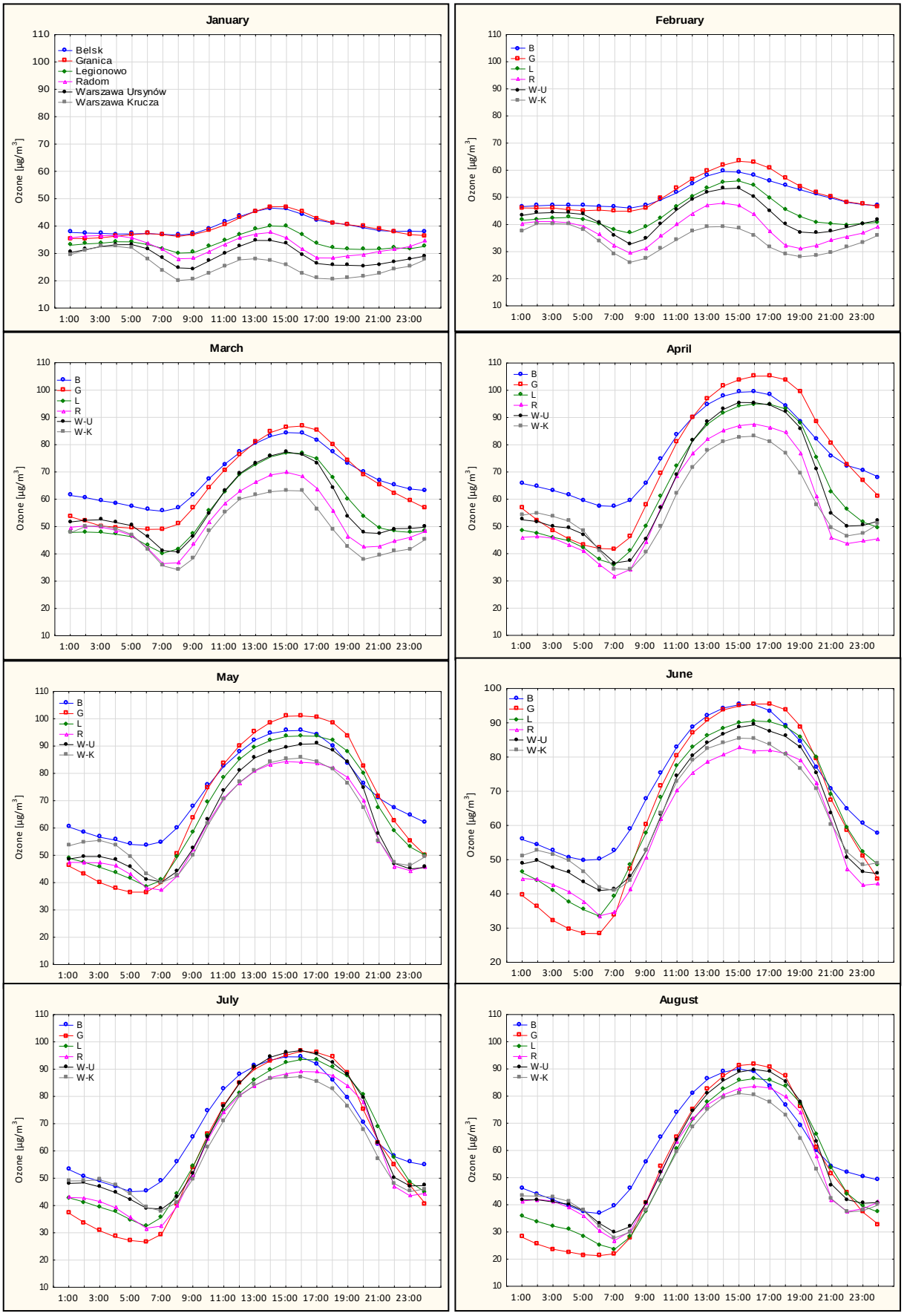

Fig. 11. Continuation on the next page.

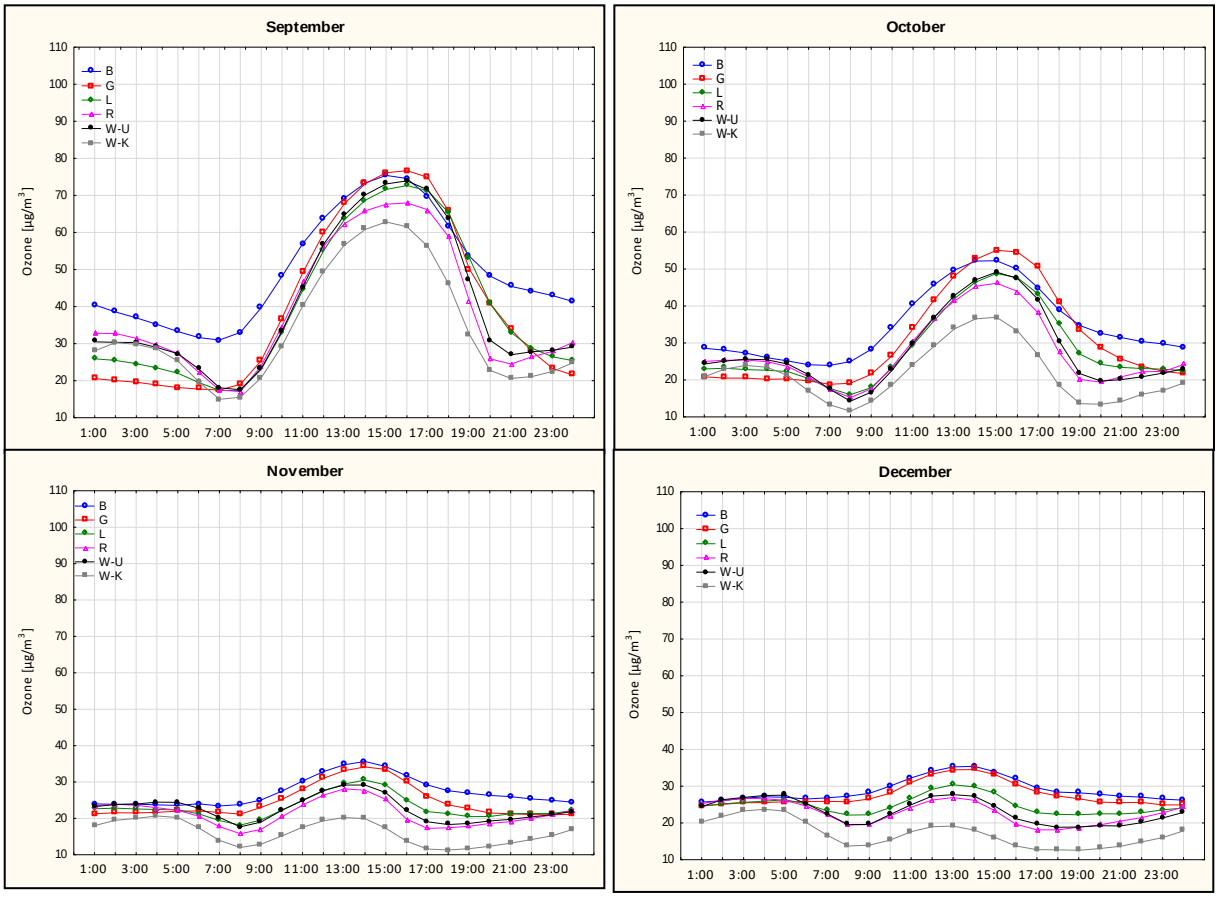

Fig. 11. Average daily ozone content waveforms in the ground layer of the atmosphere in individual months.

urban areas contributes to the reduction of ozone concentrations at the expense of production of NO_2 and O_2, especially at night when the lack of solar radiation prevents NO_2 photolysis and, as a result, ozone production. At the Warszawa-Krucza urban-background station, the phenomenon of occurrence of clearly higher ozone concentrations at night was recorded, characteristic of urban areas. The occurrence of relatively high ozone concentrations at night in urban areas during stable atmospheric conditions in the summer season is a phenomenon commonly recorded in major European and North American cities (Eliasson et al. 2003; Chung 1977; Corsmeier et al. 1997). According to the authors cited above, the occurrence of the nocturnal ozone maximum can be due to the processes of vertical mixing of ozone-rich air from higher atmospheric layers or the advection of ozone-rich air from rural areas.

In September and October, daily ozone concentrations behaved similarly as in April−August, with the difference that the maximum values were recorded between 14:00 and 16:00 and the average maximum values during the day for the analyzed period (September−October 2005−2012) were much lower.

In the period from November to February, different patterns of daily O_3 distributions were observed for regional-background stations and for urban-background stations. At the regional-background stations, no ozone concentrations characteristic for the remaining months were recorded. From the evening hours and then throughout the night, constant ozone concentrations were observed there, around 23 µg/m^3 in November, around 26 µg/m^3 in December, around 37 µg/m^3 in January, and 45 µg/m^3 in February. The increase in ozone content usually started at 9:00 am, reaching maximum concentrations in the afternoon. The average maximum values

over the day for the years 2005–2012 were recorded in the afternoon (13:00−15:00) and amounted to about 35 μg/m^3 in November and December, about 45 μg/m^3 in January, and about 60 μg/m^3 in February. From 16:00, the ozone content began to decline until late in the evening. In the case of urban background stations, especially those located in Warszawa and Radom, characteristic minima of ozone content were observed in the morning (07:00−09:00) and evening (17:00−19:00), i.e., during the most intense traffic. A high emission of nitrogen oxides promotes ozone removal processes as a result of the reaction: $NO + O_3 \rightarrow O_2 + NO_2$. Unfavorable meteorological conditions prevailing in winter make the ozone production during the day not very effective and not able to compensate for ozone losses incurred as a result of nitrogen oxide removal, thus contributing to much higher ozone content during the day than at night.

March was a transitional month between the cool (November−February) and warm (April−September) periods. At urban background stations, average minimum values over the day for the years 2005−2012 were recorded from 07:00 to 08:00. In the case of Granica it was difficult to discern a characteristic daily minimum, while at Belsk the minimum value was recorded at 07:00. The average maximum values over the day for the years 2005−2012 occurred between 14:00 and 16:00.

The daily concentrations of O_3 obtained for each month differ not only in shape but also in the amplitude of daily changes. In Table 8 the maximum values of daily amplitudes in the analyzed period 2005−2012 are presented. Amplitudes of daily changes in the ground ozone content reach the highest values in the period when the daily concentrations of this gas per year are also the highest (April−August). This effect is observed at stations located in both rural areas and urban agglomerations. Because the ozone production in the winter months is limited due to less favorable weather conditions, also the maximum ozone content on a daily basis is then smaller.

Table 8

Maximum amplitudes of daily O_3 variations in 2005−2012

Station / Month	Granica	Belsk	Legionowo	Warszawa-Ursynów	Warszawa-Krucza	Radom
			[μg/m^3]			
January	11.7	9.9	9.9	10.3	12.4	9.6
February	18.3	13.5	19.3	20.4	14.2	18.4
March	37.9	28.8	36.7	36.6	29.0	33.4
April	63.6	42.1	58.9	58.9	49.0	55.8
May	64.5	42.1	55.1	50.6	45.5	47.1
June	67.1	45.4	57.1	48.4	44.6	49.1
July	69.9	49.4	61.2	58.2	49.2	57.4
August	70.5	53.1	62.7	60.0	53.0	56.7
September	59.2	44.4	55.4	56.4	47.8	50.9
October	36.2	28.3	32.8	34.9	25.4	31.0
November	13.2	12.2	12.3	11.5	9.4	12.3
December	9.9	9.7	8.1	8.9	11.2	8.8

Of all the analyzed stations, the highest values of the amplitudes of changes in daily O_3 concentrations were recorded at Granica and the lowest at Belsk. Although both represent regional-background stations, the average values of daily amplitudes during the analyzed period (2005−2012) differ by 12 μg/m^3. In August, when the amplitudes are the highest, their values reached 70.5 μg/m^3 at Granica and 53.1 μg/m^3 at Belsk. Much greater values of the daily amplitude changes observed at the Granica station in spring and summer are probably a result of high ozone concentrations during the day and very low concentrations during the night. Among all the stations, the lowest daily minimum values were recorded in May−August on early morning (05:00−06:00) at Granica. The average values of daily amplitudes (2005−2012) in this period were higher by 32−43% than the average values of daily amplitudes at the station in Belsk, by 12% in Legionowo, by 14% in Radom, and by 25% at stations located in Warszawa. The reason for so high daily amplitude at Granica may be due to its location, the Kampinos National Park − the area of the forest complex. The immediate vicinity of the large deciduous vegetation compared to other stations may contribute to the increased dry deposition process during the growing season, which is known to be one of factors that reduce the ozone content in the ground layer of the atmosphere.

3.5 Long-term changes in ozone concentration in the ground layer of the atmosphere based on the 1995−2016 measurement series in Belsk

Having at our disposal the many-year measurement data, it is possible to make calculations and interpret long-term changes in ozone concentrations on a regional scale. The measurement series from Belsk station, where regular observations of ground-level ozone have been conducted since 1995, provided a 22-year (1995−2016) record of measurements of ozone content in the ground-level atmosphere. A sufficiently long measurement series is the basis for performing an analysis of changes in ozone concentration in various time scales and making an attempt to determine long-term changes in ozone concentration in the surface layer of the atmosphere over the region of Mazowsze. To this end, the time series for the years 1995− 2016 were analyzed in a daily and annual scale.

Figure 12, based on daily mean values, presents changes in ground-level ozone concentration at Belsk station in 1995−2016. Using the local regression method LOWESS (Locally

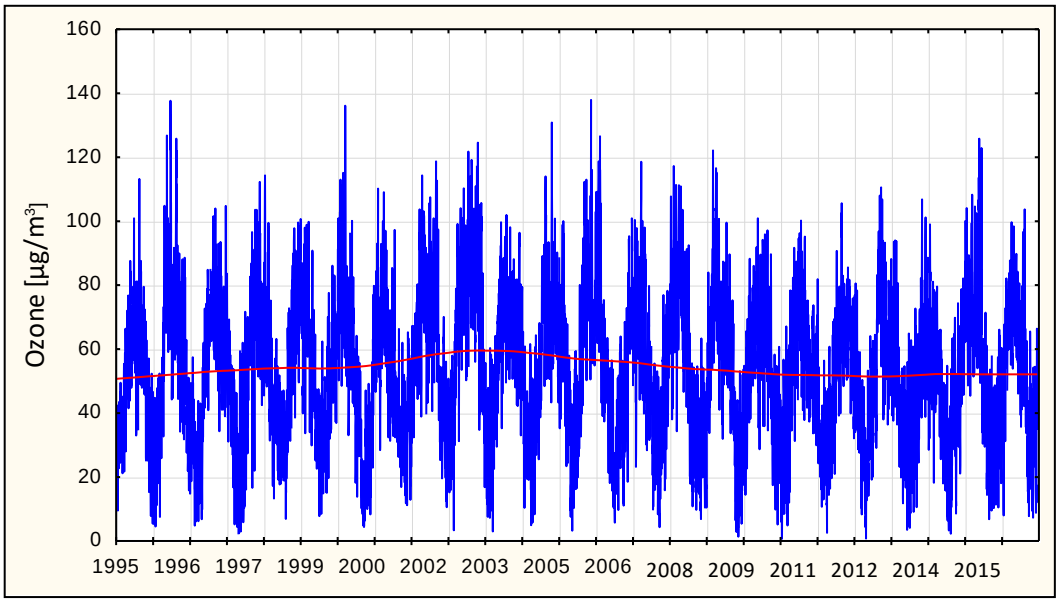

Fig. 12. Series of measurements of average daily concentrations of ground-level ozone in 1995−2016 (blue line) together with the LOWESS curve (red line).

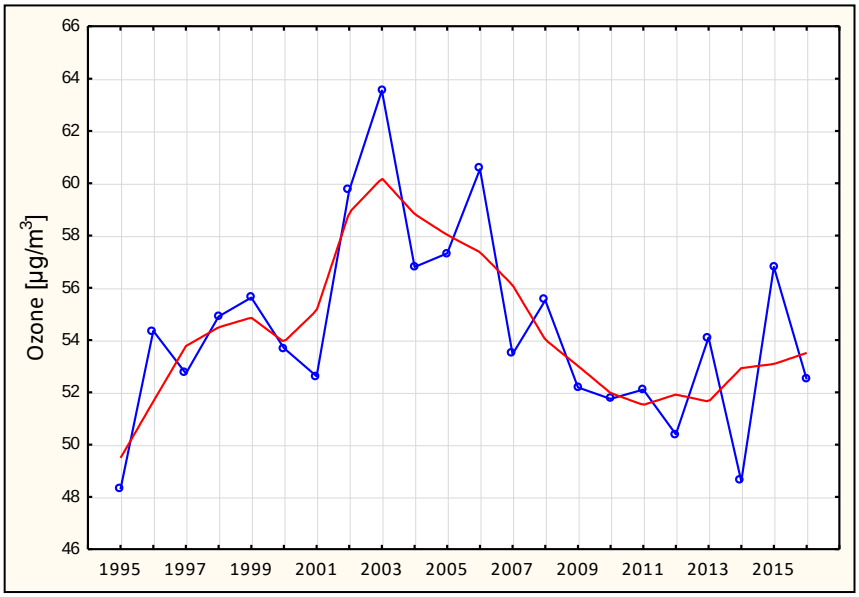

Fig. 13. Measurement series of average monthly ground-level ozone content in 1995−2016 (blue line) and a LOWESS curve (red line).

Weighted Scatterplot Smoothing) (Cleveland 1979), a smoothed curve (red line) was drawn allowing to observe the trends of long-term changes in the ozone content.

Analyzing Fig. 12 it can be stated that the measurements carried out at the Belsk station in the years 1995−2016 do not show any permanent trend of changes in the ozone content in the ground layer of the atmosphere. However, the presence of elevated ozone content is visible around 2003.

Further analysis (Fig. 13) indicates that in 1995−2016 three different time periods can be distinguished, characterizing changes in ozone concentration:

(1) 1995−2003: increase in ground-level ozone content,

(2) 2003−2010: decrease in the ground-level ozone content,

(3) 2010−2016: slow increase in ground-level ozone.

The lowest average annual ozone content in Belsk during the entire measurement series (1995−2016) was recorded in 1995 (46.7 µm/m^3), and the highest in 2003 (64.3 µg/m^3). Analyzing the chart it can be stated that 2003 was a breakthrough year that ended the period of ozone concentration increase since 1995 and began the period of ozone content decline until 2010.

The occurrence of such high ozone concentrations in 2003 was associated with exceptional meteorological conditions that significantly promoted ozone production and at the same time limited its destruction. The summer season (especially August) of 2003 was characterized by very high air temperatures resulting in the occurrence of heat waves in Europe, especially in Central Europe, which consequently produced extremely high ozone concentrations (Pellegrini et al. 2007; Solberg et al. 2008; Vieno et al. 2010). The average monthly ozone content recorded at the Belsk station in August 2003 (87.9 µg/m^3) was by 24 µg/m^3 higher than the corresponding value calculated for the years 1995−2016 (63.9 µg/m^3) (excluding 2003). Also, the average ozone content for the summer season (June−August) 2003 (86.5 µg/m^3) was much higher (by 19.1 µg/m^3) than the corresponding average seasonal value for 1995−2016 (excluding 2003). According to Solberg et al. (2008), high air temperature, intense solar radiation and related drought phenomena that occurred in Europe in the summer of 2003 contributed to the increase in the ground ozone content, in particular through:

- increasing the rate of chemical reactions,
- intensive production of biogenic VOCs (especially isoprenes),
- limited dry deposition process.

As follows from the above, the prevailing meteorological situation determining the occurrence ozone concentrations in 2003 that were higher than average significantly influenced the direction of changes in ozone content over the years 1995−2016.

4. IMPACT OF SELECTED METEOROLOGICAL PARAMETERS ON THE VARIABILITY OF GROUND-LEVEL OZONE CONTENT

Meteorological conditions, along with chemical substances that are ozone precursors, play a key role in the formation of ground-level ozone in a given area. As shown earlier (Chapter 2) photochemical ozone production, ozone transport as well as ozone deposition processes are largely determined by the prevailing synoptic situation.

Theoretical considerations regarding the impact of basic meteorological parameters on the concentration of ozone in the ground layer of the atmosphere were supplemented by an analysis of the dependence of ozone concentration on meteorological conditions, based on the measurements of ozone and the four basic meteorological parameters:

- air temperature [°C],
- global solar radiation [W/m^2],
- relative humidity of air [%],
- wind speed [m/s].

Calculations were made for all measuring stations analyzed in the present study for 2005−2012. Depending on the season of the year, data averaged over the span between local time hours listed below were used:

- spring (March, April, May): 8:00−18:00,
- summer (June, July, August): 7:00−20:00,
- autumn (September, October, November): 8:00−18:00,
- winter (January, February, December): 8:00−16:00.

On the basis of these data, the mean monthly values of individual parameters in each year were calculated, and then the average monthly value for 2005−2012 was computed as the arithmetic mean.

The first part of the assessment of the impact of selected meteorological parameters on the ground-level ozone concentration is the correlation analysis. Tables 9 through 12 present the values of the Pearson correlation coefficient (r) between the ozone concentrations and the values of selected meteorological parameters. Statistically significant values ($p < 0.05$) are marked in red. In order to characterize in detail the relationship between ground-level ozone and selected meteorological parameters, calculations of the Pearson linear correlation coefficient were made separately for each month of the year.

4.1 Air temperature

Air temperature is one of the main meteorological parameters determining the ozone content in the ground layer of the atmosphere. The impact of air temperature changes on ozone concentration can be considered in several aspects:

(1) Temperature is one of the most important factors determining the speed of chemical reactions. The mechanism assumes that an increase in temperature causes an increase in the average speed of molecules, thus enhancing the increase of their kinetic energy and the number of collisions, which results in an increase in the number of effective collisions (http://materialy.wb.

pb.edu.pl/mariolasamsonowicz/files/2012/12/Wyk%C5%82ad-9-kinetyka-reakcji-chemicznych.pdf). The temperature-dependent reaction rate constant (k) is a characteristic value for a given reaction and can generally be expressed using the Archenius equation:

$$k = A \exp\left(-Ea/T\right), \tag{25}$$

where Ea and A are constant values determined in the laboratory, characteristic for a given reaction.

For the majority of chemical reactions $Ea > 0$ which means that the rate of collisions of particles increases exponentially with increasing temperature, although reactions for which $E < 0$ exist too. Hence, when the temperature changes, there are some reactions participating in the reaction cycle which are more sensitive to temperature changes, and they will be either more or less significant compared to those that are less sensitive to temperature changes. Hence, considering the reaction chain leading to the production of ozone, the occurrence of temperature changes will result in a change in the significance of these reactions in the chemical cycle and, as a result, affect the amount of ozone formed. According to Walcek and Yuan (1995), in polluted areas, characteristic of urban sites, where the concentration of NO_x and VOC is relatively high, the increase in temperature enhances the rate of ground-level ozone formation.

Air temperature affects the lifetime in the atmosphere of PAN (peroxyacetic nitric anhydrite) chemical compounds with the general formula $RC(O)OONO_2$. The most common representative of the PAN family is peroxyethane anhydride ($CH_3C(O)OONO_2$) also commonly known as PAN, whose precursor is acetaldehyde (CH_3CHO), which is the oxidation product of many VOCs. Of importance from the point of view of ground-level ozone is the fact that PAN compounds function as effective reservoirs for both nitrogen (NO_x) and radical ($CH_3C(O)O_2$) compounds. For this reason, the life time of the PAN is very important, and since the process of thermal decay is the main way of removing this compound from the atmosphere, the effect of temperature on this mechanism is decisive. The efficiency of PAN decomposition in the troposphere is a function of altitude: the lifetime of PAN increases with increasing altitude and simultaneously with decreasing temperature (Seinfeld and Pandis 2006). At 22°C it is about 1 hour, while at –23°C it can take up to several months, which indicates a large dependence on the value of air temperature (Jacob 1999). In the mid- and upper troposphere, PAN can be transported over considerable distances and in warmer areas, often far away from the place of its origin, it undergoes decomposition as a result of the following reaction (26):

$$CH_3C(O)OONO_2 \rightarrow CH_3C(O)OO + NO_2 \tag{26}$$

being a source of NO_x, thus affecting the amount of ozone produced.

(2) Temperature affects the level of isoprene emissions − the main VOC representative in the process of ground-level ozone with NO_x. Isoprenes, due to the existence of a triple bond between carbon atoms, are a very reactive group of organic compounds. They easily react with both OH and O_3 radicals, and their lifetime in the troposphere, taking into account the reaction with the above chemical compounds, is of about 1.7 hours and 1.3 days, respectively (Seinfeld and Pandis 2006). In a situation in which VOC in the atmosphere is absent, ozone production settles at a certain constant level determined by the initial content of NO_x, O_3 and the amount of UV (see Chapter 2).

(3) Temperature affects the height of the mixing layer. The rapid increase in the height of the mixing layer is due to the increase in temperature at the earth's surface, which begins to rise

gradually just after the sunrise. At the same time, in the early morning, ozone precursors freshly emitted into the atmosphere during the morning rush hours accumulate near the earth's surface. The low altitude of the mixing layer at this time of the day and the low wind speed result in a low ventilation rate and hence a poor dispersion of pollutants. When the intensity of solar radiation increases, the conversion of ozone precursors to ozone begins as a result of photochemical processes raising the level of O_3 at the earth's surface. Over time, along with increasing height of the mixing layer and the development of vertical air exchange, one would expect a decrease in the ozone content in the surface layer due to its elevation to higher parts of the troposphere, which is true provided that there is no ozone there. In the opposite situation, when ozone is present in the night layer of vanishing turbulence (the so-called residual layer, about 1 km above the ground, which is a residue from a well mixed day layer from the previous day), vertical air mixing can actually contribute to overground ozone increase by bringing this ozone layer down to the surface of the earth (Zhang and Rao 1999). It has been proved that on days with high ozone content, the night layer of vanishing turbulence is an ozone reservoir, which, as the mixing layer develops due to the increase in temperature during the day, can contribute, during ozone episodes, to the growth of ground-level ozone on the next day morning (Zhang et al. 1998).

Table 9 presents the coefficients of correlation between ground-level ozone concentration and air temperature.

As can be seen from the Table 9, the correlation shows high variability throughout the year; a significant difference in the correlation coefficient can be sometimes observed even from month to month.

Table 9

Correlation coefficients determining the level of linear relationship between the air temperature and ground-level ozone concentration

Temperature						
Station / Month	Belsk	Granica	Legionowo	Radom	Warszawa-Krucza	Warszawa-Ursynów
January	–0.16	0.00	–0.23	–0.09	–0.07	–0.28
February	0.01	–0.12	–0.24	–0.07	–0.17	–0.04
March	–0.08	–0.09	–0.08	0.10	–0.08	0.04
April	0.59	0.62	0.63	0.52	0.53	0.64
May	0.62	0.59	0.61	0.55	0.58	0.59
June	0.59	0.59	0.66	0.51	0.61	0.64
July	0.79	0.79	0.85	0.69	0.78	0.75
August	0.72	0.73	0.76	0.60	0.74	0.76
September	0.77	0.75	0.75	0.71	0.80	0.81
October	0.37	0.27	0.22	0.42	0.13	0.41
November	0.00	0.09	–0.07	–0.05	0.11	0.13
December	–0.02	0.05	–0.14	–0.05	0.00	0.04

Note: Statistically significant values ($p < 0.05$) are marked red.

The distribution of correlations between air temperature and ozone concentration presented here indicates the dominant role of photochemical production of ozone in the warm months of the year (April−October). An increase in temperature during this time enhances the rate of chemical reactions. In addition, the April−October period is the growing season of plants. Higher temperatures during this time may contribute to more intense VOC (isoprene) emissions, increasing the efficiency of photochemical ozone production. In addition, in the spring and summer months, when the ozone content in the lower troposphere is relatively high, an increase in air temperature just after sunrise triggers convective processes and increases the vertical air exchange. The negative correlation between the value of air temperature and ozone concentration, appearing especially in the winter months, indicates the opposite situation than in the rest of the year, namely, a decrease in air temperature causes an increase in ozone concentration. This pattern can be associated with the prevailing baric situation shaping the weather in different seasons. In winter, the activity of 2 baric centers is dominant over Poland: the year-round Icelandic Low, whose maximum effect is exerted in winter, and the East Asian High. The dominance of the former results in thaw weather, with typical positive values of air temperature reaching +10°C, cloudy and frequent rain or sleet (Kaczorowska 1986). This type of weather is not conducive to photochemical production processes, hence the significantly limited temperature impact manifested by statistically insignificant correlation coefficient values. The dominance of the latter results in the inflow of dry and cold air over Poland. During this time, the temperature falls below 0°C (usually below –10°C), and the weather is cloudless and sunny (Kaczorowska 1986). Such high pressure systems stagnating for several days, resulting in low temperatures, low winds and minimal cloudiness also favor the formation of temperature inversion, which, developing in the ground layer of the atmosphere, is a kind of trap for pollution accumulated at night. During the day, photochemical reactions involving accumulated ozone precursors initiated by solar radiation contribute to an increase in ozone concentration (Schnell et al. 2009).

The negative correlation of the air temperature value with the ozone content can also be explained by the advection of Arctic air masses over Poland at this time of year. Arctic areas are characterized by relatively high ozone concentrations, with a maximum in winter (Helmig et al. 2007). The inflow of masses of cold, dry, ozone-rich air from the north partly justifies the negative correlation between air temperature and ozone content in the winter months.

4.2 Global solar radiation

The dominant sources of ozone in the ground layer of the atmosphere are chemical processes involving ozone precursors (NO_x, VOC) in the presence of solar radiation of the appropriate wavelength. Photochemical reactions are initiated by the absorption of radiation by the reacting compound, with each absorbed photon of light responsible for the transformation of only one molecule. Absorption of radiation leads to the formation of a molecule in the excited state, which can then participate in the so-called primary photochemical process and then in secondary photochemical processes taking place without the participation of solar radiation between products created in the primary process.

On the example of the ozone production cycle, the above stages can be described as follows:

$$NO_2 + h\nu\ (\lambda < 424\ \text{nm}) \rightarrow NO + O\ \text{(primary process)} \quad \text{(1), repeated}$$

$$O + O_2 + M \rightarrow O_3 + M\ \text{(secondary process)} \quad \text{(2), repeated}$$

Another aspect to mention when discussing the role of solar radiation in forming ozone concentration is its impact on the lifetime of PAN. Because PAN has the ability to absorb UV

radiation, the photolysis process is, along with thermal decay, the basic mechanism for removing PAN from the atmosphere (Seinfeld and Pandis 2006). However, while thermal decay is the dominant mechanism for PAN removal in the lower troposphere, photolysis plays a key role in the destruction of PAN at an altitude of over 7 km (Mazely et al. 1995).

Table 10 presents coefficients of correlation between ground-level ozone concentration and global solar radiation.

Table 10

Correlation coefficients determining the level of linear relationship between the solar radiation intensity and ground-level ozone concentration

Solar radiation						
Station / Month	Belsk	Granica	Legionowo	Radom	Warszawa-Krucza	Warszawa-Ursynów
January	0.35	0.13	0.35	0.23	0.12	0.27
February	0.47	0.27	0.31	0.31	0.39	0.45
March	0.64	0.44	0.59	0.59	0.57	0.58
April	0.58	0.58	0.68	0.65	0.46	0.7
May	0.71	0.64	0.73	0.72	0.66	0.7
June	0.71	0.62	0.71	0.61	0.77	0.71
July	0.66	0.6	0.65	0.66	0.26	0.6
August	0.58	0.59	0.33	0.59	0.65	0.66
September	0.73	0.66	0.8	0.63	0.45	0.76
October	0.56	0.46	0.64	0.45	0.42	0.68
November	0.38	0.3	0.31	0.28	0.43	0.32
December	0.2	0.14	0.14	0.21	0.12	0.2

Note: Statistically significant values ($p < 0.05$) are marked red.

As follows from Table 10, the correlation between ground-level ozone and solar radiation is positive each month and at each station, in the vast majority being statistically significant. Usually a positive, significant relationship between the increase of solar radiation value and the content of ground-level ozone confirms the important role of this meteorological parameter as the initiator of photochemical processes (see Chapter 2), resulting in the formation of ground-level ozone. Probably, the impact of radiation on the distribution of PAN substances as a result of photolysis is also not insignificant. PAN as a potential reservoir of NO_x compounds, undergoing decomposition, releases significant amounts of NO_2 into the atmosphere, contributing to the increase in ozone production.

4.3 Relative humidity

The content of water vapor in the air affects the ozone content in the ground layer of the atmosphere in many ways, e.g., by modifying the process of dry ozone deposition, affecting the formation of "wet aerosols", as well as affecting the course of chemical reactions, thereby regulating the concentration of reactive radicals, nitrogen oxides and ozone itself.

One of the main mechanisms of ozone removal from the atmosphere is photodissociation of the ozone molecule (see Chapter 2), which may result in the formation of an excited oxygen atom [$O(^1D)$]. The same atom can then react with H_2O to form hydroxyl radicals. Strongly reactive radicals entering the appropriate reaction cycle in an environment with a sufficiently high NO_x content contribute to the production of an ozone molecule. In a place where the amount of NO_x is too low, this cycle does not ultimately produce ozone. Hence, the increase in relative humidity will favor the reaction of the oxygen atom with H_2O, and ozone recovery as a result of subsequent reactions may be only partial, which in turn may lead to a reduction in the ozone content.

According to Lelieveld and Crutzen (1991), higher relative humidity is usually associated with more intense cloud formation and, thus, a greater cloudiness. The impact of clouds on shaping the concentration of ground-level ozone is twofold: firstly, clouds, through the processes of scattering and absorbing solar radiation, reduce its inflow to the earth's surface, thus limiting the scale of photochemical processes leading to ozone formation; and secondly, the occurrence of water clouds exerts a significant modification to the photochemical processes in the lower part of the troposphere. Relative humidity plays an important role in the dry ozone deposition process by regulating the stomal conductivity of plants. Along with solar radiation intensity and the effects during the light phase of photosynthesis, as well as CO_2 concentration and its assimilation processes, the air humidity and soil water availability are the basic factors determining the intensity of stomata conductivity of leaves (Maleszewski et al. 2003). In response to a decrease in humidity in the air, stomata of plants close up (Maleszewski et al. 1999), limiting the absorption of ozone inside the plants and increasing its concentration at the earth's surface. The absorption of ozone by plants through stomata is the main mechanism for ozone removal through dry deposition by mature plants, alongside other mechanisms such as ozone deposition on soil or plant leaves, that can play an important role in some ecosystems. According to Zhang et al. (2002), ozone deposition on the cuticle surface of plants increases exponentially as the relative humidity increases.

The high content of water vapor in the air promotes the formation of new aerosols as a result of nucleation processes, which in turn affect the inflow of solar radiation to the earth's surface through absorption and scattering processes, ultimately reducing the potential for photochemical reactions.

Table 11 presents values of correlation coefficients between ground-level ozone concentration and relative humidity.

As Table 11 shows, the correlation between ground-level ozone and relative humidity throughout the year is negative and, with only one exception (January – Warszawa-Krucza), statistically significant each month at all the stations. This means that regardless of the season, an increase in the water vapor content of the air causes a decrease in the ozone content. The highest absolute values of the correlation coefficient were recorded for warm months, from April to October. In the vast majority of cases, its absolute value was not less than 0.60, and the maximum absolute value was 0.82 (April – Warszawa-Ursynów). The negative correlation between ground-level ozone concentration and relative humidity indicates the important role of the mechanisms described above. Higher relative humidity is usually associated with greater cloudiness, and the presence of clouds makes it possible for chemical reactions to occur, which ultimately reduces the ozone concentration. The increase in relative humidity intensifies other processes that reduce the ozone content, namely the increase in the absorption of ozone by plants through stomata. This mechanism plays a special role during the growing season of plants, i.e., from April to October, due to the presence of leaves on trees and bushes. Equally important is the process of photodissociation of ozone and further reactions of the excited oxygen atom $O(^1D)$ with the participation of H_2O.

Table 11

Correlation coefficients between the relative humidity value and ground-level ozone content

Station / Month	Belsk	Granica	Legionowo	Radom	Warszawa-Krucza	Warszawa-Ursynów
January	–0.47	–0.40	–0.49	–0.56	–0.20	–0.43
February	–0.43	–0.43	–0.58	–0.57	–0.61	–0.54
March	–0.59	–0.57	–0.55	–0.65	–0.58	–0.60
April	–0.74	–0.76	–0.74	–0.77	–0.80	–0.82
May	–0.81	–0.81	–0.77	–0.77	–0.78	–0.76
June	–0.73	–0.72	–0.74	–0.69	–0.67	–0.78
July	–0.70	–0.68	–0.72	–0.74	–0.40	–0.67
August	–0.62	–0.63	–0.66	–0.57	–0.66	–0.65
September	–0.79	–0.73	–0.78	–0.77	–0.71	–0.80
October	–0.61	–0.59	–0.66	–0.70	–0.77	–0.69
November	–0.64	–0.56	–0.50	–0.60	–0.75	–0.58
December	–0.47	–0.38	–0.47	–0.47	–0.29	–0.45

Note: Statistically significant values ($p < 0.05$) are marked red.

4.4 Wind speed

The impact of wind speed on ozone concentration can be twofold, depending on whether the surface layer of the atmosphere functions as a source of ozone resulting from photochemical processes occurring in it, or as an ozone deficit site, where its production is limited. In the first case, a strong increase in wind speed with altitude will have a negative effect on ozone concentration in a given place, leading to its transport to higher parts of the troposphere as a result of vertical mixing processes. In the second case, when the production of ozone in the subsurface layer is limited, vertical air mass exchange and transport of ozone-rich air make a significant contribution to the ozone budget (Tarasova and Karpetchko 2003).

Moreover, when the wind blows from the direction of contaminated areas, which are a potential source of ozone precursors and ozone itself, the correlation between wind speed and ozone content can be significantly positive. This applies to the inflow of air masses both of a local nature as well as long-range transport (Shan et al. 2008).

Table 12 presents values of correlation coefficients between ground-level ozone concentration and wind speed.

Analyzing Table 12, it can be concluded that the dependence of ozone concentration on the value of wind speed over the year shows a large variability. The first feature which is worth attention is the positive, statistically significant correlation between the parameters in the months October–February at all measuring stations. During this period, the increase in wind speed contributes to the higher ozone concentrations recorded in the analyzed area. The months of March, April, and May, as well as August and September, turned out to be transitional months in which it is difficult to see the common pattern of the relationship between the considered parameters for all stations. In June and July, negative correlation coefficient values were recorded for all measuring stations. The fact that in the cold months all correlation coefficients

are statistically significant points to the special role of this meteorological parameter (generating transport) in this part of the year in shaping ozone concentrations in a given area.

Table 12

Correlation coefficients determining the level of the linear relationship between the wind speed and ground-level ozone concentration

Wind speed						
Station / Month	Belsk	Granica	Legionowo	Radom	Warszawa-Krucza	Warszawa-Ursynów
January	0.33	0.56	0.48	0.30	0.55	0.34
February	0.18	0.31	0.25	0.30	0.31	0.31
March	–0.02	0.09	0.02	0.17	0.08	0.12
April	–0.19	–0.11	–0.11	–0.04	–0.08	0.08
May	0.11	0.19	–0.11	–0.19	–0.06	–0.08
June	–0.16	–0.06	–0.27	–0.29	–0.09	–0.04
July	–0.23	–0.16	–0.47	–0.17	–0.18	–0.07
August	0.03	–0.02	–0.02	–0.14	0.00	0.01
September	–0.03	0.16	0.06	–0.29	0.03	0.05
October	0.28	0.55	0.50	0.15	0.40	0.39
November	0.37	0.59	0.65	0.23	0.47	0.60
December	0.37	0.60	0.48	0.27	0.52	0.52

Note: Statistically significant values ($p < 0.05$) are marked red.

5. ARTIFICIAL NEURAL NETWORKS

Neural networks, as a separate field of research, was established the 1940s by Warren McCulloch and Walter Pitts (Tadeusiewicz 1993), the scientists who were the first to present a mathematical description of the nervous system of living beings and associate it with the data processing. They claimed that any logical thesis can be coded with a properly constructed neural network because the action of a group of interrelated artificial neurons forming an artificial neural network can be identified, in a general sense, with the work of the brain (Marsalli 2006). Imitating simple cells (neurons) that, when connected together in the form of an intricate network, can process complex signals, those authors have created a very simplified model of a biological neuron, which was the foundation for the development of future research in the field of neural networks.

5.1 Structure of the artificial neural network

Due to the nature of the task set for neural networks, the Unidirectional Multi-Layer Perceptron (MLP) type will be applied in this study, and its description will be given further in this chapter. The neural network is a set of interconnected neurons and **its structure is layered** (Fig. 14). The first is the input layer (through which the original data is entered) and the last is the output layer indicating the calculation result, e.g., the forecasted value. Between them there are neurons that mediate input processing, forming layers called hidden layers (usually 1 or 2). The

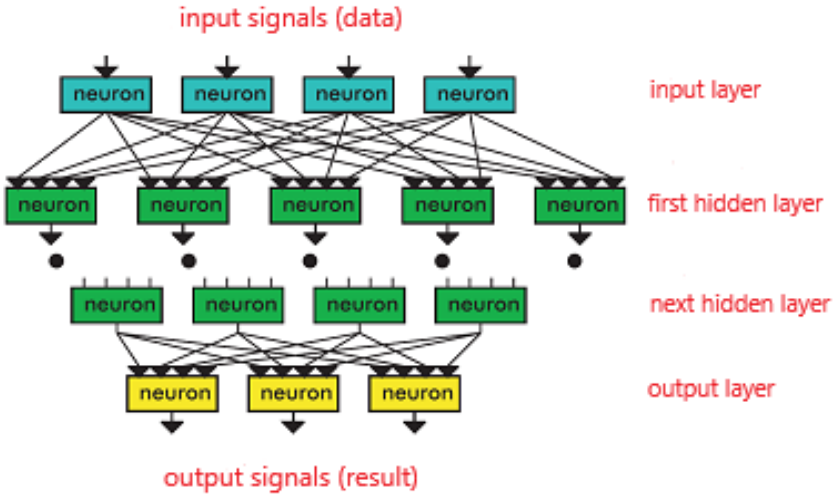

Fig. 14. Example of Unidirectional Multi-Layer Perceptron (MLP) type of neural network (source: Tadeusiewicz et al. 2007).

structure of neuron connections in the network meets the peer-to-peer principle, which means that all output and hidden neurons are connected to each neuron in the preceding layer. Such a connection is partly due to the fact that the algorithmic method of solving the modeled process is often unknown; hence, the method of data transfer is unknown either. As a result, it is not obvious which connections in the network may be necessary and which are unnecessary. During the network training process, the network structure and weighting factor values are determined, with non-zero values defining important signal processing connections and zero or very low absolute values defining connections that do not affect the determination of the output value and can be finally removed from the network. As can be seen from the above, the advantage of applying the peer-to-peer principle is that every important combination will be included in the calculation.

5.2 How do neural networks work?

Artificial neural network is a system of interconnected individual processing elements − neurons, which represent their biological counterparts. The main purpose of neurons is to convert the input signal into an output signal. In nonlinear types of neural networks, the processing consists of two parts:

- aggregation of input data,
- estimation of the neuron's output value.

Usually, neurons are characterized by the presence of multiple input data (i_1, i_2, i_3, ..., i_n) and one output value. Such a system causes the need to transform the input vector $i = (i_1, i_2, i_3, ..., i_n)$ into a single value, i.e., the so-called aggregate input value. The weight values appropriate for each neuron have a fundamental impact on this transformation. The most commonly used input aggregation formula, i.e., the linear aggregation, consists in adding up the products of all input values and the corresponding weight values. Such an aggregate input value, in a linear-type network, is automatically treated as the neuron output value. In multilayer networks (e.g., MLP), after the process of data aggregation is completed, there comes the second stage of neuron activity, i.e., the process of determining its output value using the appropriate activation function. The selected activation function is responsible for determining the method of calculating the output value on the basis of the previously calculated aggregate input value. The type of activation function used determines the behavior of the entire neural network. The activation functions commonly used are:

- linear function,
- sigmoid function (with values from the range: (0, 1)),
- tangentoid function (with values from the range: (–1, 1)),
- Gaussian function.

The choice of an appropriate activation function depends on the type of problem the network is facing to solve. In multilayer networks, nonlinear functions are usually used, because their neurons have the greatest learning ability and allow mapping the relationship between input and output data in a continuous manner.

5.3 Efficiency and usability of artificial neural networks

Neural networks are a practical modeling technique based on the structure and mode of action of the human brain. The usefulness and helpfulness of neural network models have meant that they can be used in data processing as well as prediction, classification or control. The ability to map extremely complex functions is related to the fact that the networks are non-linear. In addition to the ability to map nonlinear relationships, a very important feature of neural networks is their ability to operate in terms of multidimensionality − extremely important in the case when nonlinear processes with a large number of variables are modeled (www.statsoft.pl).

The use of neural networks is based on the effective mapping of relationships between dependent and independent variables. It can be a single dependence or a set of dependencies, even very complex and complicated, hardly discernible using classical interpretation methods, e.g., correlation coefficients.

5.4 Artificial neural network training

The effective operation of the neural network depends on:

- network structure determined by the number of layers, the number of neurons in individual layers and the selected activation function,
- network topology determined by the method of aggregation of input data or the selected activation function,
- values of weight coefficients of individual neurons.

The mechanism that allows the network to function properly by modifying weighting factors and selecting the network structure is called the neural network's training process. The training process in MLP networks is carried out under supervision, using the so-called teacher-assisted learning algorithm.

The essence of the teacher-assisted learning process is that the training data set contains both input and output data. Presenting both types of data enables the network to detect and learn the relationship between data. The training process can be defined as a cycle of searching for the appropriate parameter configuration, i.e., threshold values of neuron activation and weighting factors present in elements of the entire neural network in order to minimize the network error. The above parameters are being consistently changed using an appropriate training algorithm.

The most commonly used algorithm for multi-layer network training is the back-propagation algorithm. The idea of the algorithm is to determine and reduce the value of the error made by the network in hidden layers based on the determined backwards value of the error diagnosed in the output layer. The ultimate goal of the network training process by backward error propagation is to determine the minimum error function. To this end, this algorithm uses the gradient method − the fastest drop. As a result of the effective operation of the algorithm, the error is gradually reduced, which improves the network's performance. In order to determine the network's error, the values obtained at the output should be compared with the actual output values. Based on the error values, the weighting coefficient of the neuron is corrected in such a way that the total error made by the network is minimized for all the data forming the training

set. The network is trained stepwise: the consecutive steps, bringing the network closer to finding the optimal solution, are described as training epochs. It is to be noted that error minimization during the training process does not apply to the error for all network cases but only to the error value calculated for the training set. Therefore, there is a strong need to be able to generalize training experience in relation to new cases. The ability to generalize, i.e., determine the correct answers for input data that have not participated in the network training process is a very important attribute of neural networks. The gradual decline in generalization skills is called "network overfitting". It consists in the fact that the network begins to over-adapt to training values, losing the ability to generalize. It is important to fit the model to the overall pattern of the analyzed dependence and not to the smallest details presented by individual data. The negative effects of the "network overfitting" phenomenon necessitate the early diagnosis of the vanishing tendency of the neural network to generalize. To this end, it is practiced to split the entire data package into three sets:

- training set (presented to networks in the process of network training, used to transform the values of network parameters),
- test set (not participating in the network training process, used for ongoing, independent assessment of the training progress),
- validation set (not involved in the network training process, used to perform the final general assessment of the correctness of the network after the training process has been completed).

6. ARTIFICIAL NEURAL NETWORKS AS A TOOL FOR FORECASTING THE GROUND-LEVEL OZONE CONCENTRATION AT SELECTED MONITORING STATIONS IN THE MAZOWIECKIE VOIVODESHIP

6.1 Research methodology

The aim of the research described in this chapter was to analyze the possibility of using automatic neural networks in forecasting the content of ground-level ozone for the next day at selected measuring stations of the Mazowieckie Voivodeship. The method of ozone concentration prediction based on artificial neural networks is widely used and widely discussed in world literature (Garcia et al. 2011; Elkamel et al. 2001; de Souza et al. 2015; Gardner and Dorling 2001). Hence, keeping in mind the need for the correctness of operation and accuracy of prediction, it was planned to construct a model realizing the forecast of the maximum average 1-hour value of ozone concentration per day on the next day for the following measuring stations: Belsk, Granica, Legionowo, Radom-Tochterman, and Warszawa-Ursynów.

The aim of the work was achieved through the following actions:

(1) Acquisition of the results of forecasts of basic meteorological parameters for the period: April−September 2014 and April−September 2015 created using the global numerical weather forecast model WRF ARW (The Weather Research and Forecasting Model, Versiona ARW (Advaced Research WRF)) (Skamarock et al. 2008). The acquired data contained a forecast of the values of:

- air temperature [°C],
- solar radiation [W/m^2],
- wind speed [m/s],
- relative humidity [%],

for the next day for each of the aforementioned stations. For 2014, the data was generated every 3 hours (i.e., 00:00, 03:00, 06:00, ..., 21:00), and for 2015 every 1 hour (00:00, 01:00, 02:00, ..., 23:00). For a given hour, the parameter values were instantaneous.

The creation and search for optimal neural networks was based on data from 2015. The data from 2014 was used in the further part of the analysis to check the effectiveness of the selected neural networks.

(2) Implementation of 2015 data into a spreadsheet and compilation of tables containing the appropriate data values:

- for the prediction of the maximum 1-hour value of O_3 concentration on the next day, the maximum values of the abovementioned meteorological parameters were selected from the available prognostic data. The created data set has been supplemented with the two variables:
- value specifying the month for which the O_3 concentration prediction was carried out. The following months of the year were marked by their numerical equivalents (4 for April, 5 for May, ..., 9 for September). The forecast period per year is limited to six months, April through September, due to the high probability of occurrence of high concentrations of overground ozone at that time, so that its permissible level in terms of health protection is likely to be exceeded;
- the maximum value of 1-hour O_3 concentration per day on the day preceding the forecast.

In the author's opinion, the inclusion of the above-mentioned additional variables (in addition to variables in the form of meteorological parameters, which, as shown in previous chapters, affect the value of ground-level ozone), could have a significant influence on the quality of the neural network training process and, hence, the resulting final network.

When choosing the variables used to construct the model, the author has been taking into account:

- knowledge of the nature of the analyzed problem (processes of ground-level ozone formation and destruction),
- availability of input data.

(3) Implementation of data sets including meteorological parameter values, O_3 values on the previous day and the month number to the Statistica 10 Program with the available extension "Automatic Neural Networks". The appropriate parameters in the form of columns constituted model variables, and the values of these variables on the next day of the analyzed period (April−October 2015) in the form of rows were model cases (Table 13). All values in the data set were numerical values belonging to a specified range.

Table 13

Structure of the input set listing the number of cases and variables for the ground-level ozone concentration forecast

	Forecast 1h max	
	Cases	Variables
Belsk	158	6
Granica	146	6
Legionowo	160	6
Radom	150	6
Warszawa-Ursynów	156	6

Six input variables were used for each station and type of network. The number of cases varied, ranging from 146 to 160. The number of cases needed to carry out the correct training process is difficult to determine. In fact, there are some standards that make the number of cases dependent on the network architecture, e.g., that the number of cases should be at least ten times greater than the number of connections in the network. However, the size of the training set is determined by the complexity of the modeled phenomenon, and because the complexity of the function of the studied problem is not known, an appropriate method that would accurately determine the number of cases does not exist.

(4) Division of the entire data set into the subsets:
- training (70% of data),
- test (15% of data),
- validation (15% of data) (Table 14).

The purpose of this division was to avoid over-matching of the network to training data (i.e., loss of generalization skills). Since the minimization of error in the training process concerns the training data subset only, two additional subsets (test and validation) have been established and the cases they contained were not presented to the network during the training process. Observation and analysis of the error value in all subsets allowed to control and avoid the phenomenon of network overtraining.

Table 14

The number of data in individual neural network subsets used for the ground-level ozone concentration forecast

	1h max		
	Subset		
	Training	Test	Validation
Belsk	112	23	23
Granica	104	21	21
Legionowo	112	24	24
Radom	106	22	22
Warszawa-Ursynów	110	23	23

The assignment of cases to individual subsets was made randomly. The training subsets consisted of 104 to 112 cases, test subsets from 21 to 24 cases and validation subsets from 21 to 24 cases. All input and output data were in numeric form.

6.2 Construction of artificial neural networks

In the initial stage of the study, the "Automatic network designer" function with the regression model was applied (for each location). The analysis of the five best networks retained by the program allowed for an initial overall assessment of the quality of the generated models, serving for reference only. The author decided that the quality (expressed by correlation coefficients) of the models obtained in this way was insufficient and the error values were too large. Since the quality of the forecast in subsequent iterations of network training has not improved, at this stage of network designing the function "Automatic network designer" was each time (for each

measuring station) terminated, and we began to improve the neural model ourselves, using the "User Design" function. The process of generating the optimal model for predicting ground-level ozone concentration was based on testing various three-layer MLP neural networks using a regression model, changing the number of neurons in the hidden layer and the activation function. A supervised training method was used, which means that we knew the output (real) values, which were the correct, desired network response for a given set of input signals. The BFGS (Broyden-Fletcher-Goldfarb-Shanno) quasi-Newtonian algorithm belonging to the set of gradient methods was used to create all the networks. Networks have been trained for 200 eras. Weights were initialized randomly and then, during the network training process, their reduction was not used. The error function in all cases was the SOS (sum of squares) function, in which the difference between the output value estimated by the network and the actual value set as a standard is squared and then added:

$$E_{\mathrm{SOS}} = \sum_{i=1}^{n}(x_i - y_i)^2 \tag{27}$$

where x_i is the network output value, and y_i is the real value.

According to Cybenko (1989), the structure of a network with one hidden layer is able to forecast with a sufficiently small error any limited continuous function. Therefore, while the choice of MLP networks with three layers (input, hidden, output) was justified, the appropriate selection of the number of neurons in the hidden layer was not so obvious. A larger number of hidden neurons allows mapping more complicated phenomena but at the same time can cause excessive network development, resulting in a slower pace of its operation and a tendency of over-adapting to training values (loss of the ability of knowledge generalization). In turn, too few neurons in the hidden layer may cause the network to be inefficient in solving complicated tasks. To determine the range of the number of neurons in the hidden layer, the rule proposed by Goethals et al. (2007) was used, according to which the number of neurons in the hidden layer depends on the number of input and output signals of the network (Table 15).

Table 15

Rules defining the number of neurons in the hidden layer based on the number of input data (In) and output data (Out)

Rule	Result
2/3 × In	2/3 × (6) = 4
0.75 × In	0.75 × (6) = 4.5
0.5 × (In + Out)	0.5 × (6 + 1) = 3.5
2 × In + 1	(2 × (6)) + 1 = 13
2 × In	2 × (6) = 12

Note: Corrected version based on Goethals et al. (2007).

Following the suggestions of Goethals et al. (2007) and other authors (Hooyberghs et al. 2005; Melas et al. 2000), networks containing 3 to 13 neurons in the hidden layer were checked.

In this work, optimization of the number of neurons in the hidden layer was carried out empirically, by testing the quality of the three-layer MLP network with different numbers of neurons in the hidden layer. In the same way, the quality of network operation was analyzed with various hidden and output layer activation functions: linear, tanh, logistic, exponential and sinh. On this basis, a set of several hundred networks was generated. Optimization of the most

appropriate neural model from a set of networks with different topology (different number of neurons in the hidden layer and different activation functions in the hidden and output layer) was made based on the analysis of the basic criteria:

- Prediction error values for all subsets (training, test, validation). The greatest attention was paid to the size of error in the validation and test subsets, which were independent, not participating in the training process. It is important for the error values in all subsets to be as low as possible and for the test error to be comparable to a validation error because it indicates that the data in the subsets have been selected in a representative way. At the same time, it is important that the values of validation and test errors be not significantly different from the learning errors, as this may indicate the network's inability to generalize the training results;
- The network quality for all subsets expressed in the form of correlation coefficients between network responses and actual values set as a standard.

The analysis of the above factors made it possible to select the five best networks (one per each measuring station) realizing the forecast of the value of the maximum 1-hour O_3 concentration per day for the next day (Table 16).

Table 16

Characteristics of selected artificial neural networks for performing the forecast of the maximum daily 1-hour O_3 concentration for the next day

1 h max	Network type	Net. architecture	Correlation coefficient			Error			Training algorithm	Error function	Activation function	
			Training	Test	Validation	Training	Test	Validation			Hidden layer	Output layer
Belsk	MLP	6-6-1	0.92	0.87	0.88	57.9	55.9	48.6	BFGS 40	SOS	Tanh	Linear
Granica	MLP	6-4-1	0.92	0.90	0.89	45.7	46.2	50.2	BFGS 37	SOS	Tanh	Exponential
Legionowo	MLP	6-3-1	0.94	0.91	0.87	56.8	38.1	50.6	BFGS 63	SOS	Tanh	Exponential
Radom	MLP	6-7-1	0.93	0.89	0.90	57.8	42.4	45.9	BFGS 56	SOS	Logistic	Linear
Warszawa Ursynów	MLP	6-4-1	0.93	0.93	0.85	48.3	66.0	66.5	BFGS 33	SOS	Tanh	Logistic

6.3 Architecture of artificial neural networks for predicting the maximum 1-hour ozone concentration

In this subsection, the following network structure description system is used:

- Abbreviation of the type of neural network – Multi-Layer Perceptron, MLP;
- Designation of network architecture in the form of the number of neurons in the input layer, the number of neurons in the hidden layer, and the number of neurons in the output layer, separated by dashes. The number of neurons in the input layer (6) is constant and represents the number of input data − factors determining the content of ground-level ozone (meteorological parameter values as well as month number and ozone concentration on the day preceding the forecast). The number of neurons in the

output layer (1) is also constant, being the predicted value of ozone concentration in the ground layer of the atmosphere.

The Statistica 10 "Automatic Neural Networks" package uses the correlation coefficient values between the network output data being the values of the forecast and the actual values measured at the measuring station to assess the quality of the generated network. The interpretation of the correlation strength between the variables was made based on the values of the correlation coefficient, *r*, according to Rowntree's (1981) classification:

$0.0 < |r| \leq 0.2$ − very weak correlation,
$0.2 < |r| \leq 0.4$ − weak correlation,
$0.4 < |r| \leq 0.7$ − average correlation,
$0.7 < |r| \leq 0.9$ − high correlation,
$0.9 < |r| \leq 1.0$ − very high correlation.

6.3.1 Belsk

The selected best neural network forecasting the maximum 1-hour value of overground ozone for the Belsk measuring station had the 6-6-1 MLP structure with a hyperbolic tangent activation function for the hidden layer and a linear activation function for the output layer. The model reached the optimal level of approximation over the 40th training cycle. The prediction error for individual subsets is 57.9 for the training subset, 55.9 for the test subset, and 48.6 for the validation subset. The error values for the test and validation samples are similar, which indicates the representativeness of the data contained in them; at the same time, the error values of these tests are not significantly different from the error value in the training sample, which in turn indicates the absence of the phenomenon of network overtraining. The correlation coefficients between the actual ozone concentrations and the ozone concentrations estimated by the network are 0.92 for the training subset, 0.87 for the test subset, and 0.88 for the validation subset. The values of all correlation coefficients are statistically significant at the significance level $\alpha = 0.001$, which, according to Rowntree (1981)'s classification, testifies to a high and very high correlation between the variables.

6.3.2 Granica

The optimal neural network selected for forecasting overground ozone content at the Granica monitoring station had the 6-4-1 MLP structure with the hyperbolic tangent activation function for the hidden layer and exponential activation function for the output layer. The network has reached an optimal level of approximation over the 37th training cycle. The value of the prediction error for the training sample is 45.7, for the test sample 46.2, and for the validation sample 50.2. Similar error values in all subsets indicate good representativeness of cases in each of them and the ability of the network to generalize data. All correlation coefficients between the measured ozone concentration values and those calculated by the network are statistically significant at the significance level $\alpha = 0.001$ and amount to: 0.92 for the training set, 0.90 for the test set, and 0.89 for the validation set. This proves that the variables are in a very high and high correlation.

6.3.3 Legionowo

The selected neural network realizing the overground ozone content forecast at the Legionowo measuring station has 6-3-1 MLP architecture with hyperbolic tangent activation function and exponential activation function for the output layer. The network has achieved the approximation criterion in the 63th training cycle. The forecast error for individual subsets was: 56.8 for the training subset; 38.1 for the test subset, and 50.6 for the validation subset. The correlation coefficients between the actual ozone concentration values and the values calculated by the network were: 0.94 for the training sample, 0.91 for the test sample, and 0.87 for the validation

sample. The values of correlation coefficients are statistically significant at the significance level $\alpha = 0.001$ and testify to a very high and high correlation between the variables.

6.3.4 Radom

The neural network chosen as the best for forecasting the 1-hour maximum value of the overground ozone concentration at the Radom-Tochterman measuring station has the 6-7-1 MLP structure with a logistic activation function in the hidden layer and a linear activation function in the output layer. The network reached the level of approximation in the 56th training cycle. The prediction error for individual subsets is 57.8 for the training subset, 42.4 for the test subset, and 45.9 for the validation subset. The values of the correlation coefficient between the ozone concentrations measured at the station and the values generated by the network are 0.93 for the training sample, 0.89 for the test sample, and 0.90 for the validation sample. All coefficients are statistically significant at the significance level $\alpha = 0.001$ and testify to a very high and high correlation between the variables.

6.3.5 Warszawa-Ursynów

The selected best neural network for forecasting 1-hour maximum values of overground ozone at the Warszawa-Ursynów station is characterized by the MLP 6-4-1 structure with the hyperbolic tangent activation function for the hidden layer and the logistic activation function in the output layer. The approximation criterion was achieved in the 33rd training cycle. The values of the prediction error were: 48.3 for the training subset; 66.0 for the test subset; and 66.5 for the validation subset. Calculated values of correlation coefficients between measured data and those estimated by the network were equal to 0.93 for the training sample and also 0.93 for the test sample, as well as 0.85 for the validation sample, which testifies to very high and high correlation of variables.

6.4 Global sensitivity analysis

The quality of the modeling results is largely determined by the selection of appropriate input parameters. In order to check the correctness of using specific input variables in the model and assess how important individual variables are for the operation of the network, a global network sensitivity analysis was performed (Table 17). The analysis consists in checking the value of

Table 17

Results of the global sensitivity analysis of neural networks performing the forecast of the daily maximum 1-hour O_3 concentration for the next day

1 h max	Temperature		Solar radiation		Relative humidity		Wind speed		Previous-day ozone		Month	
	Quotient	Rank	Quotient	Rank	Quotient	Rank	Quotient	Rank	Quotient	Rank	Quotient	Rank
Belsk	5.32	1	1.53	3	1.13	5	1.04	6	1.25	4	2.67	2
Granica	5.88	1	1.26	3	1.21	5	1.24	4	1.07	6	4.82	2
Legionowo	6.38	1	1.73	2	1.07	6	1.15	5	1.57	4	1.57	3
Radom	4.94	1	1.51	4	1.10	6	1.13	5	1.97	2	1.78	3
Warszawa	5.84	1	1.68	2	1.14	6	1.16	5	1.35	4	1.47	3

the total error, while all cases of a given variable will be converted to the average of the training subset, this procedure being performed for all the variables. After such a modification of the dataset, the final prediction error can significantly/insignificantly increase/decrease, or remain unchanged. Then the quotient of network errors is calculated for a network operating without a single variable and for a network operating with a whole series of variables. The size of the error quotient indicates the usefulness of variables in the correct operation of the network − the higher the value of the quotient, the more sensitive the network is to the lack of a specific variable in the input data set. Variables for which the error quotient is above 1 are crucial for the correct operation of the network and should be kept. Variables for which the error quotient is 1 or lower usually do not affect the quality of the network, and their removal can improve the network performance. However, since the variables used as input data are usually not completely independent, you should be careful when deleting individual variables so as not to lose relevant information contained in the coexistence of mutually related variables.

6.4.1 Belsk

The global sensitivity analysis showed that the most important parameter, which has a dominant significance in shaping the 1-hour maximum concentration of ground-level ozone per day, is the value of air temperature with a rank of 1 and an error quotient of 5.32. Another important parameters are the month number of rank 2 and the quotient of 2.67, followed by solar radiation (rank 3, quotient 1.53), ozone content on the previous day (rank 4, quotient 1.25), relative humidity (rank 5 , quotient 1.13) and wind speed (rank 6, quotient 1.04). As the value of the quotient for this last parameter is close to one, modeling test was performed without taking into account wind speed, which has not significantly affected the modeling result. Finally, however, it was decided to keep the wind speed in the input data set.

6.4.2 Granica

The global sensitivity analysis showed that the main parameter affecting the value of 1-hour maximum ozone concentration per day is the value of air temperature with a rank of 1 and a quotient of 5.88. Another, also key parameter is the month number with rank 2 and the quotient value of 4.82. Other significant variables ranked in importance are: solar radiation (rank 3, quotient 1.26), wind speed (rank 4, quotient 1.24), relative humidity (rank 5, quotient 1.21), and maximum ozone content on the previous day (rank 6, quotient 1.07). The values of the error quotient for each variable used in the model were above 1. This indicates that all the input data have been affecting the final result of the forecast.

6.4.3 Legionowo

Interpretation of the global sensitivity analysis showed that the variable that most strongly affects the maximum 1-hour ground-level ozone content per day at the Legionowo monitoring station is the air temperature with a rank of 1 and an error quotient of 6.38. Other variables are characterized by much smaller error quotient values, although in each case greater than one. Sorted in order of importance for the result of the prediction are as follows: solar radiation (rank 2, quotient 1.73), month number (rank 3, quotient 1.57), maximum ozone content on the previous day (rank 4, quotient 1.57), wind speed (rank 5, quotient 1.15), and relative humidity (rank 6, quotient 1.07).

6.4.4 Radom

The global sensitivity analysis showed that the parameter to which the output variable (ozone content) is most sensitive (its lack is most influential) is the value of air temperature, with a rank of 1 and an error quotient of 4.94. The second most important parameter is the maximum ozone content on the previous day with rank 2 and an error quotient of 1.97. The next are: month

number (rank 3, quotient 1.78), solar radiation (rank 4, quotient 1.51), wind speed (rank 5, quotient 1.13), and relative humidity (rank 6, quotient 1.10). No error quotient below one was found for any of the variables used in the model.

6.4.5 Warszawa-Ursynów

From the interpretation of global sensitivity analysis it can be concluded that the key parameter affecting the final result of the prediction is the value of air temperature with a rank of 1 and an error quotient of 5.84. In the second place in terms of importance is solar radiation with rank 2 and a quotient of 1.68. Other parameters ranked by significance are: month number (rank 3, quotient 1.47), maximum ozone content on the previous day (rank 4, quotient 1.35), wind speed (rank 5, quotient 1.16), and relative humidity (rank 6, quotient 1.14). No value of the quotient smaller than one was recorded for any parameter, which indicates that all the variables used in the model are significant.

6.5 Local sensitivity analysis

In addition to the global sensitivity analysis, the results of which were discussed in the previous section, a local sensitivity analysis was also carried out to determine the ranges of input data values that are particularly important for the prediction and the ranges that do not significantly affect it. The local sensitivity analysis consists in making small changes to the quantities subject to local variations, i.e., around 10 points from the entire range of variation of a particular input. Then the model response to a given distortion of an input variable is observed. A significant difference in the result of network prediction after the introduction of the distortion determines which "areas" of variability of a given variable are particularly sensitive to modifications and therefore crucial for the correct formulation of the forecast.

The application of the local sensitivity analysis tool available in the Statistica package "Automatic neural networks" made it possible to determine the ranges of variability of those meteorological parameters that are important for the final result of the prediction, and those that are less important. Based on 10 points evenly distributed throughout the range of a given input variable, charts were created (Fig. 15) which are a graphical presentation of the results of the local sensitivity analysis. The analysis of the charts showed that the effect of air temperature values up to approx. 15°C is not significant for the result of prediction. Values from about 15°C to about 28°C are characterized by a slightly greater influence on the forecast result, but it is the range from about 28°C to maximum values, i.e., to about 34−35°C, which exerts a crucial effect on the prediction results. The importance of solar radiation in shaping the forecast result in all types of stations is minimal, although there is a noticeable tendency that the more intense the solar radiation, the minimally greater the influence of this parameter on the modeling result. The influence of wind speed on the prediction result varies depending on the type of measuring station. At regional background stations (Belsk, Granica) the lowest values, from 1 to 7 m/s, are key in shaping the modeling result. In the case of Legionowo the opposite is true − the higher the wind speed values, the greater their impact on the prediction result. In turn, at the other two city stations (Radom-Tochterman, Warszawa-Ursynów) the "area" of average values of the wind speed variability in the range from approx. 5 to 9 m/s proved to be critical. The impact of relative humidity on the ground-level ozone concentration resulting from the forecast at urban background stations is the greater the higher the value of this parameter. The situation is different at regional stations. Relative humidity values between 60 and 70% and 80 to 100% are of key importance there. Values between 70 and 80% have the smallest share in shaping the prediction result.

Further analysis of the curves presented in the graphs allowed to notice a non-linear nature of the dependence of changes in the values of individual meteorological parameters on the

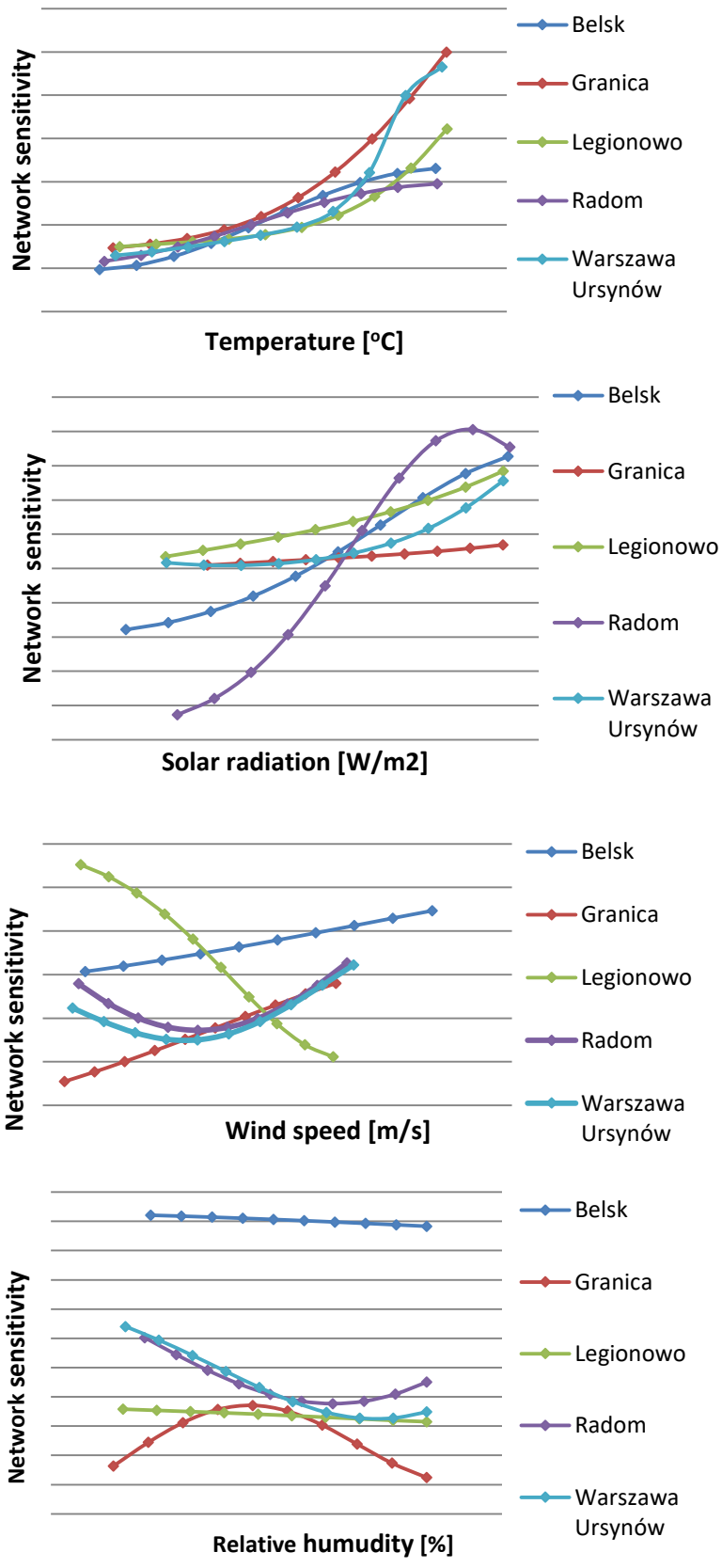

Fig. 15. Graphic interpretation of the results of local sensitivity analysis for meteorological parameters.

ground-level ozone content characteristic for each measuring station. This demonstrates the varied impact of local meteorological and chemical conditions on the formation of ozone concentrations in places located in a relatively small area (Mazowieckie Voivodeship).

6.6 Quality assessment of neural prognostic models

The following graphs are the determinants showing the extent to which the selected model approximates the values of ground-level ozone concentration in individual measuring stations:

- bar graphs: ground-level ozone concentrations calculated by the network and measured at the station,
- dispersion: ozone content measured at the station relative to the content calculated by the network,
- relative error values informing how the value calculated by the network differs (in percent) from the value measured at the monitoring station. The relative error was calculated according to the formula:

$$\delta = \frac{|X_{\text{meas}} - X_{\text{calc}}|}{X_{\text{meas}}} \times 100\% \tag{28}$$

where X_{meas} are the measured values [μg/m^3], and X_{calc} are the calculated values [μg/m^3].

The most important feature of neural models is their ability to generalize, and that is why only the charts for data from the validation subset are presented in this chapter, i.e., those that were not used during the training process.

An additional criterion for the quality of selected models are error values that are a measure of the deviations of modeled ground-level ozone content. Using different types of measures, you can examine the properties of prognostic errors such as load and precision. Load of the forecast is determined on the basis of ME (Mean Error) and MPE (Mean Percentage Error), whose values provide information on the average systematic deviation of the forecasted values from the actual ones (how much the forecast values are overestimated or underestimated in relation to real values). Forecast precision can be determined based on both the absolute measures, i.e., MAE (Mean Absolute Error) or MAPE (Mean Absolute Percentage Error) and the square measures, such as: MSE (Mean Squared Error) or RMSE (Root Mean Squared Error). Precision errors tell us what is the average deviation of the predicted values from the actual values (http://gszafranski.w.interiowo.pl/download/prog/Modul5.pdf). In order to achieve the minimum error, it is important to choose the right network structure and correctly match the weight values in the training process. In such a situation, the global model error (GE) value generated for the validation set is the smallest.

In this study, in order to examine the predictive properties of the model, the following kinds of forecast error measures were calculated:

(1) ME − Mean Error of the forecast: allows us to determine the average load of the forecast, i.e., check whether the model results are subject to a systematic error. With the assumed formula shown below, a positive deviation from zero indicates that the forecasts are underestimated and negative forecasts that they are overestimated.

$$\text{ME} = \frac{1}{n}\sum_{i=1}^{n}(x_i - y_i) \tag{29}$$

where x_i is the actual value, y_i the forecasted value, and n is the number of cases.

(2) MAE – Mean Absolute Error of the forecast: allows us to determine how much the average forecast values will deviate (in absolute terms) from the actual values.

$$\mathrm{MAE} = \frac{1}{n}\sum_{i=1}^{n} |x_i - y_i| \tag{30}$$

(3) MAPE – Mean Absolute Percentage Error of the forecast: allows us to specify the average percentage forecast error. The MAPE meter is the basis for comparing the accuracy of forecasts for different models.

$$\mathrm{MAPE} = \frac{1}{n}\sum_{i=1}^{n} \left|\frac{x_i - y_i}{x_i}\right| \times 100\% \tag{31}$$

(4) RMSE − Root Mean Square Error: interpretation similar to MAE, but RMSE is more sensitive to extremely high and low values.

$$\mathrm{RMSE} = \sqrt{\frac{1}{n}\sum_{i=1}^{\mathrm{n}} (x_i - y_i)^2} \tag{32}$$

(5) GE − Global Error of the model: allows us to assess the model's ability to reproduce the analyzed phenomenon.

$$\mathrm{GE} = \sqrt{\frac{\sum_{i=1}^{n} (x_i - y_i)^2}{\sum_{i=1}^{n} x_i^2}} \tag{33}$$

(6) R − Correlation Coefficient: allows to determine the compliance of the directions of changes (increases and decreases) of forecasted values and actual values.

6.6.1 Belsk

As can be seen from the graphs (Fig. 16), the general nature of changes in ozone content has been correctly reproduced; most cases of ozone content are predicted with high accuracy and the points focus around a fitted regression line. The difference in the forecast of the two maximum values of ozone concentrations (143.6 and 140.8 μg/m^3) from the validation set was 11.3 and 9.2 μg/m^3, respectively.

Further analysis of the plots indicates that the relative error made by the selected neural model for the validation sample ranges from 1.9 to 31.4%. The highest error (31.4%) was recorded at the end of September when the measured ozone concentrations were relatively low (62.4 μg/m^3). The average relative error was 9.7%, with 61% of the values estimated by the model obtained with an error below this value. Also, 61% of the results calculated by the model were obtained with an error below 10%, and 91% with an error below 20%. The values of the model fit quality measures for the training, test and validation subsets are presented in Table 18.

The values of Pearson's linear correlation coefficients for all subsets give evidence for a high and very high correlation between real values and those generated by the network, indicating the network's ability to correctly reproduce relationships typical for the considered situation. The analysis of the remaining measures shows that usually the error values for the training sample are smaller compared to the test and validation samples. This situation is the evidence of the proper selection of the network structure and indicates the ability of the network to generalize. The value of global error plays a dominant role in assessing the quality of model fit. As can be seen from the table, the selected neural network, when predicting the maximum 1-hour value of ozone concentration, makes an error of 0.11, which indicates a fairly good representation of the actual values network.

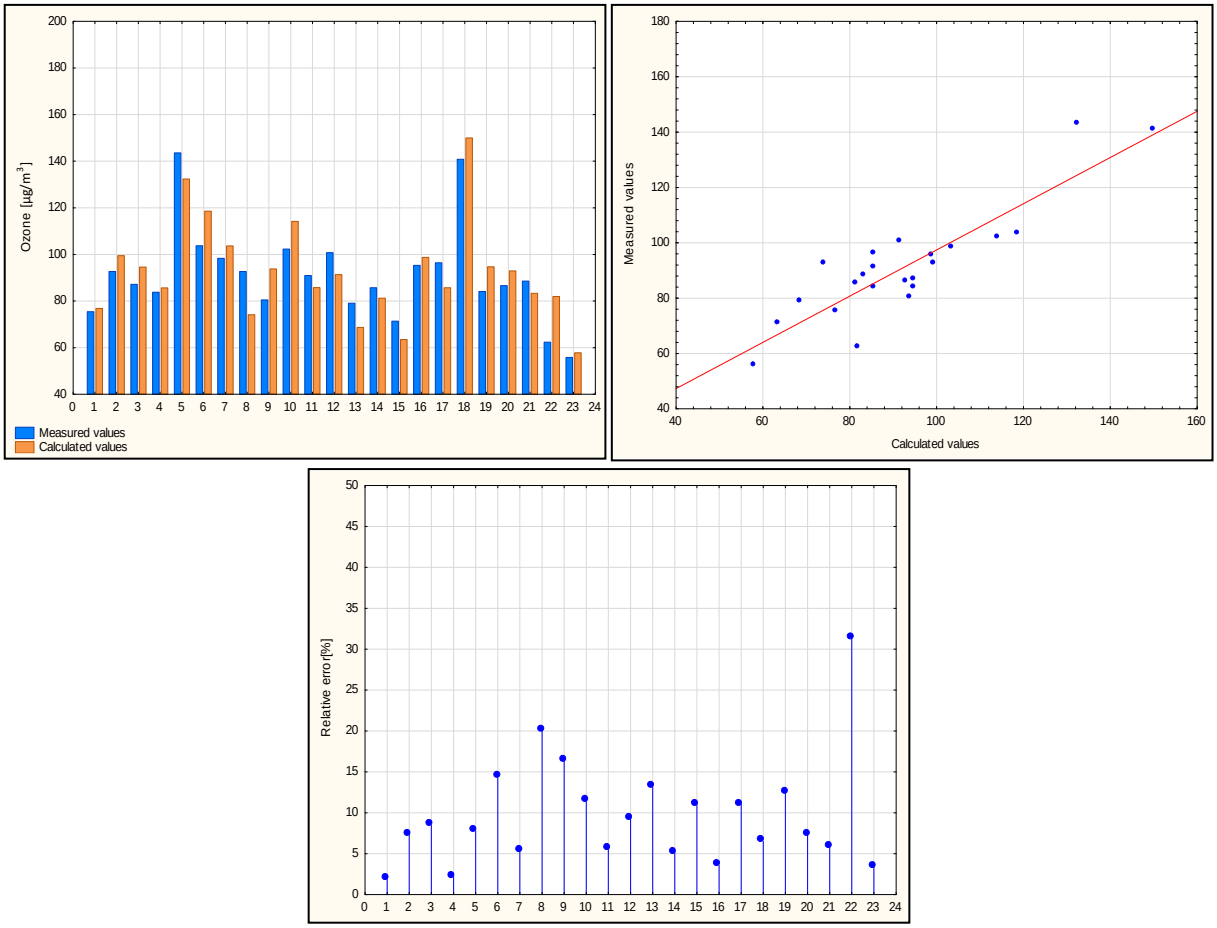

Fig. 16. Modeling results of the maximum 1-hour value of ozone concentration for validation test (Belsk station). Top left: chart of measured and calculated ozone concentrations; top right: chart of scattering of measured ozone concentrations against calculated values; bottom: chart of relative errors.

Table 18

Values of the model fit measures for the validation sample (Station Belsk)

Belsk			
Measure\Sample	Training	Test	Validation
ME	0.0811	0.2379	–1.3385
MAE	7.9015	8.7835	8.5784
MAPE	7.7741	8.4086	9.6667
RMSE	10.7573	10.5700	9.8544
Correlation	0.9199	0.8663	0.8847
GE			0.1056

6.6.2 Granica

The analysis of plots in Fig. 17 shows that the majority of ozone concentration values are forecasted with high accuracy. It is important that the predictions of the highest (the most dangerous) ozone concentrations be burdened with the smallest possible error.

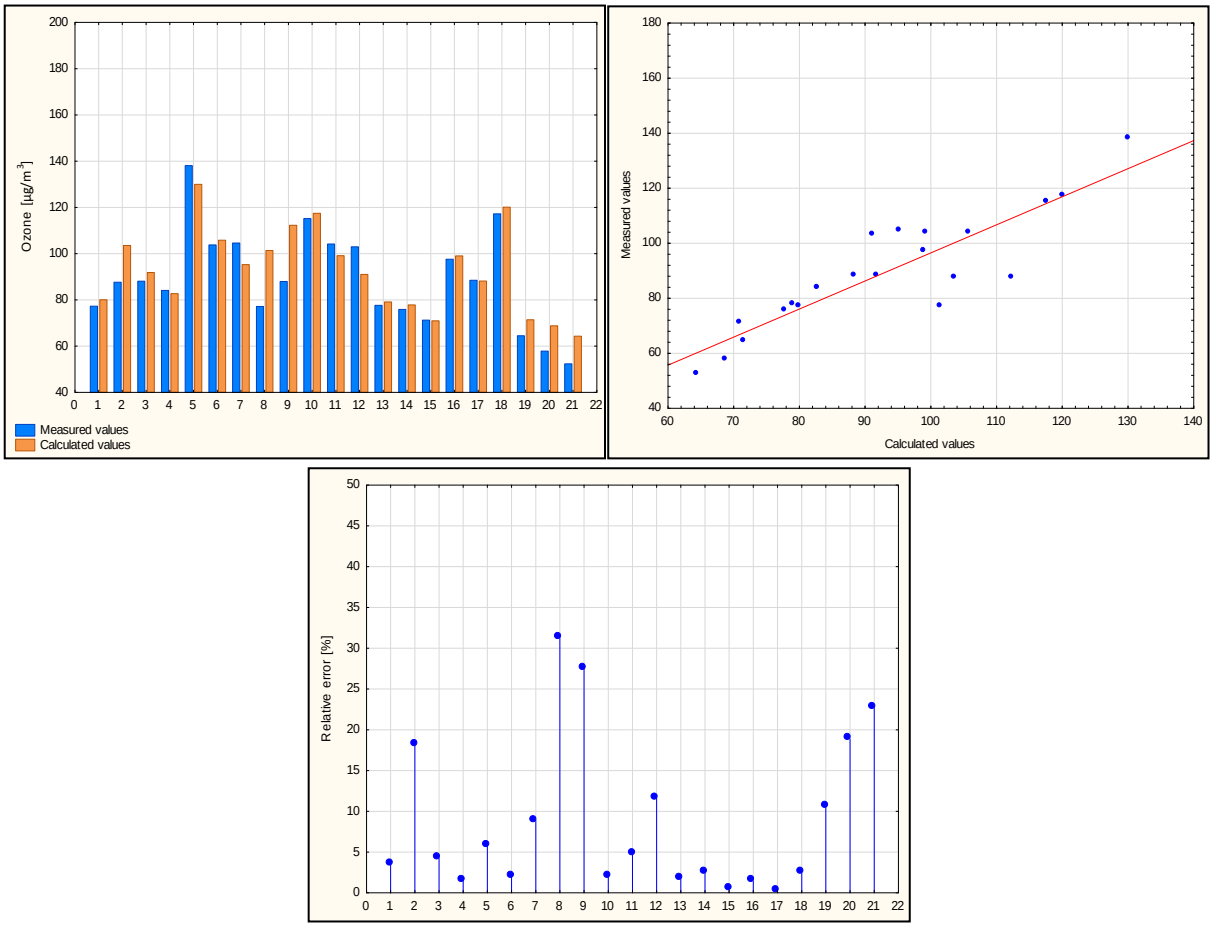

Fig. 17. Modeling results of the maximum 1-hour value of ozone concentration for validation test (Station Granica). Top left: chart of measured and calculated ozone concentrations; top right: chart of scattering of measured ozone concentrations against calculated values; bottom: chart of relative errors.

Table 19

Values of the model fit measures for the validation sample (Station Granica)

Granica			
Measure\Sample	Training	Test	Validation
ME	0.0041	1.9984	-3.6225
MAE	7.3748	6.8747	7.1023
MAPE	8.0746	6.9985	8.7243
RMSE	9.5576	9.6115	10.0160
Correlation	0.9162	0.9012	0.8884
GE			0.1094

The difference between the maximum measured ozone concentration (138.1 μg/m^3) and the corresponding calculated value was 8.2 μg/m^3. Even smaller differences in the measured and calculated values were recorded for two consecutive high ozone concentrations, 117 and 115 μg/m^3, for which the differences were 2.9 and 2.3 μg/m^3, respectively. The relative error made by the network ranges from 0.3 to 31.3%. The average relative error value is 8.7%, with 62% of the results generated by the network obtained with an error below this value. 67% of forecasts were contaminated with an error below 10%, while 86% of forecasts with an error below 20%. The values of the model fit quality measures for the training, test and validation subsets are presented in Table 19.

The values of Pearson's linear correlation coefficients for all subsets indicate a very high and high correlation between the measured values set as a standard and the modeled values, and testify to the correctness of mapping the relationships characterizing the studied phenomenon. For test and validation samples, higher error values were recorded than for the training sample. The value of the global model error indicates that the prediction of the maximum 1-hour ozone content per day is contaminated by an error of the order of 0.11.

6.6.3 Legionowo

The analysis of plots in Fig. 18 indicates that the nature of the data variability in the validation sample has been correctly reproduced and the points are grouped along the regression line. At the Legionowo monitoring station, the maximum value of 1-hour maximum ground-level ozone

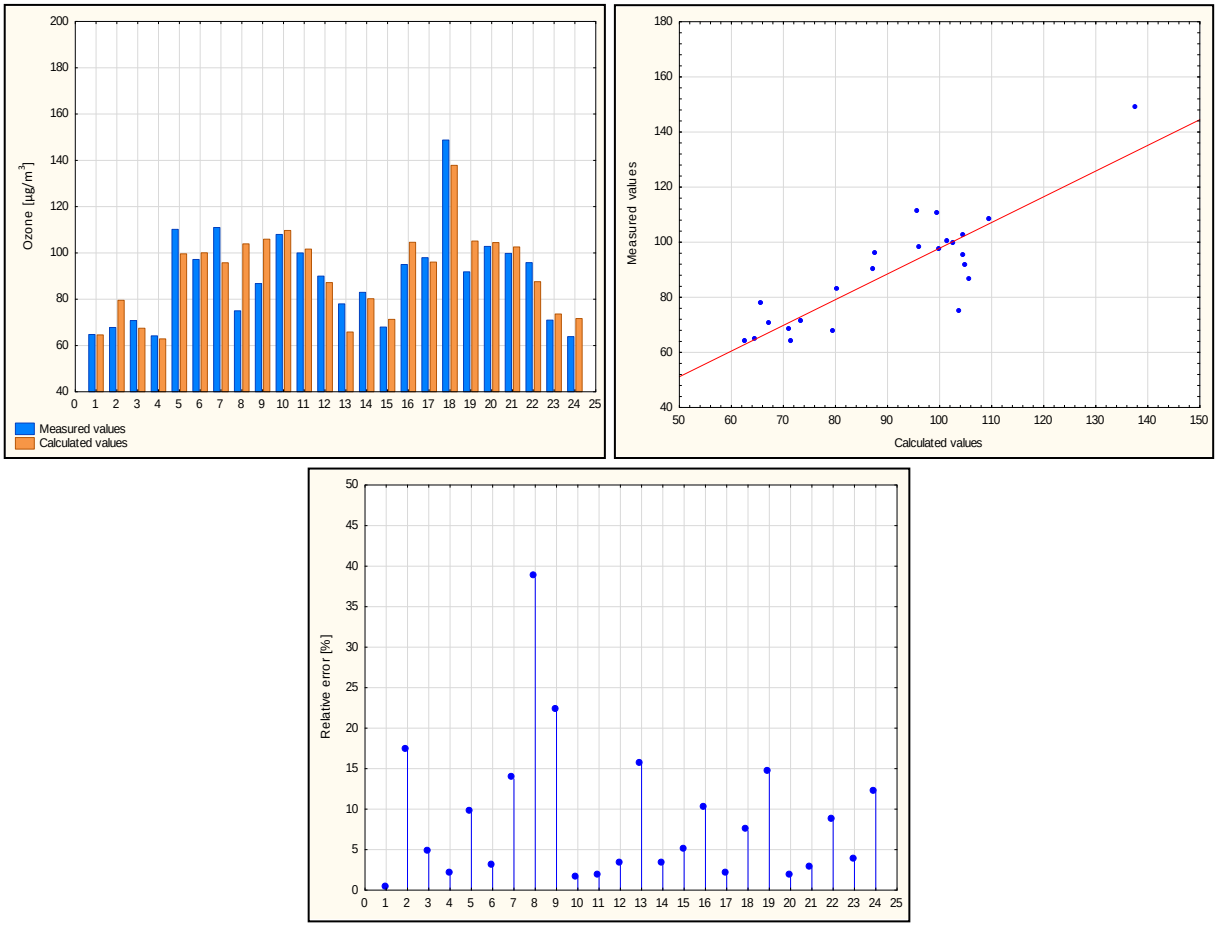

Fig. 18. Modeling results of the maximum 1-hour value of ozone concentration for validation test (Station Legionowo). Top left: chart of measured and calculated ozone concentrations; top right: chart of scattering of measured ozone concentrations against calculated values; bottom: chart of relative errors.

content in the validation set was 148.8 μg/m^3. The result of the forecast by the selected neural network for that day was 137.8 μg/m^3. When the concentration values are so high, the 11 μg/m^3 difference in prediction is the evidence for high accuracy of mapping.

The value of the relative error made by the network ranges from 0.3 to 38.6%. The highest error (38.6%) was observed at the end of May, when the 1-hour maximum value of ozone concentration was relatively low (72 μg/m^3). The average relative error value is 8.5%, with 58% of network results obtained with an error below this value. 67% of network results were contaminated with an error below 10 and 92% with an error below 20%. Table 20 presents the values of the model fit quality measures for the training, test and validation subsets.

Table 20

Values of the model fit measures for the validation sample (Station Legionowo)

Legionowo			
Measure\Sample	Training	Test	Validation
ME	0.1911	0.1286	-1.5818
MAE	8.3434	6.7703	7.3618
MAPE	8.5177	6.6733	8.5113
RMSE	10.6554	8.7254	10.0556
Correlation	0.9403	0.9069	0.8652
GE			0.1100

The values of Pearson's linear correlation coefficients for all subsets testify to a very good and almost full correlation between the standard values and the values estimated by the network and testify to the correct representation of the relationships describing the studied phenomenon. In most cases, higher error values were obtained for the test and validation samples compared to the training sample. The value of the global model error means that the prediction of the maximum 1-hour ozone content per day is contaminated with an error of 0.11.

6.6.4 Radom

The analysis of the presented plots (Fig. 19) indicates the correct representation of the nature of ground-level ozone concentration variability: the points are grouped along the regression line. The differences between the two maximum ozone concentration values (139.1 and 118.6 μg/m^3) and their forecasted values were minimal, amounting to 2.2 and 3.2 μg/m^3, respectively.

The relative errors committed by the network range from 0.3 to 46.1%. The largest error (46.1%) was recorded at the end of May, when the maximum ozone content was relatively low (60.1 μg/m^3) (the forecast value was 87.8 μg/m^3). The average value of relative error is 9.5% with 54% of network results obtained with an error below this value. 59% of network results were contaminated by an error below 10%, and 95% of results by an error below 20%. The quality measures of the model fit for the training, test and validation subsets are presented in Table 21.

The values of Pearson's linear correlation coefficients for all subsets give evidence of a very high and high correlation between real values and values generated by the network. In general, higher error values were recorded for the test and validation samples than for the training sample. The value of the global error of the model indicates that, while predicting the maximum 1-hour ozone content, the selected network makes an error of 0.11.

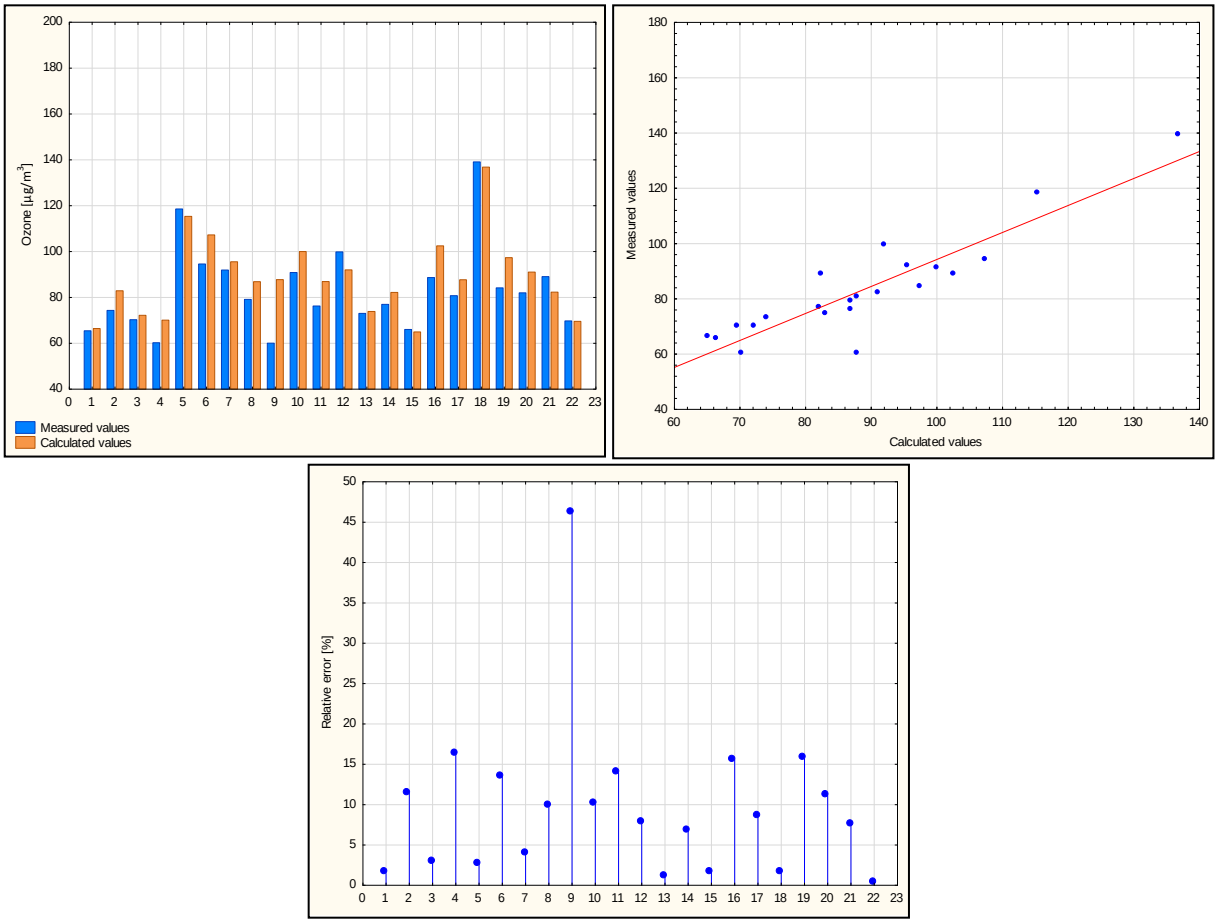

Fig. 19. Modeling results of the maximum 1-hour value of ozone concentration for validation test (Station Radom). Top left: chart of measured and calculated ozone concentrations; top right: chart of scattering of measured ozone concentrations against calculated values; bottom: chart of relative errors.

Table 21

Values of the model fit measures for the validation sample (Station Radom)

Radom			
Measure\Sample	Training	Test	Validation
ME	0.0205	–2.5176	–5.4801
MAE	8.1855	7.2665	7.4182
MAPE	8.3553	7.5123	9.5332
RMSE	10.7498	9.2059	9.5830
Correlation	0.9260	0.8883	0.9022
GE			0.1124

6.6.5 Warszawa-Ursynów

The analysis of the plots (Fig. 20) confirmed the compliance of the pattern of the mapped changes in the ground-level ozone content at the Station Warszawa-Ursynów. The maximum ozone concentration values (155, 139.8, and 120.5 µg/m^3) were mapped by the network with

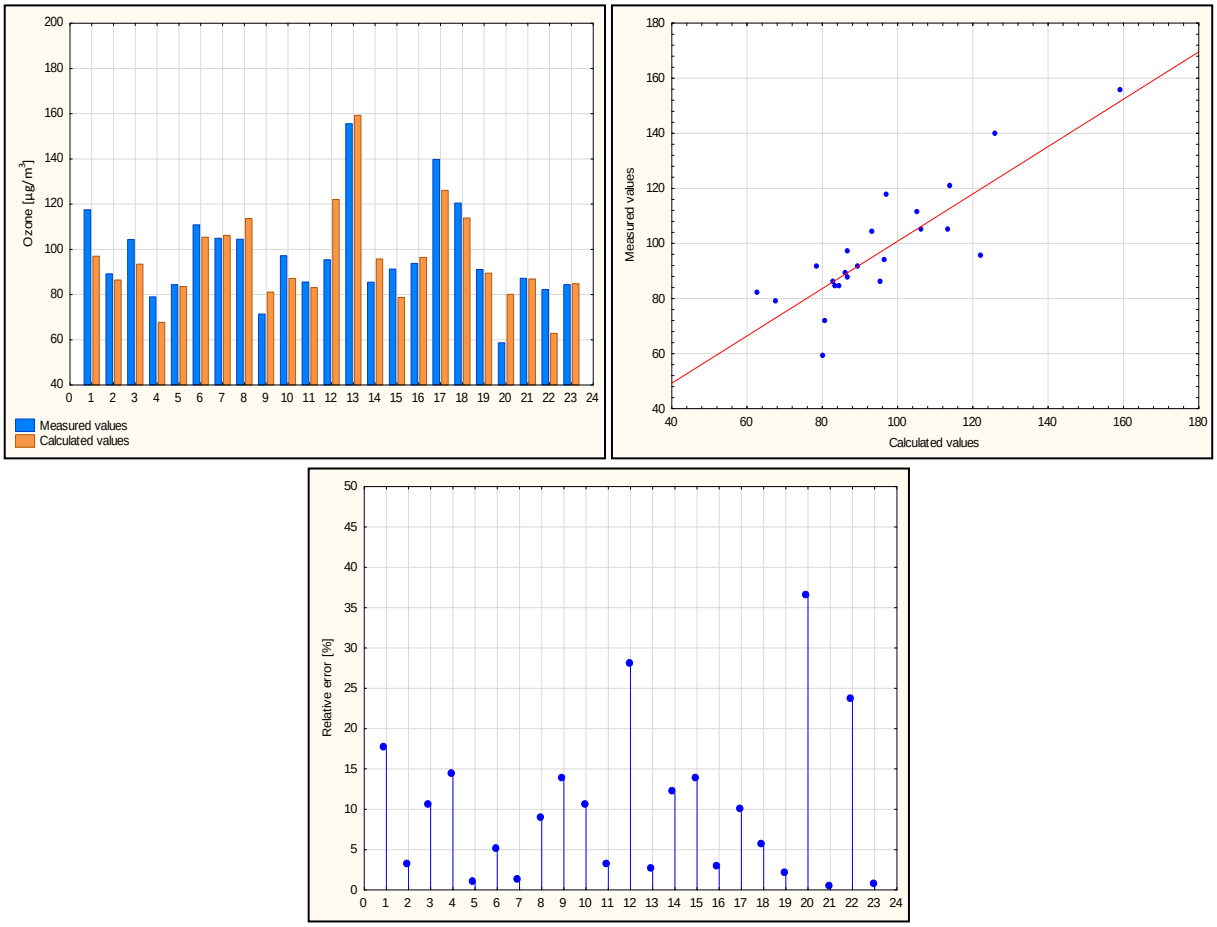

Fig. 20. Modeling results of the maximum 1-hour value of ozone concentration for validation test (Station Warszawa-Ursynów). Top left: chart of measured and calculated ozone concentrations; top right: chart of scattering of measured ozone concentrations against calculated values; bottom: chart of relative errors.

Table 22

Values of the model fit measures for the validation sample (Station Warszawa-Ursynów)

Warszawa-Ursynów			
Measure\Sample	Training	Test	Validation
ME	–0.2797	–0.0065	1.4383
MAE	7.3938	8.9199	8.8648
MAPE	8.2244	9.3894	9.7855
RMSE	9.8322	11.4903	11.5356
Correlation	0.9300	0.9290	0.8488
GE			0.1161

relatively small differences (3.7, 13.7, and 6.6 µg/m^3, respectively). The relative error calculated for the data from the validation subset ranges from 0.3 to 36.5%. The highest error (36.5%) was found in early September, when the ozone concentration measured at the station was rather

low: 58.7 μg/m^3. The average relative error value is 9.8%, with 56% of the ozone concentration estimated with an error below this value. Also, 56% of the results had an error below 10%, and 87% of the results had an error below 20%.

The values of the quality measures of the model fit for the training, test and validation subsets are given in Table 22. The values of Pearson's linear correlation coefficients for all subsets give evidence for a very good and almost full correlation between real values and network response values, as well as an accurate mapping of dependencies characterizing a given phenomenon.

Usually, lower error values recorded for the training sample testify to the properly selected network structure, ensuring its ability to generalize knowledge for cases that have not been presented yet. The value of the global model error indicates that the prediction of the maximum 1-hour ozone content is realized with an error of 0.12.

7. FORECAST OF THE MAXIMUM 1-HOUR OZONE CONCENTRATION FOR THE YEAR 2014 (APRIL−SEPTEMBER)

One of the aims of this study was to create a set of neural networks that would be able to generalize the acquired knowledge into new cases, i.e., such that had not been presented before.

The future exploitation of the model was taken into account already at the stage of constructing the network architecture. Both the number (only 6) and the specificity (only key predictors) of information used in the network as a vector of input variables were strictly conditioned by the future use of the model. The reason is that it is important to have the input information set containing the data that can be obtained on the day the forecast is being made.

In order to check the effectiveness (ability to generalize) of selected neural networks when applied to new cases, the networks were used to forecast ground-level ozone for the next day through the period from April to September 2014. The forecast of the maximum 1-hour value of ozone concentration per day for the next day was based on the input data for 2014, analogous to the input data for 2015 used for the construction of the network (see Chapter 6).

7.1 Presentation of results

The results of selected models were presented using the diagrams of:

- time variability of the predicted maximum 1-hour value of ground-level ozone concentration per day,
- dispersion of the maximum 1-hour values of ground-level ozone concentrations during the day, as measured at the measuring station, versus the values calculated by the network,
- histogram of deviations of values generated by the network from the actual values,
- values of relative errors.

Moreover, like in the case of assessing the quality of networks generated for 2015, the errors constituting the measure of deviations of modeled ozone concentration values (ME, MAE, MAPE, RMSE, and Pearson's linear correlation coefficient) were used as the criterion of forecast accuracy. In order to obtain additional information regarding the quality assessment of selected prognostic neural models, the respective error measures were compared, namely ME and MAE as well as MAE and RMSE. The comparison of the first pair of error measures provides information on the systematic "loading" of projected values, i.e., whether they have been systematically undervalued or overvalued relative to actual values. Equal or similar absolute ME and MAE error values mean that the forecast values were systematically overestimated or underestimated. Comparing the second pair of error measures with each other allows to conclude about the occurrence of various values of differences (both small and large) between the forecasted and actual values. This is demonstrated by the significant difference between the MAE and RMSE values.

7.1.1 Belsk

Figure 21 presents a set of graphs showing the relationships between ground-level ozone concentrations measured at the station and calculated by the selected model in relation to the maximum 1-hour O_3 concentration per day during the period 1 April – 30 September 2014.

Analysis of the diagrams shows that the prognostic model well reproduces the actual time variation of ozone concentrations. The exceptions are the first half of April, when the model slightly overestimated the low ozone concentrations, and the turn of August and September, when the model undervalued the high ozone levels. The maximum value of ozone concentration measured in the analyzed period at the Station Belsk was 145.4 µg/m^3. The value estimated for this day by the model was 141.5 µg/m^3.

Analysis of the residual histogram shows that the residual values range from about –60 to about +40 µg/m^3. Deviations of the forecast from the value observed for 52% of cases ranged from –10 to +10 µg/m^3, for 81% of cases between –20 and +20 µg/m^3, for 93% of cases within –30 to +30 µg/m^3 and for 98% of the cases between –40 and +40 µg/m^3. On average, about 3% of cases were characterized by a deviation from actual value in the range from –40 to –60 µg/m^3.

The maximum residual value was 53.6 µg/m^3 (27 July 2014, x_i (measured value) was 79 µg/m^3, y_i (calculated value) was 132.6 µg/m^3) and was the only value above 50 µg/m^3. Interpretation of the scatter graph shows the existence of a relationship between variables at the correlation coefficient level of 0.73. The relative error values range from 0.2 to 136.4%. The

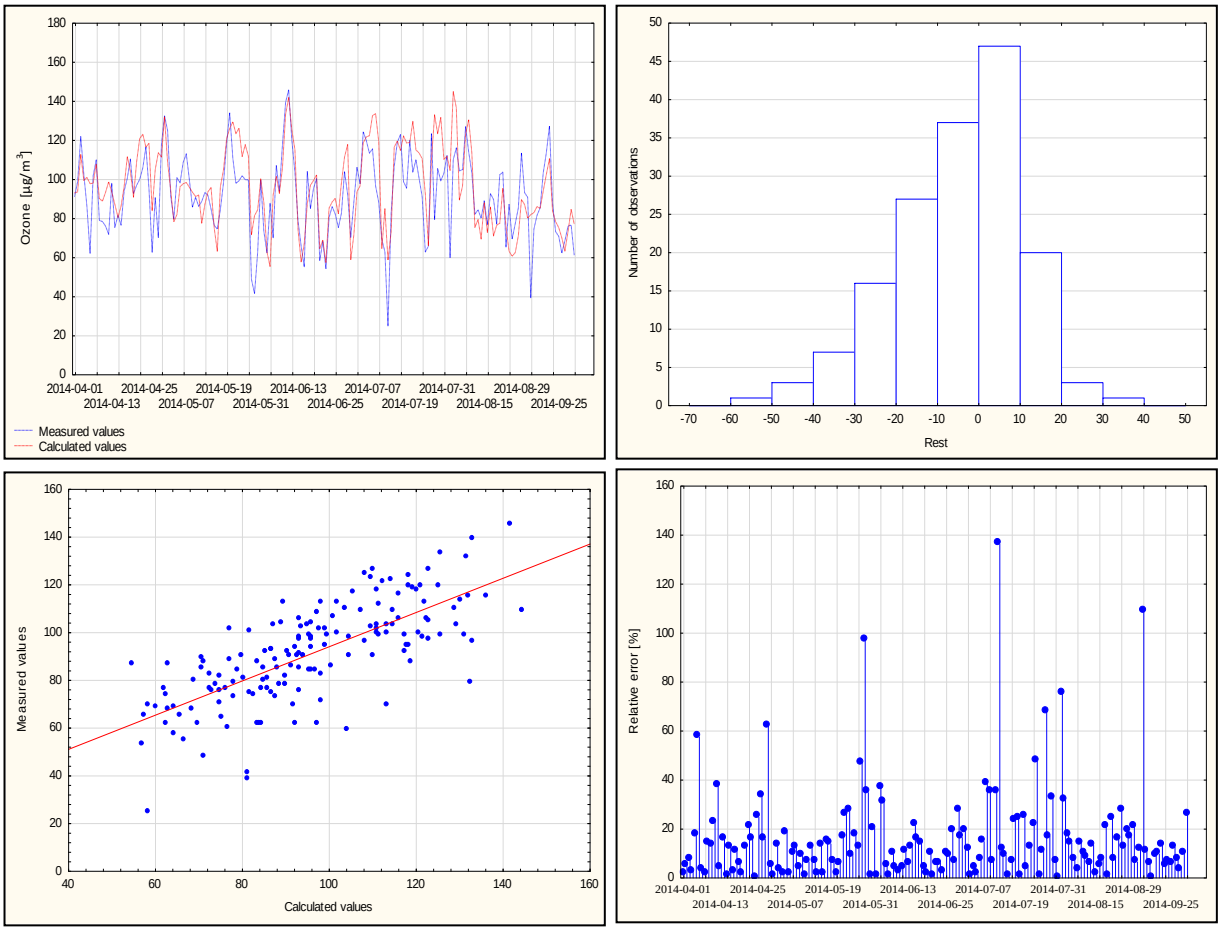

Fig. 21. Modeling results of the maximum 1-hour value of ozone concentration for the period from April to September 2014 (Station Belsk). Top left: measured and calculated ozone concentrations; top right: histogram of residues; bottom left: scatter graph of measured ozone concentrations versus calculated values; bottom right: relative errors.

Table 23
Model fit values for the period from April to September 2014 (Station Belsk)

Station\Measure	ME	MAE	MAPE [%]	RMSE	Correlation
Belsk	–4.8	12.1	15.4	15.9	0.73

average value of relative error is 15.3%, with 67% of forecasts obtained with an error below this value. Table 23 presents the calculated basic measures of deviations of real ozone values from the forecasts estimated by the selected neural network model for the period 1 April – 30 September 2014.

A negative ME value indicates that the model tends to overestimate the maximum 1-hour ozone concentration. It can be stated that the actual values were lower than the forecast by an average of 4.8 μg/m^3. The MAE value indicates that the forecast values differed from the values observed by of 12.1 μg/m^3, on average. The MAPE value indicates that the forecast values differed from real values by an average of 15.4%. According to the RMSE value, the average difference between the measured value and the forecast is 15.9 μg/m^3. Pearson's linear correlation coefficient of 0.73 gives evidence for a high correlation and compliance of directions of the forecasted and real values. The absolute values of ME and MAE are very different, which indicates that the forecasts are not subject to any systematic overestimation or underestimation. The higher RMSE error compared to MAE is probably due to the existence of extremely high residuals (above 30 μg/m^3) between measured and forecasted values.

7.1.2 Granica

Figure 22 presents a set of graphs showing the relationships between ground-level ozone concentrations measured at the station and calculated by the selected model in relation to the maximum 1-hour O_3 concentration per day during the period 1 April – 30 September 2014.

Analysis of the diagrams indicates good compliance of the forecast with the actual concentration values from April to the first half of July and in the first half of August. In the second half of July, the model systematically overestimated the forecast values, while at the turn of August and September the model tended to average the high and low ozone concentrations. The maximum ozone content measured at the Station Granica during the analyzed period was 150.8 μg/m^3 (7 July 2014). The forecast value for this day was characterized by a minimal (5.7 μg/m^3) underestimation. Analysis of the residual histogram indicates that the residual values range from –60 to +40 μg/m^3. The deviations of the forecast value from the actual value for 47% of cases ranged from –10 to +10 μg/m^3, for 73% of cases from –20 to +20 μg/m^3, for 94% of cases within –30 to +30 μg/m^3, and for 98% of cases between –40 and +40 μg/m^3. The remaining approx. 3% of forecasts had a deviation from the observed value within the range of –40 to –60 μg/m^3. Maximum residual values between the observation and the forecast were 52.2 and 53.9 μg/m^3, and both were associated with significant overestimation of the observations. A scatter plot indicates the existence of a relationship between variables at the correlation coefficient level of 0.74. The relative error values range from 0 to 77.4%. The average relative error value is 15.4%, with 59% of forecasts obtained with an error below this value. Table 24 provides information on the main measures of deviations of forecast ozone values from actual values for the period 1 April – 30 September 2014.

A negative ME value indicates the general tendency of the model to overestimate the maximum 1-hour ozone concentration by an average of 7.1 μg/m^3. The MAE value indicates that the projected values differ from the actual values by an average of 13.5 μg/m^3. According to the MAPE value, the forecasts differed from observations by an average of 15.4%. The average

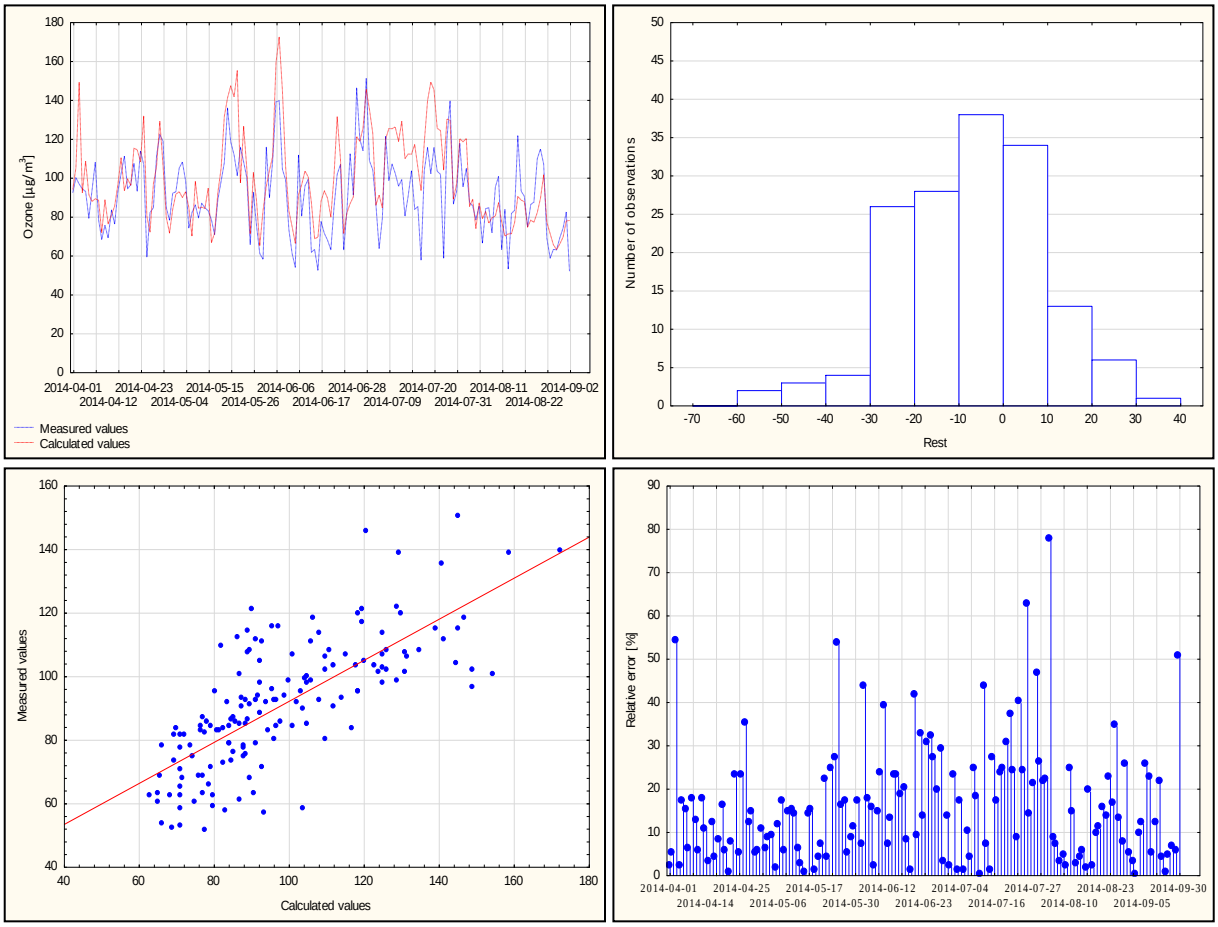

Fig. 22. Modeling results of the maximum 1-hour value of ozone concentration for the period from April to September 2014 (Station Granica). Top left: measured and calculated ozone concentrations; top right: histogram of residues; bottom left: scatter graph of measured ozone concentrations versus calculated values; bottom right: relative errors.

Table 24

Model fit values for the period from April to September 2014 (Station Granica)

Station\Measure	ME	MAE	MAPE [%]	RMSE	Correlation
Granica	–7.1	13.5	15.4	17.4	0.74

difference between the measured and forecast values, according to RMSE, is 17.4 µg/m^3. The value of Pearson's linear correlation coefficient is 0.74, which indicates a high correlation and a good mapping of the directions of changes in real values by the predicted values. The almost two-fold absolute value of the MAE measure (13.5) compared to the ME measure (–7.1) means that there is neither systematic overestimation nor underestimation of the forecasted values. The difference between the MAE and RMSE values of 3.9 µg/m^3 may be due to high residual values.

7.1.3 Legionowo

Figure 23 presents a set of graphs showing the relationships between ground-level ozone concentrations measured at the station and calculated by the selected model in relation to the maximum 1-hour O_3 concentration per day during the period 1 April – 30 September 2014.

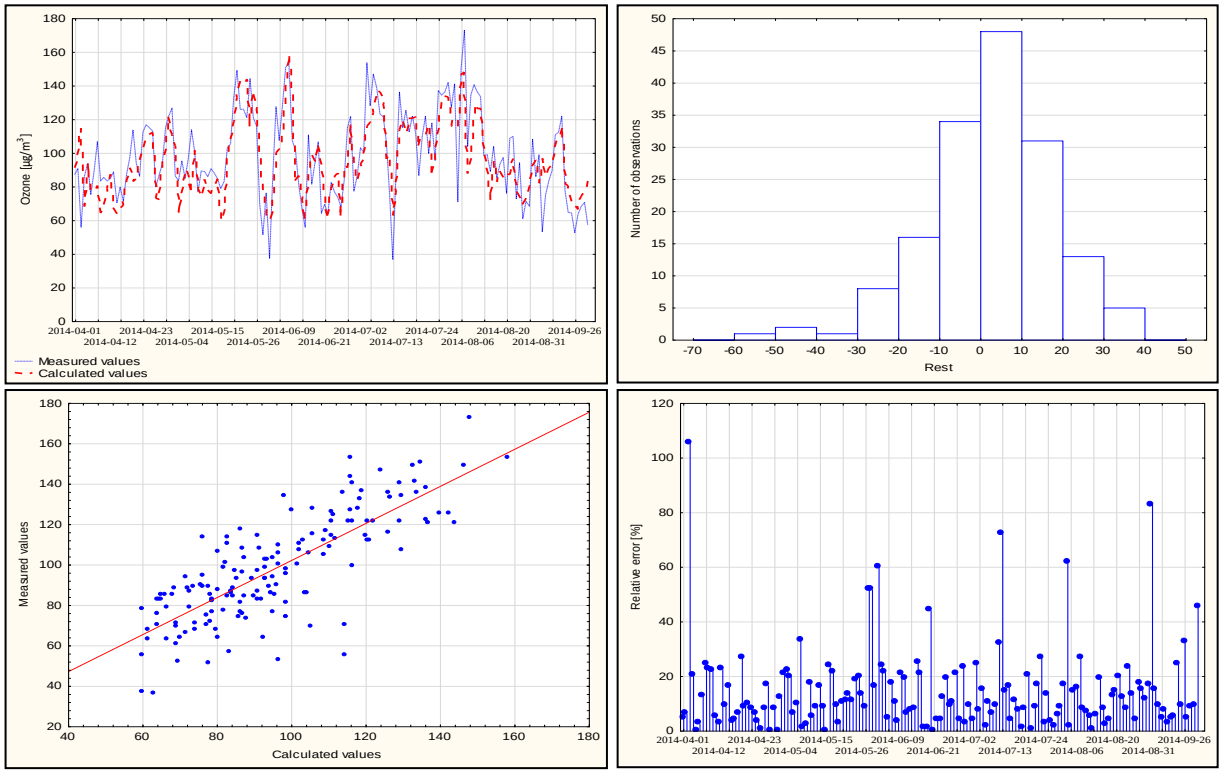

Fig. 23. Modeling results of the maximum 1-hour value of ozone concentration for the period from April to September 2014 (Station Legionowo). Top left: measured and calculated ozone concentrations; top right: histogram of residues; bottom left: scatter graph of measured ozone concentrations versus calculated values; bottom right: relative errors.

Analysis of the graphs indicates good compliance of the forecast with the actual concentration values over the entire analyzed period. The maximum measured ozone concentration was 172.9 µg/m^3. The forecast value for that day was 147.9 µg/m^3, generating a difference of 25 µg/m^3. Other very high ozone concentrations with a value above 150 µg/m^3 were the following: 150.7 µg/m^3 (8 June 2014), 153.2 µg/m^3 (9 June 2014), and 153.3 µg/m^3 (4 July 2014). The corresponding forecast values were: 134.8, 158.2, and 115.7 µg/m^3, respectively. Analysis of the residual histogram shows that the residual values range from –60 to +40 µg/m^3. The deviations of the predicted value from the actual value for 51% of cases ranged from –10 µg/m^3 to +10 µg/m^3, for 80% of cases between –20 and +20 µg/m^3, for 93% of cases between –30 to +30 µg/m^3 and for 97% of cases within the range of –40 to +40 µg/m^3. The remaining 3% of cases were characterized by a deviation from –40 to –60 µg/m^3. The maximum value of the remainder between the actual value and the forecast, resulting from the overestimation of the low ozone content by the model, was 58.8 µg/m^3 (3 April 2014, x_i = 55.7 µg/m^3, y_i = 114.5 µg/m^3). The analysis of the scatter graph shows the existence of a correlation between variables at the coefficient level of 0.79. The relative error values range from 0 to 105.6%. The average value of relative error is 14.3%, with 62% of the results obtained with an error value below this value.

Table 25 contains the results of calculations of the measures of deviations of the ozone concentration values estimated by the selected neural model from the actual values for the period 1 April – 30 September 2014.

A positive sign of the ME error indicates that the selected model has a tendency to understate the predicted maximum 1-hour ozone concentrations in relation to actual values by an average of 2.7 µg/m^3. According to the MAE, the forecasts differed from the actual values by

Table 25

Model fit values for the period from April to September 2014 (Station Legionowo)

Station\Measure	ME	MAE	MAPE [%]	RMSE	Correlation
Legionowo	2.7	12.6	14.3	16.2	0.79

12.6 µg/m^3, on average. The RMSE indicates that the average difference between the observation and the forecast was 16.2 µg/m^3. The MAPE value indicates that actual values differed from forecasts by 14.3%, on average. The value of Pearson's linear correlation coefficient (0.79) gives evidence for a high correlation between variables and compliance of directions of changes in forecasted values. The absolute values of ME (2.7) and MAE (12.6) differ significantly, hence it can be concluded that the forecast values are not systematically undervalued or overestimated. The difference of MAE and RMSE measures, amounting to 3.6, indicates the existence of extreme values of differences between the forecast and actual values.

7.1.4 Radom

Figure 24 presents a set of graphs showing the relationships between ground-level ozone concentrations measured at the station and calculated by the selected model as concerns the maximum 1-hour O_3 concentration per day during the period 1 April – 30 September 2014.

The time variability of ozone concentrations is well reproduced by the predicted values, except for the second half of August and the first days of September, when the model underes-

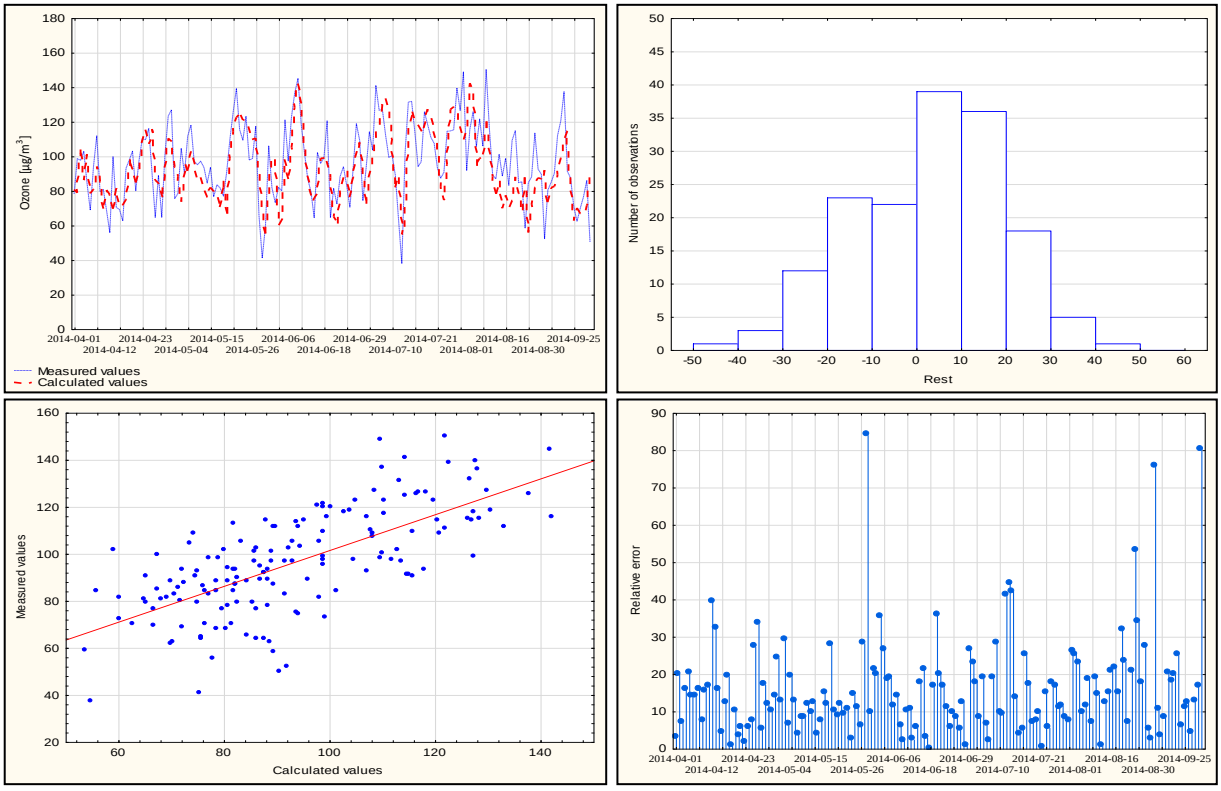

Fig. 24. Modeling results of the maximum 1-hour value of ozone concentration for the period from April to September 2014 (Station Radom). Top left: measured and calculated ozone concentrations; top right: histogram of residues; bottom left: scatter graph of measured ozone concentrations versus calculated values; bottom right: relative errors.

timated the high ozone concentrations and overestimated the low ones twice. The maximum measured ozone concentration is 150.2 μg/m^3, while the corresponding forecast value is 121.8 μg/m^3. Analysis of the residual histogram shows that the residual values range from –50 to +50 μg/m^3. Forecast deviations from observations for 38% of cases are in the range from –10 to +10 μg/m^3, for 75% in the range from –20 to +20 μg/m^3, for 94% in the range from –30 to +30 μg/m^3, for 99% in the range from –40 to +40 μg/m^3. Only 1% of cases had a deviation from –40 to –50 μg/m^3 (1 case) and from +40 to +50 μg/m^3. The maximum residual values between forecast and actual values are 43.2 μg/m^3 (13 July 2014: x_i = 102.1 μg/m^3, y_i = 58.9 μg/m^3) and 40.3 μg/m^3 (30 September 2014: x_i = 50.2 μg/m^3, y_i = 90.5 μg/m^3). As can be seen from the above, the former is a result of an underestimation of the high ozone value and the latter follows from an overestimation of the low ozone value. A scatter plot indicates the existence of a relationship between variables at the correlation coefficient level of 0.69. The relative error values range from 0.1 to 84.1%. The average relative error value is 15.8%, with 60% of the prediction results obtained with an error below this value. Table 26 presents values of basic measures of deviations of forecast from actual values for the period from 1 April to 30 September 2014.

Table 26

Model fit values for the period from April to September 2014 (Station Radom)

Station\Measure	ME	MAE	MAPE [%]	RMSE	Correlation
Radom	3.3	14.1	15.8	16.8	0.69

The value of ME indicates the tendency of the model to underestimate the value of forecasts by 3.3 μg/m^3, on average. The MAE value indicates that the average difference between the measured and modeled values is 14.14 μg/m^3. The average percentage difference between the forecast and the observation according to the MAPE measure is 15.8%. According to RMSE, projections differed from observations by 16.8 μg/m^3, on average. The value of Pearson's linear correlation coefficient (0.69) indicates that the correlation between the forecast and real variables was on the average level. The MAE error that is almost 4 times higher (14.1 μg/m^3) than the ME error (3.3 μg/m^3) rules out the occurrence of a systematic underestimation or overestimation of the forecast value by the selected model. The relatively low value of the difference (2.6) between MAE and RMSE, as compared to other stations (3.8 in Belsk; 3.9 in Granica; 3.6 in Legionowo), probably results from the occurrence of lower maximum absolute values of differences between the actual and forecasted values (between 40 and 50 μg/m^3 in contrast to 50 to 60 μg/m^3).

7.1.5 Warszawa-Ursynów

Figure 25 presents a set of graphs showing the relationships between ground-level ozone concentrations measured at the station and calculated by the selected model concerning the maximum 1-hour O_3 concentration per day during the period 1 April – 30 September 2014.

Analysis of the diagrams indicates good compliance of the forecast with the actual concentration values. The exceptions are two periods: the first half of May and the turn of August and September, when the model underestimated the value of ozone concentrations. The maximum 1-hour ozone content measured at Station Warszawa-Ursynów during the analyzed period was 150 μg/m^3. The forecast value estimated for that day was 132.0 μg/m^3, i.e., less than the measured value by 18 μg/m^3. The residual histogram analysis shows that the residual values range from –50 to +40 μg/m^3. For 49% of cases, the residual values ranged from –10 to +10 μg/m^3;

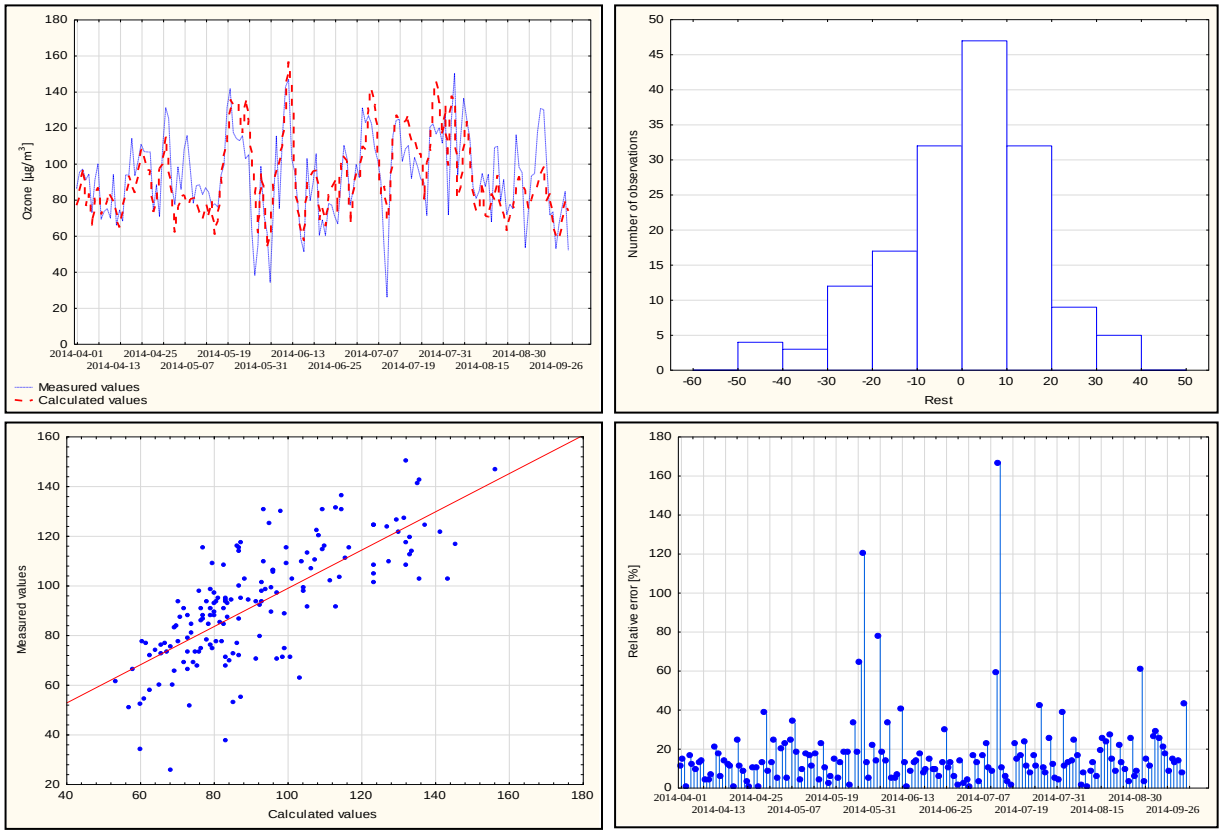

Fig. 25. Modeling results of the maximum 1-hour value of ozone concentration for the period from April to September 2014 (Station Warszawa-Ursynów). Top left: measured and calculated ozone concentrations; top right: histogram of residues; bottom left: scatter graph of measured ozone concentrations versus calculated values; bottom right: relative errors.

Table 27

Model fit values for the period from April to September 2014 (Station Warszawa-Ursynów)

Station\Measure	ME	MAE	MAPE [%]	RMSE	Correlation
Warszawa-Ursynów	0.9	13.0	15.7	16.3	0.74

for 80% of cases between –20 and +20 µg/m^3; for 93% of cases from –30 to +30 µg/m^3; for 98% of the cases from –40 to +40 µg/m^3. The remaining 2% of forecast cases were characterized by a deviation from the actual value in the range from –40 to –50 µg/m^3. The maximum absolute residual value (45.3 µg/m^3) was associated with an actual ozone concentration of only 37.8 µg/m^3 and was due to model's overestimation of a low ozone concentration. The arrangement of points on the scatter plot indicates the existence of a relationship between variables at the correlation coefficient level of 0.69, but at the same time shows the existence of several outliers. The relative error values range from 0.1 to 166.0%. The average value of relative error is 15.7%, with 67% of forecast results obtained with an error below this value. Table 27 presents the results of calculations of the main measures of deviations of the forecast values relative to the actual values for the period from 1 April to 30 September 2014.

The ME value indicates the model's tendency to understate the projected values by 0.9 µg/m^3 on average. The MAE measure indicates that the projections differed from real values

by 13.0 $\mu g/m^3$ on average. The percentage difference between the forecast and the measured value (MAPE measure) is 15.7%, on average. According to RMSE, the average difference between the observation and the forecast is 16.3 $\mu g/m^3$. The value of Pearson's linear correlation coefficient of 0.74 indicates a high correlation between variables and good implementation of changes in the directions of modeled value. A significant difference between the ME and MAE values indicates that there is no regularity in underestimating or overestimating the predicted ozone concentrations. The difference between the MAE and RMSE, amounting to 3.3 $\mu g/m^3$, indicates the existence of large residual values between observation and forecast.

7.2 Comparison of the results of the forecast by artificial neural networks and the GEM-AQ model

In this section, a comparison is made of the ground ozone forecasts for 1 day forward generated by selected neural networks with an analogous forecast created by the latest-generation global troposphere chemistry model GEM-AQ (Global Environmental Multiscale-Air Quality). Data in the form of tropospheric ozone concentration maps for the Mazowieckie Voivodeship, covering the analyzed period from 1 April to 30 September 2014, were downloaded from the website of the Chief Inspectorate for Environmental Protection (air.gios.gov.pl), which provides the forecast of air contamination by ground-level ozone on the country and voivodeship scale calculated through the EkoPrognoza forecasting system based on the GEM-AQ model.

7.2.1 Description of the GEM-AQ model

The GEM-AQ model, belonging to the group of Euler models, was developed by a network of cooperating Canadian scientific institutions MAQNet (Multiscale Air Quality Network). The GEM-AQ model was based on the GEM (Global Environmental Multiscale Model) numerical weather forecast model used by the Canadian Meteorological Center (Côté et al. 1998). The characteristics of transport processes and physical phenomena in the GEM-AQ model come from the meteorological model, while the chemical description of the gas phase is based on the ADOM (Acid Deposition and Oxidants Model) model (Lurmann et al. 1986). Currently, the improved system determining the chemical properties of the gas phase includes 50 chemical compounds (35 transported by advection and 15 with short lifetime not suitable for transport), 116 chemical reactions and 19 photochemical reactions. In addition, the model includes the CAM aerosol module (Canadian Aerosol Model; Gong et al. 2003) covering physico-chemical interactions involving five types of aerosols: organic, sulfate, mineral dust, sea salt, and soot (Kaminski et al. 2008).

Generation of a forecast for the concentration of a given atmospheric air pollutant is based on a number of input data that are an integral part of the entire forecasting system. In addition to the chemical data described above (including aerosols), the most important are the following:

- geophysical and topographic data characterizing the earth's surface: land/sea recognition, mean height and roughness of the ground, surface temperature, soil temperature, soil moisture, albedo, and snow/ice cover,
- meteorological data at the earth's surface: pressure and, at a constant pressure level or at hybrid levels: air temperature, relative humidity, geopotential, wind vector components,
- emission data covering the total volume of emissions of relevant chemical compounds (NO_x, VOC) (http://powietrze.gios.gov.pl/pjp/documents/download/101102).

The forecast of atmospheric air pollution by ozone for the area of Poland in the voivodeship scale is carried out every day for 3 consecutive days on a computational grid with a resolution of 5 km (0.05°). One-hour ozone concentrations are the basis for calculating the following average values:

- maximum 1-hour ozone concentration per day,
- maximum 8-hour moving average ozone concentration per day,
- 24-hour average ozone concentration.

The results of the weather forecast carried out by the GEM-AQ model, available for download from the GIOŚ website, are presented in graphic form (maps and animations) both on the national and voivodeship scale. The degree of atmospheric air pollution with ozone is presented by means of a color scale (Fig. 26).

In this work, the use was made of the Mazowieckie Voivodeship maps presenting the forecast values for the maximum 1-hour value of ozone concentration per day on the next day.

Each of the forecasts has different ozone concentration ranges (Table 28). Different colors on the maps (the same as in the table) characterize the respective ranges of ozone content in the air.

To enable comparative analysis of ozone concentration forecasts generated by selected neural networks with those created by the GEM-AQ model, the forecasted ozone concentration ranges were read from available maps for all analyzed stations (Belsk, Granica, Legionowo, Radom, Warszawa-Ursynów) in the period from 1 April to 30 September 2014 for a specific

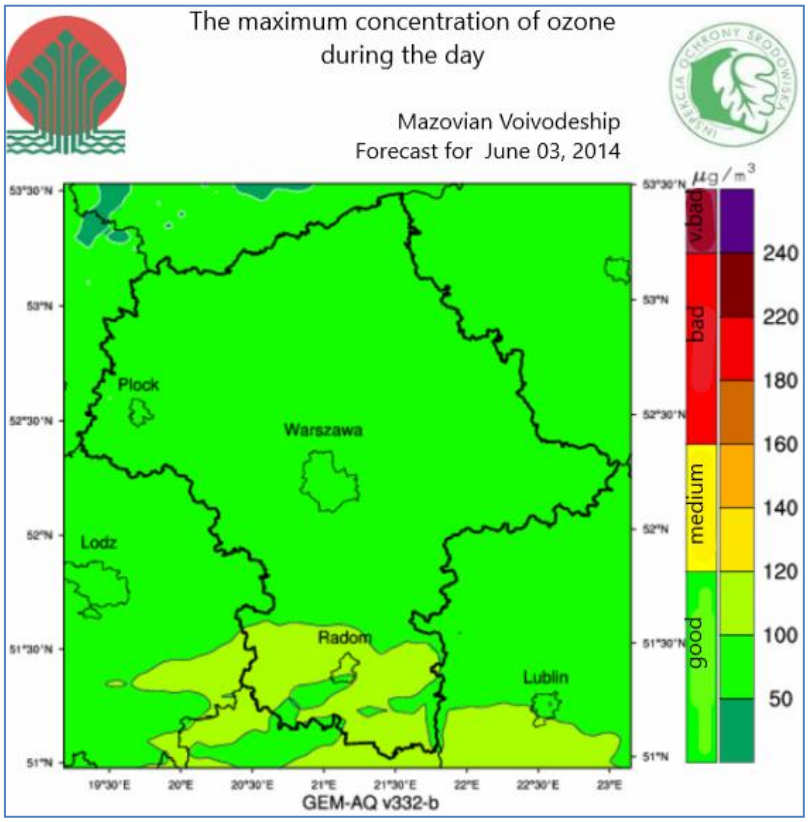

Fig. 26. Maps of ozone air pollution in the Mazowieckie Voivodeship (maximum ozone concentration per day) (source: powietrze.gios.gov.pl).

Table 28

Ranges of ozone concentration values and the corresponding color scale

Forecast	Range [µg/m^3]								
1h max	0-50	50-100	100-120	120-140	140-160	160-180	180-220	220-240	240-

type of forecast. Then, neural network prediction results were assigned to concentration ranges appropriate for the GEM-AQ model. In this way, comparable data sets containing forecasts in the form of a range of ozone concentrations for a given day for both neural networks and the GEM-AQ model were obtained.

7.2.2 Comparison results

7.2.2.1 Belsk

The total number of forecasts of ground-level ozone concentration carried out by the selected neural network for the Belsk measuring station for the period from 1 April to 30 September 2014 was 161. For these days, the results of network prediction were compared with those obtained by the GEM-AQ model. The number of accurate predictions made by the neural network was 105, which constitutes 65% of the total number of all predictions, while the number of correct predictions made by the GEM-AQ model was 81, which constitutes 50% of the total number of forecasts. Figure 27 presents the correct and incorrect forecasts for each month covered by the analysis in the period from April to September 2014 for the results of the neural network and the GEM-AQ model.

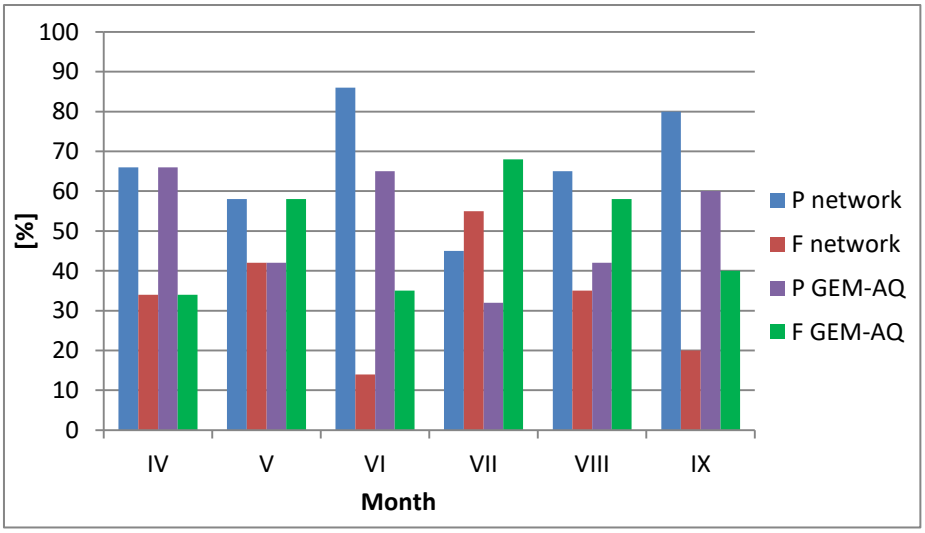

Fig. 27. Comparison of forecasts of the maximum 1-hour ozone concentration obtained from the neural network and the GEM-AQ model in the period from April to September 2014 (Station Belsk). Legend: P − correct forecast, F − incorrect forecast.

Analyzing the results of calculations for neural networks, it can be stated that in all the months covered by the analysis, except for July, correct forecasts constitute from 58% (May) to 86% (June) of the total number of forecasts. In July, only 45% of all forecasts were correct. Analyzing the results of the GEM-AQ model, it was found that in the months of April, June, and September the percentage value of the prediction was 66, 65, and 60%, respectively. In the remaining three months, i.e., May, July, and August, the percentage of correctly calculated forecasts was 42, 32, and 42%, respectively.

7.2.2.2 Granica

The total number of forecasts of ground-level ozone concentration carried out by the selected neural network for the measuring Station Granica for the period from 1 April to 30 September 2014 was 154. For these days, the results of network prediction were compared with those obtained by the GEM-AQ model. The number of forecasts correctly made by the neural network

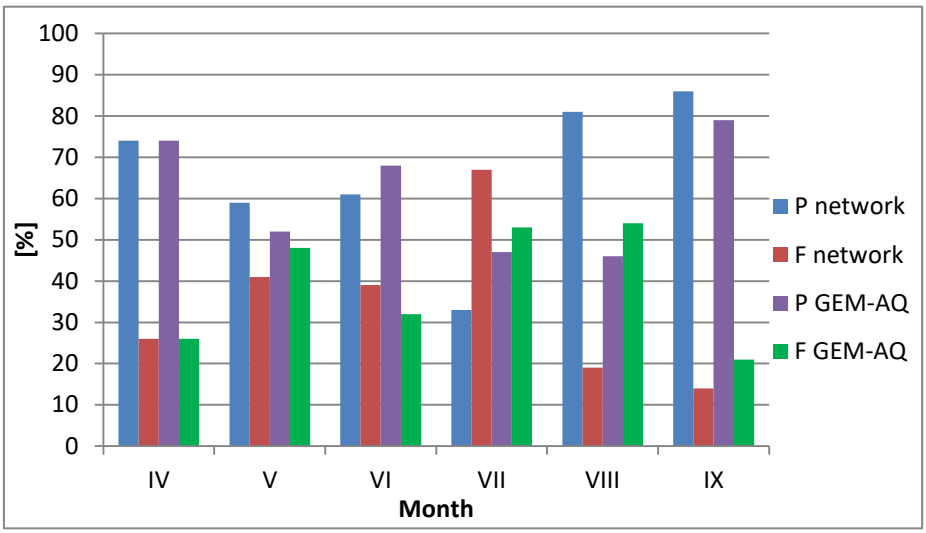

Fig. 28. Comparison of forecasts of the maximum 1-hour ozone concentration obtained from the neural network and the GEM-AQ model in the period from April to September 2014 (Station Granica). Legend: P − correct forecast, F − incorrect forecast.

was 97, which constitutes 63% of the total number of all forecasts, while the number of correct forecasts made by the GEM-AQ model was 91, which constitutes 59% of the total number of forecasts. Figure 28 presents the results of correct and incorrect forecasts for each month covered by the analysis in the period from April to September 2014 for the results of the neural network and the GEM-AQ model.

Analyzing the results of calculations for neural networks, it can be stated that in all the months covered by the analysis, except of July, correct forecasts constitute from 59% (May) to 86% (September) of the total number of forecasts. In July, only 33% of all forecasts were correct. Analyzing the results of the GEM-AQ model, in the months of April, May, June, and September it was found that the percentage of the prediction was: 74, 52, 68, and 79%, respectively. In the other two months, i.e., July and August, the percentage of correctly calculated forecasts was 47 and 46%, respectively.

7.2.2.3 Legionowo

The total number of forecasts of ground-level ozone concentration carried out by the selected neural network for the Legionowo measuring station for the period from 1 April to 30 September 2014 was 158. For these days, a comparative analysis of the prediction results generated by the network with those obtained by the GEM-AQ model was performed. The number of forecasts correctly made by the neural network was 106, which constitutes 67% of the total number of all forecasts, while the number of correct forecasts made by the GEM-AQ model was 88, which constitutes 56% of the total number of forecasts.

Figure 29 presents the results of correct and incorrect forecasts for each month under study in the period from April to September 2014 for the results of the neural network and the GEM-AQ model.

Analyzing the results of calculations for neural networks, it can be stated that in all months covered by the analysis, except for July, correct forecasts constitute from 63% (May) to 93% (September) of the total number of forecasts. In July, correct forecasts constituted only 39% of the realized forecasts. Analyzing the results of the GEM-AQ model, it was found that in the months of April, June, and September the percentage of the prediction was 65, 81, and 79%, respectively. In the months of May and July, the percentage of correctly calculated forecasts was 43 and 32%, respectively. In August, the correct forecasts constituted 50%.

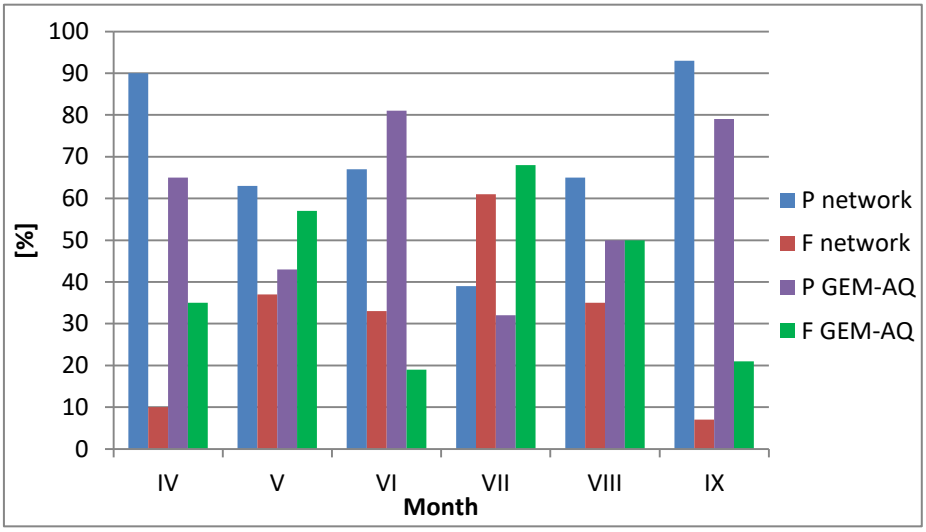

Fig. 29. Comparison of forecasts of the maximum 1-hour ozone concentration obtained from the neural network and the GEM-AQ model in the period from April to September 2014 (Station Legionowo). Legend: P − correct forecast, F − incorrect forecast.

7.2.2.4 Radom

The total number of forecasts of the ground-level ozone concentration made by the selected neural network for the Radom measuring station for the period from 1 April to 30 September 2014 was 159. For these days, the results of forecasts created by the network were compared with those made by the GEM-AQ model. The number of correct forecasts made by the neural network was 98, which constitutes 62% of the total number of all predictions, while the number of correct forecasts made by the GEM-AQ model was 88, which constitutes 55% of the total number of forecasts. Figure 30 presents the results of correct and incorrect forecasts for each month under study in the period from April to September 2014 for the results of the neural network and the GEM-AQ model.

Analyzing the results of calculations for neural networks, it can be stated that in all months covered by the analysis, with the exception of July, correct forecasts constitute from 54% (Au-

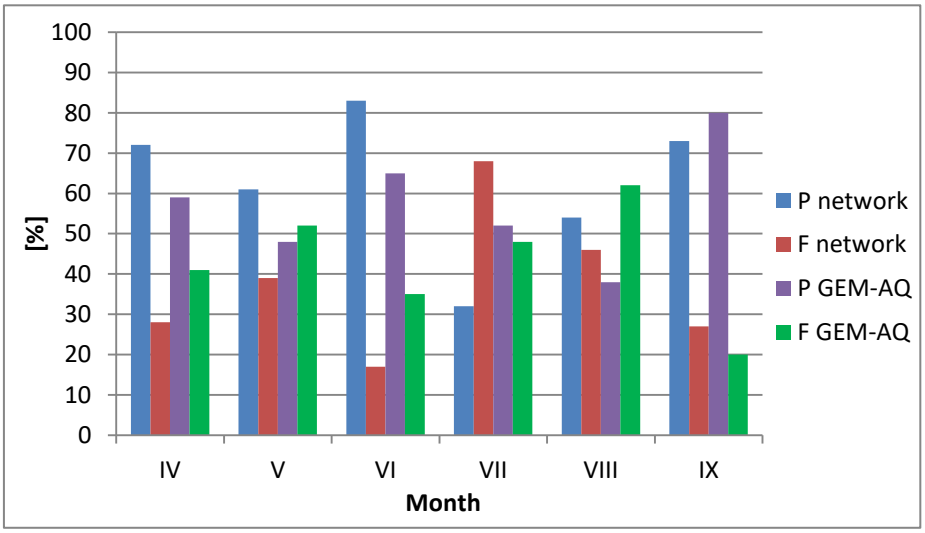

Fig. 30. Comparison of forecasts of the maximum 1-hour ozone concentration obtained from the neural network and the GEM-AQ model in the period from April to September 2014 (Station Radom). Legend: P − correct forecast, F − incorrect forecast.

gust) to 83% (June) of the total number of forecasts. In July, correctly made forecasts constitute 32% of all forecasts. Analyzing the results of the GEM-AQ model, in the months of April, June, July, and September, it was found that the percentage of the prediction was 59, 65, 52, and 80%, respectively. In the remaining months, i.e., May and August, the percentage of correctly calculated forecasts was 48% and 38%, respectively.

7.2.2.5 Warszawa-Ursynów

The total number of forecasts of the ground-level ozone concentration made by the selected neural network for the Warszawa-Ursynów measuring station for the period from 1 April to 30 September 2014 was 160. The results of network prediction were compared with those obtained by the GEM-AQ model for the appropriate 160 days of the analyzed period. The number of correct forecasts made by the neural network was 111, which constitutes 69% of the total number of all forecasts, while the number of correct forecasts made by the GEM-AQ model was 93, which constitutes 58% of the total number of forecasts. Figure 31 presents the results of correct and incorrect forecasts for each month subject to the analysis in the period from April to September 2014 for the results of the neural network and the GEM-AQ model.

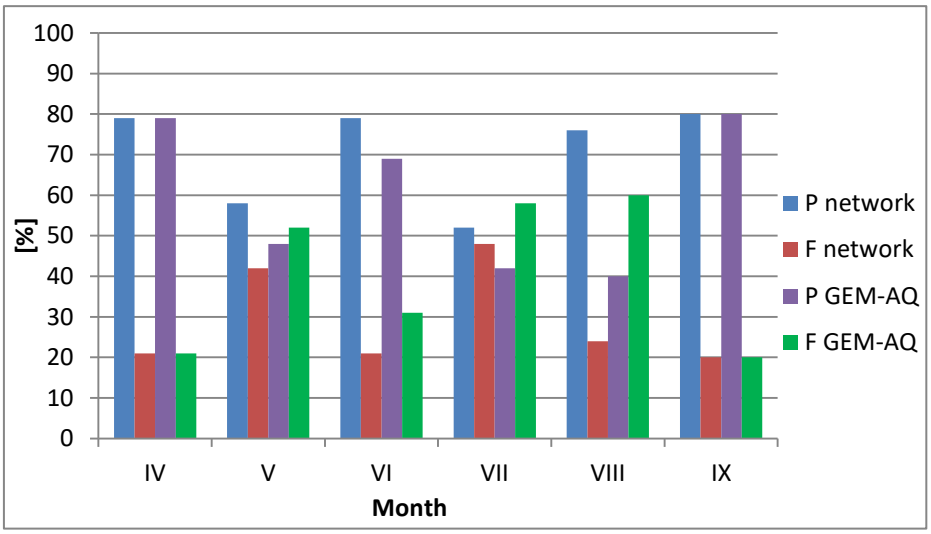

Fig. 31. Comparison of forecasts of the maximum 1-hour ozone concentration obtained from the neural network and the GEM-AQ model in the period from April to September 2014 (Station Warszawa-Ursynów). Legend: P − correct forecast, F − incorrect forecast.

Analyzing the results of calculations for neural networks, it can be stated that in all the months analyzed, the correct forecasts constitute from 52% (July) to 80% (September) of the total number of forecasts. Analyzing the results of the GEM-AQ model, it was found that in the months of April, June and September the percentage of the prediction was: 79, 69, and 80%, respectively. In the remaining three months, i.e., in May, July, and August, the percentage of correctly calculated forecasts was 48, 42, and 40%, respectively.

7.2.3 Forecast analysis with relative error value above 50%

The results of modeling the maximum 1-hour ozone concentration on the following day for the period from April to September 2014 were characterized by the occurrence of forecasts with an unusually high value of the relative error. In this paper, it was assumed that an unusually high value of relative error means a value above 50%. The adopted criterion is related to Directive 2008/50/EC, according to which the deviation from the observed value for at least 90% of forecast results should be below 50%. In this section, an analysis is made of forecasts with a relative

Table 29

Comparison of results of two forecasts: taking into account forecasted input data and actual input data, made for days on which the modeling result was contaminated by an error above 50%

Date	Measured value [μg/m^3]	Forecast 1		Forecast 2	
		Forecast [μg/m^3]	Relative error [%]	Forecast [μg/m^3]	Relative error [%]
Belsk					
6 April 2014	61.8	97.4	57.6	96.1	55.4
28 April 2014	69.8	113.2	62.1	86.9	24.4
29 May 2014	41.1	81.0	97.1	67.6	64.4
12 July 2014	24.6	58.2	136.4	54.5	121.6
27 July 2014	79.0	132.6	67.9	142.9	80.9
1 August 2014	59.4	104.2	75.4	81.0	36.4
1 September 2014	39.0	81.4	108.8	73.2	87.7
Granica					
3 April 2014	96.5	148.7	54.1	117.1	21.4
24 May 2014	100.8	154.7	53.4	132.8	31.8
25 July 2014	57.3	93.2	62.6	83.0	44.8
1 August 2014	58.5	103.8	77.4	85.0	45.3
30 September 2014	51.7	77.8	50.4	72.0	39.2
Legionowo					
3 April 2014	55.7	114.5	105.6	79.8	43.3
28 May 2014	69.3	105.2	51.8	67.7	2.3
29 May 2014	51.3	77.8	51.7	59.4	15.7
3 June 2014	37.2	59.6	60.2	58.6	57.5
12 July 2014	36.4	62.7	72.2	60.7	66.7
1 August 2014	70.8	114.4	61.6	93.2	31.7
1 September 2014	52.8	96.5	82.8	67.9	28.6
Radom					
29 May 2014	40.9	75.3	84.1	78.6	92.1
26 August 2014	58.4	89.4	53.1	84.5	44.7
1 September 2014	52.2	91.9	76.0	94.5	81.1
30 September 2014	50.2	90.5	80.4	88.5	76.3
Warszawa-Ursynów					
28 May 2014	63.1	103.4	63.8	69.9	10.9
29 May 2014	37.8	83.1	119.9	57.1	51.0
3 June 2014	34.0	60.3	77.2	54.0	58.8
11 July 2014	55.2	87.4	58.4	76.4	38.5
12 July 2014	25.7	68.4	166.0	52.3	103.3
1 September 2014	53.2	85.2	60.1	58.2	9.4

error of over 50%. Table 29 presents a list of days in which this situation took place. Additionally, the results of the forecast for the input data including the forecasted meteo parameters (Forecast 1) and for the input data including the actual meteo parameters (Forecast 2) are presented. In this way, a potential source of error can be detected, e.g., in the incorrect forecast of the input data.

As shown in Table 29, the occurrence of forecast values with an error of over 50% was recorded at all measuring stations. Their number, depending on the station, ranged from 4 (Radom) to 7 (Belsk, Legionowo).

It has been observed that errors above 50% are associated with relatively low values of observed maximum 1-hour ozone concentrations, in the range from 25.7 to 79 $\mu g/m^3$. The exceptions are 2 cases at the Station Granica, where the concentration values were higher (96.5 and 100.8 $\mu g/m^3$). It is important to note that in each case the network had a tendency to overestimate the actual ozone content and this usually took place with a sharp decrease in ozone concentration. Figure 32 presents such an example that occurred on 12 July 2014, and plots over 7 days before and 7 days after it, as recorded at the Station Warszawa-Ursynów. As shown in Fig. 32, the maximum ozone concentration dropped by about 70 $\mu g/m^3$ within two days, and on the next day it increased by over 60 $\mu g/m^3$. The network correctly detected the direction of changes, but it failed to forecast such a low ozone content. In order to determine the origin of such high error values generated by the network, an additional forecast of ozone concentrations was made for the days listed in Table 29. This time, the forecasted meteorological parameter values were replaced by the actual ones. A comparative analysis of the errors the two types of forecasts showed that:

- for Belsk, the error value was reduced in six out of seven cases, and in two cases the forecast result had an error below 50%;
- for Granica, in addition to reducing the error value in each case, it was possible to generate a forecast with an error below 50%;
- for Legionowo, in each case the error value decreased and in five out of seven cases the error was less than 50%;
- for Radom in two out of four cases a smaller error was obtained and in one the error below 50% was achieved;
- for Warszawa-Ursynów, in all six cases there was a decrease in error and in four cases an error below 50% was obtained.

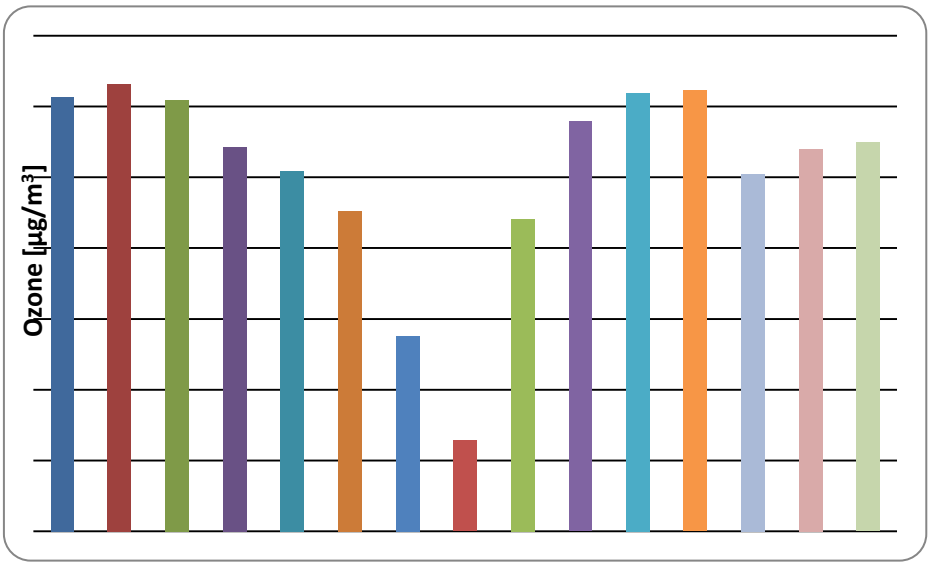

Fig. 32. Values of ozone concentration in the period from 5 to 19 July 2014.

As follows from the above, the use of real meteorological parameters instead of forecasted ones significantly improved the quality of the forecast. In 93% of cases, the forecast results were contaminated by a smaller error and in 55% the obtained error values were less than 50%. This demonstrates the ability of the network to correctly reproduce the relationships between variables, and high relative error values of generated forecasts may be partly a consequence of incorrect input data.

8. SUMMARY AND CONCLUSIONS

The presence of ozone in the ground layer of the atmosphere is a widely discussed issue in recent decades, especially in the context of the occurrence of high ozone concentrations − dangerous to human health and plant conditions. Ground-level ozone is a secondary air pollutant arising as a result of photochemical reactions involving, i.e., nitrogen oxides and volatile organic compounds. Ozone production processes, involving the content of ozone precursors and their quantitative ratio, are strongly non-linear (Lin et al. 1988). The significant impact of ozone on the formation of the greenhouse effect on Earth, the formation of photochemical smog and the production of free radicals makes it a very important component of air, and the recognition and description of its time-space variability and factors determining its concentration is of fundamental importance.

The main goal of this work was a detailed analysis of the variability of ozone content in the ground layer of the atmosphere in the Mazowieckie Voivodeship. The considerations presented concern six measuring stations: Belsk, Granica, Legionowo, Radom-Tochterman, Warszawa-Krucza, and Warszawa-Ursynów selected to represent the stations of the urban background as well as the regional background. The goal was achieved through the following actions:

(1) A detailed analysis of the variability of ozone concentration values in the ground layer of the atmosphere, at all the stations under study, on an annual, weekly, and daily scale. This analysis covered a period of 8 years, from 2005 to 2012. Average long-term ozone concentration values ranged from 41.2 to 54.1 $\mu g/m^3$. The highest values were recorded at the regional background stations: Belsk and Granica, and the lowest at the urban background stations: Warszawa-Krucza and Radom. The variability of ozone concentrations is determined by a number of factors, among which the most important are: the state of air pollution and the associated availability of potential ozone precursors, as well as the prevailing meteorological conditions affecting the rate of photochemical reactions. Changes in the above factors on an annual or daily basis are reflected in the variability of ozone content. At all analyzed stations, a characteristic cycle of changes in ozone concentrations was observed with a maximum in the spring and summer and a minimum in the autumn and winter. The existence of a clear April maximum for regional background stations and a wide spring-summer maximum for urban background stations was recognized. The highest ozone concentration values per week, regardless of the type of station, were recorded on Sundays and the lowest on Wednesdays at regional background stations and on Fridays at urban background stations. In addition, the existence of ozone weekend phenomenon (occurrence of higher ozone concentrations on working days than on Saturdays and Sundays) has been demonstrated annually at a statistically significant level ($\alpha = 0.05$) for the Station Warszawa-Krucza. The analysis of the phenomenon in individual seasons showed the existence of the weekend phenomenon in all seasons only at the Station Warszawa-Krucza and additionally at the Warszawa-Ursynów, Radom and Belsk stations in winter. During the analysis of the pattern in the scale of individual seasons, an unusual phenomenon of lower ozone concentrations on workdays was detected on Saturdays and Sundays at regional background stations in summer. An application of the comparative method for the O_x content on workdays and on Saturdays and Sundays made it possible to detect the main reason for the occurrence of the ozone weekend phenomenon at the measuring stations of the

Mazowieckie Voivodeship, namely the reduction of NO emissions on Saturdays and Sundays, and hence the reduction of ozone destruction processes with the participation of NO particles. The universal pattern of ground-level ozone variability throughout the day, with a clear maximum in the afternoon and a minimum just before sunrise, undergoes significant changes throughout the year. Depending on the month, the changes concern the ozone concentration values, amplitudes of diurnal changes as well as the occurrence time of the maximum. In addition, during the winter, a specific double minimum, in the morning and evening, has occurred at the urban-background stations.

(2) Assessment of the variability in the ground-level ozone content trend at Belsk in 1995−2016. Based on the average annual values of ozone concentrations and the curve determined by the LOWESS local regression method, three periods were distinguished (1995−2003, 2003−2010, 2010−2016), during which the following pattern was observed: increase, decrease and then again a slow increase of ground-level ozone.

(3) A statistical analysis to learn what relationship exists between the ground ozone content and selected meteorological parameters on a monthly basis at the stations under study. The relationship between the value of ozone concentration and air temperature shows a positive, statistically significant correlation in the months from April to October. In the remaining months, correlation coefficients have different character and are usually not statistically significant. Of interest is the correlation between ozone content and relative humidity, which is negative throughout the year and statistically significant. An opposite situation is in the case of the dependence of the ozone content on the solar radiation, in which the correlation throughout the year is positive and almost always statistically significant. The impact of wind speed on the ozone concentration value varies significantly throughout the year. Noticeable is a positive, statistically significant correlation in the months from October to February, proving that the transport of ozone-rich air is a key factor in shaping the ozone budget in the autumn and winter. In the remaining months, correlation coefficient values are much lower and usually indicate a negative correlation between wind speed and ozone concentration.

(4) Construction of five (for 5 measuring stations) models of neural networks that forecast the value of the maximum 1-hour ozone concentration per day on the following day for the period from April to September 2015. The Statistica 10 "Automatic neural networks" model package was used to build the models. The model input data were the following: predictive data (WRF model forecast) of four basic meteorological parameters (air temperature, solar radiation, relative humidity and wind speed) identified as having key significance for the processes of ozone formation and destruction in the atmosphere, as well as two parameters relating to the ozone concentration on the day preceding the forecast and time the forecast was made. For approximation, three-layer MLP networks were used, with a properly selected number of neurons in the hidden layer and the appropriate activation function for the hidden and output layers. The quasi-Newtonian algorithm BFGS was used to create all the networks, and the SOS function was the error function in all cases. Optimization of the best model was based on network quality indicators and error values for each subset (training, test, and validation). Selected neural networks were of simple topology. The number of neurons in the input layer was 6, in the hidden layer from 3 to 7 and in the output layer 1. The global sensitivity analysis showed that the parameters constituting the input data of the model were chosen correctly. The local sensitivity analysis made it possible to find the variability ranges of input variables, particularly important for the result of the prediction and at the same time to reflect the non-linear nature of the relationship between ground-level ozone content and meteorological parameters, of different character, depending on the station type. Hence, one can conclude that there is a significant impact of local environmental conditions (meteorological and chemical) on shaping the nature of the non-linear relationship between ground-level ozone and the values of meteorological

parameters. It can be stated that the correlation analysis based on the values of Pearson's coefficient was a preliminary, visual assessment of the interdependence of variables. Thanks to the neural networks (or more precisely the tool in the form of local sensitivity analysis), it was possible to detect a non-linear correlation that actually characterizes the ground-level ozone content and selected meteorological parameters.

(5) Verification of the quality of operation of all selected neural networks over the period from April to September 2014, using the same set of input data as in the year 2015. The purpose of the verification was to assess the ability of the network to generalize the knowledge acquired during the training process for new cases previously not presented to the network. The values of correlation coefficients for all stations, varying from 0.69 (Radom) to 0.79 (Legionowo), show that in most cases the correlation between the actual and forecast values is high. The average values of relative errors range from 14.3% (Legionowo) to 15.8% (Radom). Forecasts characterized by the highest value of relative errors (above 50%) were the effect of overestimation of relatively low ozone concentrations, associated with a sharp decrease in measured values.

(6) Comparison of the modeling results of maximum 1-hour values of ground-level ozone for the next day using the artificial neural networks constructed by the author and the global troposphere chemistry model GEM-AQ. The comparative analysis covered the period from April to September 2014. The results for neural models indicate that the percentage of correctly made predictions, depending on the measuring station, ranged from 62% (Radom) to 69% (Warszawa-Ursynów), while the percentage of correct predictions generated by the GEM-AQ model fluctuated in the range from 50% (Belsk) to 59% (Granica). Ultimately, it can be stated that the use of artificial neural networks with the MLP structure is an effective tool supporting the prediction of ground-level ozone for the next day and the accuracy of forecasts is at least equivalent, or in some cases better than the accuracy of forecasts obtained using modern global troposphere chemistry models.

References

Andrews, T. (1874), Address on ozone, *J. Scot. Meteorol. Soc.* **4**, 41-42, 122–134.

Aneja, V.P., C.S. Claiborn, Z. Li, and A. Murthy (1994), Trends, seasonal variations, and analysis of high-elevation surface nitric acid, ozone, and hydrogen peroxide, *Atmos. Environ.* **28**, 10, 1781–1790, DOI: 10.1016/1352-2310(94)90140-6.

Atkinson, R. (2000), Atmospheric chemistry of VOCs and NO_x, *Atmos. Environ.* **34**, 12-14, 2063–2101, DOI: 10.1016/S1352-2310(99)00460-4.

Atkinson, R., D.L. Baulch, R.A. Cox, J.N. Crowley, R.F. Hampson, R.G. Hynes, M.E. Jenkin, M.J. Rossi, and J. Troe (2006), Evaluated kinetic and photochemical data for atmospheric chemistry, Tech. Rep., IUPAC Subcommittee on Gas Kinetic Data Evaluation for Atmospheric Chemistry, Cambridge, UK, available from: http://www.iupac-kinetic.ch.cam.ac.uk.

Atkinson-Palombo, C.M., J.A. Miller, and R.C. Balling Jr. (2006), Quantifying the ozone "weekend effect" at various locations in Phoenix, Arizona, *Atmos. Environ.* **40**, 39, 7644–7658, DOI: 10.1016/j.atmosenv.2006.05.023.

Beekmann, M., G. Ancellet, S. Blonsky, D. De Muer, A. Ebel, H. Elbern, J. Hendricks, J. Kowol, C. Mancier, R. Sladkovic, H.G.J. Smit, P. Speth, T. Trickl, and Ph. Van Haver (1997), Stratosphere-troposphere exchange – regional and global tropopause folding occurrence. **In:** P. Borrell and P.M. Borrell (eds.), *Transport and Chemical Transformation of Pollutants in the Troposphere*, Vol. 6, Springer, Berlin Heidelberg, 131–151.

Bithell, M., L.J. Gray, and B.D. Cox (1999), A three-dimensional view of the evolution of midlatitude stratospheric intrusions, *J. Atmos. Sci*. **56**, 5, 673–688, DOI: 10.1175/1520-0469(1999)056 <0673:ATDVOT>2.0.CO;2.

Bojkov, R.D. (1986), Surface ozone during the second half of the nineteenth century, *J. Climate Appl. Meteor*. **25**, 3, 343–352, DOI: 10.1175/1520-0450(1986)025<0343:SODTSH>2.0.CO;2.

Bonasoni, P., F. Evangelisti, U. Bonafe, F. Ravegnani, F. Calzolari, A. Stohl, L. Tositti, O. Tubertini, and T. Colombo (2000), Stratospheric ozone intrusion episodes recorded at Mt. Cimone during the VOTALP project: case studies, *Atmos. Environ.* **34**, 9, 1355–1365, DOI: 10.1016/S1352-2310(99)00280-0.

Bonasoni, P., P. Laj, F. Angelini, J. Arduini, U. Bonafè, F. Calzolari, P. Cristofanelli, S. Decesari, M.C. Facchini, S. Fuzzi, G.P. Gobbi, M. Maione, A. Marinoni, A. Petzold, F. Roccato, J.C. Roger, K. Sellegri, M. Sprenger, H. Venzac, G.P. Verza, P. Villani, and E. Vuillermoz (2008), The ABC-Pyramid Atmospheric Research Observatory in Himalaya for aerosol, ozone and halocarbon measurements, *Sci. Total Environ.* **391**, 2–3, 252–261, DOI: 10.1016/j.scitotenv.2007.10.024.

Brönnimann, S., and U. Neu (1997), Weekend-weekday differences of near-surface ozone concentrations in Switzerland for different meteorological conditions, *Atmos. Environ.* **31**, 8, 1127–1135, DOI: 10.1016/S1352-2310(96)00311-1.

Cape, J.N. (2008), Surface ozone concentrations and ecosystem health: past trends and a guide to future projections, *Sci. Total Environ.* **400**, 1–3, 257–269, DOI: 10.1016/j.scitotenv.2008.06.025.

Chevalier, A., F. Gheusi, R. Delmas, C. Ordóñez, C. Sarrat, R. Zbinden, V. Thouret, G. Athier, and J.-M. Cousin (2007), Influence of altitude on ozone levels and variability in the lower troposphere: a ground-based study for western Europe over the period 2001–2004, *Atmos. Chem. Phys.* **7**, 16, 4311–4326.

Chou, C.C.K., S.C. Liu, C.Y. Lin, C.J. Shiu, and K.H. Chang (2006), The trend of surface ozone in Taipei, Taiwan, and its causes: implications for ozone control strategies, *Atmos. Environ.* **40**, 21, 3898–3908, DOI: 10.1016/j.atmosenv.2006.02.018.

Chung, Y.S. (1977), Ground-level ozone and regional transport of air pollutants, *J. Appl. Meteor*. **16**, 11, 1127-1136, DOI: 10.1175/1520-0450(1977)016<1127:GLOART>2.0.CO;2.

Cleveland, W.S. (1979), Robust locally weighted regression and smoothing scatterplots, *J. Am. Statist. Assoc*. **74**, 368, 829–836, DOI: 10.1080/01621459.1979.10481038.

Cleveland, W.S., T.E. Graedel, B. Kleiner, and J.L. Warner (1974), Sunday and workday variations in photochemical air pollutants in New Jersey and New York, *Science* **186**, 4168, 1037–1038, DOI: 10.1126/science.186.4168.1037.

Cooper, O.R., D.D. Parrish, J. Ziemke, N.V. Balashov, M. Cupeiro, I.E. Galbally, S. Gilge, L. Horowitz, N.R. Jensen, J.F. Lamarque, V. Naik, S.J. Oltmans, J. Schwab, D.T. Shindell, A.M. Thompson, V. Thouret, Y. Wang, and R.M. Zbinden (2014), Global distribution and trends of tropospheric ozone: An observation-based review, *Elementa: Sci. Anthropocene* **2**, 29, DOI: 10.12952/journal.elementa.000029.

Corsmeier, U., N. Kalthoff, O. Kolle, M. Kotzian, and F. Fiedler (1997), Ozone concentration jump in the stable nocturnal boundary layer Turing a LLJ-event, *Atmos. Environ.* **31**, 13, 1977–1989, DOI: 10.1016/S1352-2310(96)00358-5.

Côté, J., S. Gravel, A. Méthot, A. Patoine, M. Roch, and A. Staniforth (1998), The operational CMC–MRB Global Environmental Multiscale (GEM) model: Part I – Design considerations and formulation, *Month. Weather Rev.* **126**, 6, 1373–1395, DOI: 10.1175/1520-0493(1998)126<1373: TOCMGE>2.0.CO;2.

Crutzen, P.J., and P.H. Zimmermann (1991), The changing photochemistry of the troposphere, *Tellus A* **43**, 4, 136–151, DOI: 10.3402/tellusa.v43i4.11943.

Cybenko, G. (1989), Approximation by superposition's of a sigmoidal function, *Math. Control Sign. Syst*. **2**, 303–314, DOI: 10.1007/BF02551274.

Davies, T.D., and E. Schuepbach (1994), Episodes of high ozone concentrations at the earth's surface resulting from transport down from the upper troposphere / lower stratosphere: a review and case studies, *Atmos. Environ.* **28**, 1, 53–68, DOI: 10.1016/1352-2310(94)90022-1.

de Souza, A., F. Aristone, and I. Sabbah (2015), Modeling the surface ozone concentration in Campo Grande (MS) – Brazil using neural networks, *Natural Sci.* **7**, 4, 171–178, DOI: 10.4236/ns.2015.74020.

Debaje, S.B., and A.D. Kakade (2006), Measurements of surface ozone in rural site of India, *Aerosol Air Qual. Res*. **6**, 4, 444–465, DOI: 10.4209/aaqr.2006.12.0002.

Dlugokencky, E.J., E.G. Nisbet, R. Fisher, and D. Lowry (2011), Global atmospheric methane: budget, changes and dangers, *Philos. Trans. Roy. Soc*. **369**, 1943, 2058–2072, DOI: 10.1098/rsta.2010.0341.

Eliasson, I., S. Thorsson, and Y. Andersson-Sköld (2003), Summer nocturnal ozone maxima in Göteborg, Sweden, *Atmos. Environ.* **37**, 19, 2615–2627, DOI: 10.1016/S1352-2310(03)00205-X.

Elkamel, A., S. Abdul-Wahab, W. Bouhamra, and E. Alper (2001), Measurement and prediction of ozone levels around a heavily industrialized area: a neural network approach, *Adv. Environ. Res*. **5**, 1, 47–59, DOI: 10.1016/S1093-0191(00)00042-3.

Fabian, P., and P.G. Pruchniewicz (1977), Meridional distribution of ozone in the troposphere and its seasonal variations, *J. Geophys. Res.* **82**, 15, 2063–2073, DOI: 10.1029/JC082i015p02063.

Falkowska, L., and K. Korzeniewski (1998), *Chemia Atmosfery*, Wydawnictwo Uniwersytetu Gdańskiego, Gdańsk (in Polish).

Finlayson-Pitts, B.J., and J.N. Pitts Jr. (1993), Atmospheric chemistry of tropospheric ozone formation: scientific and regulatory implications, *Air & Waste* **43**, 8, 1091–1100, DOI: 10.1080/1073161X.1993.10467187.

Fishman, J., and P.J. Crutzen (1977), A numerical study of tropospheric photochemistry using a one-dimensional model, *J. Geophys. Res.* **82**, 37, 5897–5906, DOI: 10.1029/JC082i037p05897.

Fishman, J., and P.J. Crutzen (1978), The origin of ozone in the troposphere, *Nature* **274**, 855–858, DOI: 10.1038/274855a0.

Fishman, J., V. Ramanathan, P.J. Crutzen, and S.C. Liu (1979), Tropospheric ozone and climate, *Nature* **282**, 818–820, DOI: 10.1038/282818a0.

Fujita, E.M., W.R. Stockwell, D.E. Campbell, L.R. Chinkin, H.H. Main, and P.T. Roberts (2002), Weekend/weekday ozone observations in the South Coast Air Basin: Volume I – executive summary, Final Report prepared by the Desert Research Institute, Reno, NV, and Sonoma Technology, Petaluma, CA, for the National Renewable Energy Laboratory, Golden, CO, and the Coordinating Research Council, Alpharetta, GA, 12 June 2002.

Garcia, I., J.G. Rodriguez, and Y.M. Tenorio (2011), Artificial neural network models for prediction of ozone concentrations in Guadalajara, Mexico. **In:** D. Popović (ed.), *Air Quality-Models and Applications*, InTech, Rijeka, 35–52, available from: https://www.intechopen.com/books/air-quality-models-and-applications/artificial-neural-network-models-for-prediction-of-ozone-concentrations-in-guadalajara-mexico.

Gardner, M., and S. Dorling (2001), Artificial neural network-derived trends in daily maximum surface ozone concentrations, *J. Air & Waste Manage. Assoc*. **51**, 8, 1202–1210, DOI: 10.1080/10473289.2001.10464338.

Gilge, S., C. Plass-Duelmer, W. Fricke, A. Kaiser, L. Ries, and B. Buchmann (2010), Ozone, carbon monoxide and nitrogen oxides time series at four Alpine GAW mountain stations in Central Europe, *Atmos. Chem. Phys.* **10**, 24, 12295–12316, DOI: 10.5194/acp-10-12295-2010.

Goethals, P.L.M., A.P. Dedecker, W. Gabriels, S. Lek, and N. De Pauw (2007), Applications of artificial neural networks predicting macroinvertebrates in freshwaters, *Aquatic Ecol.* **41**, 3, 491–508, DOI: 10.1007/s10452-007-9093-3.

Gong, S.L., L.A. Barrie, J.-P. Blanchet, K. von Salzen, U. Lohmann, G. Lesins, L. Spacek, L.M. Zhang, E. Girard, H. Lin, R. Leaitch, H. Leighton, P. Chylek, and P. Huang (2003), Canadian Aerosol

Module: A size-segregated simulation of atmospheric aerosol processes for climate and air quality models, 1. Module development, *J. Geophys. Res.* **108**, D1, AAC3-1–AAC3-16, DOI: 10.1029/2001JD002002.

Guicherit, R., and M. Roemer (2000), Tropospheric ozone trends, *Chemosphere – Global Change Sci.* **2**, 2, 167–183, DOI: 10.1016/S1465-9972(00)00008-8.

Güsten, H., G. Heinrich, E. Mönnich, D. Sprung, J. Weppner, A.B. Ramadan, M.R.M. Ezz El-Din, D.M. Ahmed, and G.K.Y. Hassan (1996), On-line measurements of ozone surface fluxes: Part II. Surface-level ozone fluxes onto the Sahara desert, *Atmos. Environ.* **30**, 6, 911–918, DOI: 10.1016/1352-2310(95)00270-7.

Haagen-Smit, A.J. (1952), Chemistry and physiology of Los Angeles smog, *Industr. Eng. Chem*. **44**, 6, 1342–1346, DOI: 10.1021/ie50510a045.

Helmig, D., S.J. Oltmans, T.O. Morse, and J.E. Dibb (2007), What is causing high ozone at Summit, Greenland? *Atmos. Environ.* **41**, 24, 5031–5043, DOI: 10.1016/j.atmosenv.2006.05.084.

Heuss, J.M., D.F. Kahlbaum, and G.T. Wolff (2003), Weekday/weekend ozone differences: what can we learn from them? *J. Air & Waste Manage. Assoc.* **53**, 7, 772–788, DOI: 10.1080/10473289.2003.10466227.

Hocking, W.K., T. Carey-Smith, D.W. Tarasick, P.S. Argall, K. Strong, Y. Rochon, I. Zawadzki, and P.A. Taylor (2007), Detection of stratospheric ozone intrusions by windprofiler radars, *Nature* **450**, 281–284, DOI: 10.1038/nature06312.

Holton, J.R., P.H. Haynes, M.E. McIntyre, A.R. Douglass, R.B. Rood, and L. Pfister (1995), Stratosphere-troposphere exchange, *Rev. Geophys*. **33**, 4, 403–439, DOI: 10.1029/95RG02097.

Hooyberghs, J., C. Mensink, G. Dumont, F. Fierens, and O. Brasseur (2005), A neural network forecast for daily average PM_{10} concentrations in Belgium, *Atmos. Environ.* **39**, 18, 3279–3289, DOI: 10.1016/j.atmosenv.2005.01.050.

IPCC (2013), Working Group I contribution to the IPCC fifth assessment report "Climate Change 2013: The Physical Science Basis", Final Draft Underlying Scientific-Technical Assessment. IPCC (Intergovernmental Panel on Climate Change), available from http://www.ipcc.ch.

Jacob, D.J. (1999), *Introduction to Atmospheric Chemistry*, Princeton University Press, Princeton.

Johnson, W.B., and W. Viezee (1981), Stratospheric ozone in the lower troposphere – I. Presentation and interpretation of aircraft measurements, *Atmos. Environ.* **15**, 7, 1309–1323, DOI: 10.1016/0004-6981(81)90325-5.

Juda-Rezler, K. (2006), *Oddziaływanie Zanieczyszczeń Powietrza na Środowisko*, Oficyna Wydawnicza Politechniki Warszawskiej, Warszawa (in Polish).

Kaczorowska, Z. (1986), *Pogoda i Klimat*, Wydawnictwa Szkolne i Pedagogiczne, Warszawa (in Polish).

Kaminski, J.W., L. Neary, J. Struzewska, J.C. McConnell, A. Lupu, J. Jarosz, K. Toyota, S.L. Gong, J. Côté, X. Liu, K. Chance, and A. Richter (2008), GEM-AQ, an on-line global multiscale chemical weather modelling system: model description and evaluation of gas phase chemistry processes, *Atmos. Chem. Phys*. **8**, 12, 3255-3281, DOI: 10.5194/acp-8-3255-2008.

Lal, S., M. Naja, and B.H. Subbaraya (2000), Seasonal variations in surface ozone and its precursors over an urban site in India, *Atmos. Environ.* **34**, 17, 2713–2724, DOI: 10.1016/S1352-2310(99)00510-5.

Lee, H.J., S.W. Kim, J. Brioude, O.R. Cooper, G.J. Frost, C.H. Kim, R.J. Park, M. Trainer, and J.H. Woo (2014), Transport of NOx in East Asia identified by satellite and in situ measurements and Lagrangian particle dispersion model simulations, *J. Geophys. Res. Atmospheres* **119**, 5, DOI: 10.1002/2013JD021185.

Lelieveld, J., and P.J. Crutzen (1991), The role of clouds in tropospheric photochemistry, *J. Atmos. Chem*. **12**, 229–267, DOI: 10.1007/BF00048075.

Lin, X., M. Trainer, and S.C. Liu (1988), On the nonlinearity of the tropospheric ozone production, *J. Geophys. Res.* **93**, D12, 15879–15888, DOI: 10.1029/JD093iD12p15879.

Logan, J.A. (1985), Tropospheric ozone: Seasonal behavior, trends, and antropogenic influence, *J. Geophys. Res.* **90**, D6, 10463–10482, DOI: 10.1029/JD090iD06p10463.

Logan, J.A., J. Staehelin, I.A. Megretskaia, J.P. Cammas, V. Thouret, H. Claude, H. De Backer, M. Steinbacher, H.E. Scheel, R. Stübi, M. Fröhlich, and R. Derwent (2012), Changes in ozone over Europe: Analysis of ozone measurements from sondes, regular aircraft (MOZAIC) and alpine surface sites, *J. Geophys. Res.* **117**, D9, D09301, DOI: 10.1029/2011JD016952.

Lurmann, F.W., A.C. Lloyd, and R. Atkinson (1986), A chemical mechanism for use in long-range transport/acid deposition computer modeling, *J. Geophys. Res.* **91**, D10, 10905–10936, DOI: 10.1029/JD091iD10p10905.

Maleszewski, S., E. Burchacka, M. Rakus, and B. Kozłowska-Szerenos (1999), Stomatal responses of bean (Phaseolus vulgaris L.) leaves to changing irradiance, air humidity, and water potential of root medium, *Photosynthetica* **37**, 39–46, DOI: 10.1023/A:1007062712048.

Maleszewski, S., B. Kozłowska-Szerenos, and A. Jurga (2003), Znaczenie aparatów szparkowych dla współdziałania wody i światła w metabolizmie roślin, *Wiadomości Botaniczne* **47**, 1/2, 27–39 (in Polish).

Marenco, A., H. Gouget, P. Nédélec, J.P. Pagés, and F. Karcher (1994), Evidence of a long-term increase in tropospheric ozone from Pic du Midi series: Consequences: Positive radiative forcing, *J. Geophys. Res.* **99**, D8, 16617–16632, DOI: 10.1029/94JD00021.

Marsalli, M. (2006), McCulloch-Pitts Neurons, available from: http://www.mind.ilstu.edu/curriculum/mcp_neurons/ mcp_neuron_5.php?mdGUI=212&compGUI=1749&itemGUI=3022.

Mazely, T.L., R.R. Friedl, and S.P. Sander (1995), Production of NO_2 from photolysis of peroxyacetyl nitrate, *J. Phys. Chem*. **99**, 20, 8162–8169, DOI: 10.1021/j100020a044.

Melas, D., I. Kioutsioukis, and I.C. Ziomas (2000), Neural network model for predicting peak photochemical pollutant levels, *J. Air & Waste Manage. Assoc*. **50**, 4, 495–501, DOI: 10.1080/10473289.2000.10464039.

Mohanakumar, K. (2008), *Stratosphere-Troposphere Interactions. An Introduction*, Springer Science & Business Media, 416 pp.

Monks, P.S. (2000), A review of the observations and origins of the spring ozone maximum, *Atmos. Environ.* **34**, 21, 3545–3561, DOI: 10.1016/S1352-2310(00)00129-1.

Moore, G.W.K., and J.L. Semple (2005), A Tibetan Taylor Cap and a halo of stratospheric ozone over the Himalaya, *Geophys. Res. Lett*. **32**, 21, L21810, DOI: 10.1029/2005GL024186.

Moore, G.W.K., and J.L. Semple (2009), High concentration of surface ozone observed along the Khumbu Valley Nepal, April 2007, *Geophys. Res. Lett.* **36**, 14, L14809, DOI: 10.1029/2009GL038158.

Moore, G.W.K., S. Abernethy, and J.L. Semple (2009), Spatial and temporal variability in surface ozone at a high elevation remote site in Nepal, *Atmos. Chem. Phys. Discuss*. **9**, 16233–16266, DOI: 10.5194/acpd-9-16233-2009.

Naja, M., H. Akimoto, and J. Staehelin (2003), Ozone in background and photochemically aged air over central Europe: Anlysis of long-term ozonesonde data from Hohenpeissenberg and Payerne, *J. Geophys. Res.* **108**, D2, 4063–4073, DOI: 10.1029/2002JD002477.

Novelli, P.C., K.A. Masarie, P.M. Lang, B.D. Hall, R.C. Myers, and J.W. Elkins (2003), Reanalysis of tropospheric CO trends: Effects of the 1997–1998 wildfires, *J. Geophys. Res.* **108**, D15, 4464, DOI: 10.1029/2002JD003031.

Ordóñez, C., H. Mathis, M. Furger, S. Henne, Ch. Hüglin, J. Staehelin, A.S.H. Prévôt (2005), Changes of daily surface ozone maxima in Switzerland in all seasons from 1992 to 2002 and discussion of summer 2003, *Atmos. Chem. Phys.* **5**, 1187–1203, DOI: 10.5194/acp-5-1187-2005.

Parrish, D.D., M. Trainer, M.P. Buhr, B.A. Watkins, and F.C. Fehsenfeld (1991), Carbon monoxide concentrations and their relation to concentrations of total reactive oxidized nitrogen at two rural U.S. sites, *J. Geophys. Res.* **96**, D5, 9309–9320, DOI: 10.1029/91JD00047.

Pawlak, I., and J. Jarosławski (2014), Analysis of surface ozone variations based on the long-term measurement series in Kraków (1854–1878), (2005–2013) and Belsk (1995–2012). **In:** R. Bialik, M. Majdański, and M. Moskalik (eds.), *Achievements, History and Challenges in Geophysics*, GeoPlanet: Earth and Planetary Sciences, Springer, Cham, 313–335, DOI: 10.1007/978-3-319-07599-0_18.

Pawlak, I., and J. Jarosławski (2015), The influence of selected meteorological parameters on the concentration of surface ozone in the central region of Poland, *Atmos. Ocean* **53**, 1, 126–139, DOI: 10.1080/07055900.2014.969189.

Pellegrini, E., G. Lorenzini, and C. Nali (2007), The 2003 European Heat Wave: Which role for ozone? Some data from Tuscany, Central Italy, *Water Air Soil Poll*. **181**, 401–408, DOI: 10.1007/s11270-006-9310-z.

Pio, C.A., and M.S. Feliciano (1996), Dry deposition of ozone and sulphur dioxide over low vegetation in moderate southern European weather conditions. Measurements and modelling, *Phys. Chem. Earth* **21**, 5-6, 373–377, DOI: 10.1016/S0079-1946(97)81126-3.

Pont, V., and J. Fontan (2001), Comparison between weekend and weekday ozone concentration in large cities in France, *Atmos. Environ.* **35**, 8, 1527–1535, DOI: 10.1016/S1352-2310(00)00308-3.

Rani, B., U. Singh, A.K. Chuhan, D. Sharma, and R. Maheshwari (2011), Photochemical smog pollution and its mitigation measures, *J. Adv. Sci. Res*. **2**, 4, 28–33.

Rowntree, D. (1981), *Statistics without Tears: A Primer for Non-mathematicians*, Charles Scribner's Sons, New York, 170 pp.

Rubin, M.B. (2001), The history of ozone. The Schönbein period, 1839–1868, *Bull. Hist. Chem*. **26**, 1, 40–56.

Sadanaga, Y., S. Shibata, M. Hamana, N. Takenaka, and H. Bandow (2008), Weekday/weekend difference of ozone and its precursors in urban areas of Japan, focusing on nitrogen oxides and hydrocarbons, *Atmos. Environ.* **42**, 19, 4708–4723, DOI: 10.1016/j.atmosenv.2008.01.036.

Sadanaga, Y., M. Sengen, N. Takenaka, and H. Bandow (2012), Analyses of the ozone weekend effect in Tokyo, Japan: Regime of oxidant (O_3 + NO_2) production, *Aerosol Air Qual. Res*. **12**, 2, 161–168, DOI: 10.4209/aaqr.2011.07.0102.

Saitanis, C.J. (2003), Background ozone monitoring and phytodetection in the greater rural area of Corinth – Greece, *Chemosphere* **51**, 9, 913–923, DOI: 10.1016/S0045-6535(03)00041-9.

Schnell, R.C., S.J. Oltmans, R.R. Neely, M.S. Endres, J.V. Molenar, and A.B. White (2009), Rapid photochemical production of ozone at high concentrations in a rural site during winter, *Nature Geosci.* **2**, 120–122, DOI: 10.1038/ngeo415.

Seinfeld, J.H., and S.N. Pandis (2006), *Atmospheric Chemistry and Physics: From Air Pollution to Climate Change*, 2nd ed., John Wiley & Sons.

Semple, J.L., and G.W.K. Moore (2008), First observations of surface ozone concentration from the summit region of Mount Everest, *Geophys. Res. Lett.* **35**, 20, L20818, DOI: 10.1029/2008GL035295.

Shan, W.P., Y.Q. Yin, J.D. Zhang, and Y.P. Ding (2008), Observational study of surface ozone at an urban site in East China, *Atmos. Res*. **89**, 3, 252–261, DOI: 10.1016/j.atmosres.2008.02.014.

Sillman, S. (1999), The relation between ozone, NO_x and hydrocarbons in urban and polluted rural environments, *Atmos. Environ.* **33**, 12, 1821–1845, DOI: 10.1016/S1352-2310(98)00345-8.

Skamarock, W.C., J.B. Klemp, J. Dudhia, D.O. Gill, D. Barker, M.G. Duda, X.Y. Huang, W.Wang, and J.G. Powers (2008), A description of the advanced research WRF. Version 3, NCAR Tech. Note No. NCAR/TN-475+STR, 113, University Corporation for Atmospheric Research, Boulder, USA, DOI: 10.5065/D68S4MVH.

Solberg, S., Ø. Hov, A. Søvde, I.S.A. Isaksen, P. Coddeville, H. De Backer, C. Forster, Y. Orsolini, and K. Uhse (2008), European surface ozone in the extreme summer 2003, *J. Geophys. Res.* **113**, D7, D07307, DOI: 10.1029/2007JD009098.

Staehelin, J., J. Thudium, R. Buehler, A. Volz-Thomas, and W. Graber (1994), Trends in surface ozone concentrations at Arosa (Switzerland), *Atmos. Environ.* **28**, 1, 75–87, DOI: 10.1016/1352-2310(94)90024-8.

Stevenson, D.S., F.J. Dentener, M.G. Schultz, K. Ellingsen, T.P.C. van Noije, O. Wild, G. Zeng, M. Amann, C.S. Atherton, N. Bell, D.J. Bergmann, I. Bey, T. Butler, J. Cofala, W.J. Collins, R.G. Derwent, R.M. Doherty, J. Drevet, H.J. Eskes, A.M. Fiore, M. Gauss, D.A. Hauglustaine, L.W. Horowitz, I.S.A. Isaksen, M.C. Krol, J.-F. Lamarque, M.G. Lawrence, V. Montanaro, J.-F. Müller, G. Pitari, M.J. Prather, J.A. Pyle, S. Rast, J.M. Rodriguez, M.G. Sanderson, N.H. Savage, D.T. Shindell, S.E. Strahan, K. Sudo, and S. Szopa (2006), Multimodel ensemble simulations of present-day and near-future tropospheric ozone, *J. Geophys. Res.* **111**, D8, D08301, DOI: 10.1029/2005JD006338.

Stohl, A., P. Bonasoni, P. Cristofanelli, W. Collins, J. Feichter, A. Frank, C. Forster, E. Gerasopoulos, H. Gäggeler, P. James, T. Kentarchos, H. Kromp-Kolb, B. Krüger, C. Land, J. Meloen, A. Papayannis, A. Priller, P. Seibert, M. Sprenger, G.J. Roelofs, H.E. Scheel, C. Schnabel, P. Siegmund, L. Tobler, T. Trickl, H. Wernli, V. Wirth, P. Zanis, and C. Zerefos (2003), Stratosphere-troposphere exchange: A review, and what we have learned from STACCATO, *J. Geophys. Res.* **108**, D12, 8516, DOI: 10.1029/2002JD002490.

Tadeusiewicz, R. (1993), *Sieci Neuronowe*, Akademicka Oficyna Wydawnicza, Warszawa (in Polish).

Tadeusiewicz, R., T. Gąciarz, B. Borowik, and B. Leper (2007), *Odkrywanie Właściwości Sieci Neuronowych przy Użyciu Programów w Języku C*, Polska Akademia Umiejętności, Kraków (in Polish).

Tarasick, D.W., and R. Slater (2008), Ozone in the troposphere: Measurements, climatology, budget and trends, *Atmosphere-Ocean* **46**, 1, 93–115, DOI: 10.3137/ao.460105.

Tarasova, O.A., and A.Y. Karpetchko (2003), Accounting for local meteorological effects in the ozone time-series of Lovozero (Kola Peninsula), *Atmos. Chem. Phys*. **3**, 4, 941–949, DOI: 10.5194/acp-3-941-2003.

The Royal Society (2008), Ground-level ozone in the 21st century: Future trends, impacts and policy implications, Royal Society Science Policy Report No. 15/08, RS1276, available from: https://royalsociety.org/~/media/Royal_Society_Content/policy/publications/2008/7925.pdf.

van Aardenne, J.A., F.J. Dentener, J.G.J. Olivier, C.G.M. Klein Goldewijk, and J. Lelieveld (2001), A 1°×1° resolution data set of historical antropogenic trace gas emissions for the period 1890–1990, *Global Biogeochem. Cycles* **15**, 4, 909–928, DOI: 10.1029/2000GB001265.

vanLoon, G.W., and S.J. Duffy (2008), *Chemia Środowiska*, Wydawnictwo Naukowe PWN, Warszawa (in Polish).

Vestreng, V., L. Ntziachristos, A. Semb, S. Reis, I.S.A. Isaksen, and L. Tarrasón (2009), Evolution of NOx emissions in Europe with focus on road transport control measures, *Atmos. Chem. Phys*. **9**, 1503–1520, DOI: 10.5194/acp-9-1503-2009.

Vieno, M., A.J. Dore, D.S. Stevenson, R. Doherty, M.R. Heal, S. Reis, S. Hallsworth, L. Tarrason, P. Wind, D. Fowler, D. Simpson, and M.A. Sutton (2010), Modelling surface ozone during the 2003 heat-wave in the UK, *Atmos. Chem. Phys.* **10**, 16, 7963–7978, DOI: 10.5194/acp-10-7963-2010.

Viezee, W., H.B. Singh, and H. Shigeishi (1982), The impact of stratospheric ozone on tropospheric air quality: Implications from an analysis of existing field data, Report, Proj. 1140, SRI International Corp., Menlo Park, Ca, USA.

Viezee, W., W.B. Johnson, and HB. Singh (1983), Stratospheric ozone in the lower troposphere – II. Assessment of downward flux and ground-level impact, *Atmos. Environ.* **17**, 10, 1979–1993, DOI: 10.1016/0004-6981(83)90354-2.

Vingarzan, R. (2004), A review of surface ozone background levels and trends, *Atmos. Environ.* **38**, 21, 3431–3442, DOI: 10.1016/j.atmosenv.2004.03.030.

Volz, A., and D. Kley (1988), Evaluation of the Montsouris series of ozone measurements made in the nineteenth century, *Nature* **332**, 6161, 240–242, DOI: 10.1038/332240a0.

Walcek, C.J., and H.H. Yuan (1995), Calculated influence of temperature-related factors on ozone formation rates in the lower troposphere, *J. Appl. Meteor*. **34**, 5, 1056–1069, DOI: 10.1175/1520-0450(1995)034<1056:CIOTRF>2.0.CO;2.

Wang, Y.H., D.J. Jacob, and J.A. Logan (1998), Global simulation of tropospheric O_3–NO_x-hydrocarbon chemistry: 3. Origin of tropospheric ozone and effects of nonmethane hydrocarbons, *J. Geophys. Res.* **103**, D9, 10757–10767, DOI: 10.1029/98JD00156.

Wang, Y., L. Shen, S. Wu, L. Mickley, J. He, and J. Hao (2013), Sensitivity of surface ozone over China to 2000–2050 global changes of climate and emissions, *Atmos. Environ.* **75**, 374–382, DOI: 10.1016/j.atmosenv.2013.04.045.

Wierzbicki, D. (1882), Ozon atmosferyczny i roczny ruch jego według dwudziesto-pięcioletnich spostrzeżeń obliczony, (Atmospheric ozone and its annual variation calculated from 25-year observations), Rozprawy i Sprawozdania z Posiedzeń Wydziału Matematyczno-Przyrodniczego Akademii Umiejętności, Tom IX, Kraków (in Polish).

Yarwood, G., T.E Stoeckenius, and J. Heiken (2002), Proximate modeling of weekday/weekend ozone differences for Los Angeles, Final Report; prepared by Environ International Corp. and Air Improvement Resource, Inc., for the National Renewable Energy Laboratory, Golden, CO, and the Coordinating Research Council, Alpharetta, GA.

Yarwood, G., T.E. Stoeckenius, J.G. Heiken, and A.M. Dunker (2003), Modeling weekday/weekend ozone differences in the Los Angeles region for 1997, *J. Air & Waste Manage. Assoc*. **53**, 7, 864–875, DOI: 10.1080/10473289.2003.10466232.

Zaveri, R.A., R.D. Saylor, L.K. Peters, R. McNider, and A. Song (1995), A model investigation of summertime diurnal ozone behaviour in rural mountainous locations, *Atmos. Environ.* **29**, 9, 1043–1065, DOI: 10.1016/1352-2310(94)00319-G.

Zhang, J., and S.T. Rao (1999), The role of vertical mixing in the temporal evolution of ground-level ozone concentrations, *J. Appl. Meteor*. **38**, 12, 1674–1691, DOI: 10.1175/1520-0450(1999)038<1674:TROVMI>2.0.CO;2.

Zhang, J., S.T. Rao, and S.M. Daggupaty (1998), Meteorological processes and ozone exceedances in the northeastern United States during the 12–16 July 1995 episode, *J. Appl. Meteor*. **37**, 8, 776–789, DOI: 10.1175/1520-0450(1998)037<0776:MPAOEI>2.0.CO;2.

Zhang, Y., N. Shabanov, Y. Knyazikhin, and R.B. Myneni (2002), Assessing the information content of multiangle satellite data for mapping biomes: II. Theory, *Remote Sens. Environ*. **80**, 3, 435–446, DOI: 10.1016/S0034-4257(01)00320-0.

Received 28 May 2020
Received in revised form 18 August 2020
Accepted 31 August 2020

"Publications of the Institute of Geophysics, Polish Academy of Sciences: Geophysical Data Bases, Processing and Instrumentation" appears in the following series:

A – Physics of the Earth's Interior

B – Seismology

C – Geomagnetism

D – Physics of the Atmosphere

E – Hydrology (formerly Water Resources)

P – Polar Research

M – Miscellanea

Every volume has two numbers: the first one is the consecutive number of the journal and the second one (in brackets) is the current number in the series.